

ABSTRACT

Title of Document: THE EQUILIBRIUM GEOMETRY THEORY
FOR BONE FRACTURE HEALING

Alvin Garwai Yew, M.S. 2008
Mechanical Engineering

Directed By: Assistant Professor Adam Hsieh
Department of Bioengineering

Models describing the impact of mechanical stimuli on bone fracture healing can be used to design improved fixation devices and optimize clinical treatment. Existing models however, are limited because they fail to consider the changing fracture callus morphology and probabilistic behavior of biological systems. To resolve these issues, the Equilibrium Geometry Theory (EGT) was conceptualized and when coupled with a mechanoregulation algorithm for differentiation, it provides a way to simulate cell processes at the fracture site. A three-dimensional, anisotropic random walk model with an adaptive finite element domain was developed for studying the entire course of fracture healing based on EGT fundamentals. Although a coarse cell dispersal lattice and finite element mesh were used for analyses, the computational platform provides exceptional latitude for visualizing the growth and remodeling of tissue. Preliminary parameter and sensitivity studies show that simulations can be fine-tuned for a wide variety of clinical and research applications.

THE EQUILIBRIUM GEOMETRY THEORY FOR BONE FRACTURE HEALING

By

Alvin Garwai Yew

Thesis submitted to the Faculty of the Graduate School of the
University of Maryland, College Park, in partial fulfillment
of the requirements for the degree of
Master of Science
2008

Advisory Committee:

Dr. Adam Hsieh, Chair

Dr. Abhijit Dasgupta

Dr. Charles Schwartz

Dr. Chandrasekhar Thamire

© Copyright by
Alvin Garwai Yew
2008

Dedication

Mommy, Daddy and Calinda

Acknowledgements

My time at the Orthopaedic Mechanobiology Lab in the past year has been a phenomenal experience. First and foremost, I thank Dr. Adam Hsieh for generously allowing me to explore the world, both inside and outside of the laboratory. The opportunities that he has provided to me have made me feel like the most fortunate graduate student on Earth. It is rare for Adam to say “no”, and whether or not this was a conscious effort, the outcome is still the same – I have grown in my ability to think independently and have learned to better anticipate and manage the consequences of my actions. In all, my interactions with Adam have been rewarding. He has been a gentle advisor who has deep perception and forethought, yet also has the ability to metaphorically, move along the gradients of a flowing river. I have enjoyed our sometimes lengthy philosophical conversations and have always looked forward to debating the EGT.

Adam probably doesn't remember, but as an undergraduate student not more than one year ago, he asked me to take more risks. I never told him, but part of my drive to take on an all-or-nothing pursuit, to completely build a computational platform in a matter of months, was meet his challenge. Without his encouragement and willingness to allow me to take risks, this thesis would never have come to be.

In much the same way, Dr. Charles Schwartz gave me great freedom in pursuing my project for his Computational Geomechanics class in Fall 2007. Like no other person, Dr. Schwartz saw the birth and early workings of what eventually came to be my thesis. If Dr. Schwartz had stopped me from pursuing the class project, this thesis would also have never come to be. Regis Carvalho, who is one of Dr. Schwartz's PhD students,

helped me to work out some of my difficulties in ABAQUS and taught me the finer details of the “Mona Lisa” mesh. Thanks, Regis!

All of my efforts here are based on solid research foundations. The efficiency with which I attacked the thesis was nurtured by Dr. Chandrasekhar Thamire. From Fall 2006 to Summer 2007, I worked with Dr. Thamire in my first scholarly research endeavor – Thermal Therapy Protocols for Benign Prostatic Hyperplasia. By working with him, I learned how to thoroughly conduct good and relevant research. Having also taken my first graduate-level class with him as an undergraduate, I became fully-prepared to tackle a full load of graduate coursework in Fall 2007, which has made me a more productive student and has therefore, partially equipped me to complete my Master’s thesis with such speed.

Besides his invaluable seeding, Dr. Thamire, like Adam has served as a reliable mentor, always ready to share an insight or to lend an open ear. His work ethic is relentless and though I have strived to mimic his productivity when I am at work, I find it very difficult to endure and produce as much as him. For this and other reasons, Dr. Thamire has been a role model for me since the very beginning and he was instrumental in reviving a previously dying interest in me to pursue bioengineering.

Another member of my thesis committee, whom I have had little contact with is Dr. Abhijit Dasgupta. I have heard only positive things from the faculty and students and so, I am honored to have him serve on my committee. It is my hope that Dr. Dasgupta will be able to provide advice on how to refine the simulations in future work. I also hope that he will keep his door open for me if I should ever need his expertise on aerospace components and hardware when I begin working full-time at NASA.

Most importantly, I would like to acknowledge and thank my fellow graduate and undergraduate friends at the University of Maryland. There are far too many to name here, but I would like to give special attention to the Orthopaedic Mechanobiology Lab cohort: Hyunchul Kim who has been my most consistent lab buddy this past year; Anshu Rastogi for her motherly love; David Hwang for always making sure that I am constantly entertained; Mike Morchauser for his subtle ways in keeping me focused; Danial Shahmirzadi for watching my back; Ryan Schmidt for being co-king of the undergrads; Rita Pal for working with me on designing the control system for the cartilage loading fixture; Monica Machado for feeding me every so often; Richie Booth for being the other running guy in the lab; Synthia Mariadhas for working with me shortly on the bracket design; Chetan Pasrija for being such a hard worker; Anike Freeman for her many talents; Valerie Loewensberg for reminding me of the beauty of Switzerland; Pratiksha Thakore for always visiting me while waiting on the Quarentine Chamber stuff; Aaron Johnson for first introducing me to ABAQUS; Matt Love for his always-happy attitude; Ben Yang for being my replaceable BFF; Augusta Vigfusdottir for her alien head candy and wonderful Icelandic accent; Adam Gabai for teaching me how to “grab” a rat; Traci Berkman for all the good old times; Magda Benavides for her superb acting skills; Khine Lwin for all her wonderful reflections on life; Charlie Sun for pretending to love programming; David Ryan for demonstrating the qualities of a good leader; and there’s so many more . . . thank you all!

Table of Contents

Dedication	ii
Acknowledgements	iii
Chapter 1: Introduction	1
1.1 Bone Fracture Healing	1
1.2 Stages in Fracture Healing	2
1.3 Clinical and Societal Impact	3
1.4 Mechanobiology Theories	4
1.5 Limitations of Current Models	7
Chapter 2: Model Development	10
2.1 The Equilibrium Geometry Theory	10
2.2 Implementation of the EGT	12
2.2.1 Convergence Criteria	12
2.2.2 The Random Walk	14
2.2.3 Cell Dispersal: Migration	15
2.2.4 Cell Dispersal: Mitosis	17
2.2.5 Cell Dispersal: Apoptosis	18
2.2.6 Poroelastic Finite Element Model	20
Chapter 3: Simulation Results	28
3.1 Scope of the Studies	28
3.2 Apoptosis Proximity Scaling	28
3.3 Age Requirement for Differentiation	30
3.4 Mechanical Loading Protocols	35
3.5 Computational Histology	39
3.6 Statistical Analysis	43
Chapter 4: Conclusion	45
4.1 Summary of Results and Future Work	45
4.2 Philosophical Implications of the EGT	49
Appendix A	53
References	82

Chapter 1: Introduction

1.1 Bone Fracture Healing

The primary function of bone is to provide local and global structural stiffness in the body [6, 22]. As a load-bearing structure, bone has impressive mechanical properties [9, 18, 26]. In longitudinal tension, the human femur is only about one-tenth the strength of steel, but its composite makeup and efficient geometry gives long bone excellent strength-weight ratio. Unlike inorganic materials however, living bone has remarkable adaptive capabilities that allows it to respond to changes in its environment [27]. Moreover, early experiments studying the behavior of bone show that the mechanical environment strongly modulates cell processes [20, 22, 30]. The study of this effect is called mechanobiology. The term can be broadened to include not only bone-related studies, but also the study of mechanical stimuli on the response of any biological system.

Acute bone fractures introduce drastic changes to bone's mechanical environment and therefore, a series of biological responses is elicited to repair the damaged tissue. Bone repair can be attributed to either primary or secondary healing processes [7]. Primary fracture healing (intramembranous bone formation) is the formation of bone directly from the cortex. Secondary fracture healing (endochondral bone formation) involves the formation of soft tissues and its subsequent mineralization, or ossification, in both the endosteal and periosteal regions. In fractures where interfragmentary gap sizes are large and there is minimal structural stability, primary healing plays a minimal role in the reestablishment of bone integrity when compared to the secondary processes [6]. For this reason, secondary fracture healing (henceforth, "fracture healing") will be our focus.

1.2 Stages in Fracture Healing

Following the initial injury, it is generally understood that bone fracture healing progresses through four stages [8], as depicted in Figure 1: (1) the formation of a hematoma or blood clot, which helps to usher in specialized cells, thus forming soft tissue known as (2) the granulation tissue. Among other substances, the granulation tissue is composed of unorganized, fibrous tissue formed from cells called fibroblasts. As the tissue continues to mineralize, it stiffens and becomes (3) the fracture callus. Chondrocytes (cartilage forming cells) and osteoblasts (bone forming cells) are types of cells that appear in greater abundance during this stage. Once the callus is formed and significantly mineralized, (4) remodeling processes dominate to restore the bone to its most efficient geometry. For convenience, the differentiating tissue at the bone fracture site will henceforth be called the “callus.” For example, stage two of fracture healing can be described as a fracture callus consisting of granulation tissue.

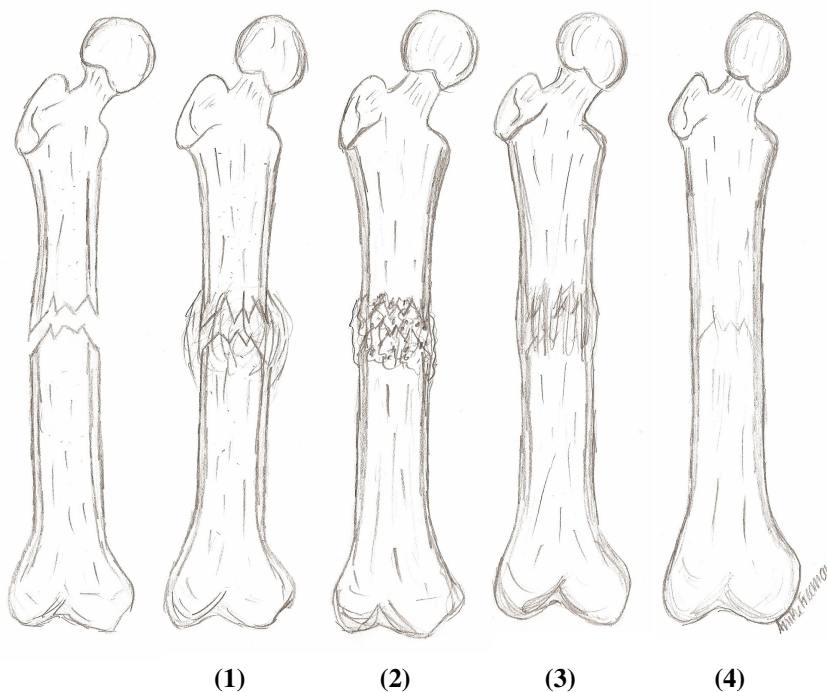


Figure 1 The four stages in bone fracture healing. 1) hematoma; 2) granulation tissue; 3) callus; 4) healed bone after remodeling. Courtesy of Anike Freeman.

1.3 Clinical and Societal Impact

In 2005, there were over 3.4 million hospital visits in the United States for injuries due to fractures [19]. These incidents often require hospitalization for many days, and full recovery can take many weeks. Furthermore, this can be compounded by osteopenia, or abnormally low bone density; estimates in 2007 report more than 200 million osteoporotic subjects worldwide whose condition makes them more susceptible to fragility fractures [25]. Accordingly, a number of authorities including the United Nations (UN) and the World Health Organization (WHO) have named 2000-2010 the “Bone and Joint Decade” [29]. In 2002, President Bush followed by declaring 2002-2011 the “National Bone and Joint Decade.” The instant limelight on musculoskeletal issues could not have come at a better time; trends show that the incidence of fractures is on the rise (partially due to the aging baby-boomer population) and so, there is motivation to find ways to expedite the time to recovery.

The use of mechanobiologic theories to design therapeutic regimens or to optimize fracture fixation implants is one viable solution for speeding up recovery and it proposes that fracture healing is facilitated by the appropriate magnitudes and durations of mechanical stimuli. Identifying the key stimuli is a challenge and many theories have been proposed. Once the underlying stimuli are determined and the appropriate assumptions are made, one can model a bone fracture within a simulation to determine the mechanical protocols needed to ensure that an effective treatment is undertaken. If inappropriate protocols are prescribed during the healing process, a number of complications can occur. These complications can encompass a wide variety of issues, including poor healing, delayed healing, refractures, myelofibrosis and nonunions [7, 8].

1.4 Mechanobiology Theories

Although Wolff (1892) indirectly linked mechanical stress with trabecular structure [28], Pauwels in his 1960 paper, is often credited for being the first to identify a means for which mechanical forces can be associated with bone fracture healing [2, 27]. Through his clinical observations, he theorized that fracture healing was influenced by the first invariant (volume changed caused by dilatational stresses) and second invariant (shape change caused by distortional stresses) of the stress tensor. Further, he proposed that bone can only form in an environment with high dilatational and low distortional stresses and in fracture healing, through the differentiation of softer tissues. Also, hydrostatic compression leads to the formation of cartilage while shearing deformation leads to the formation of fibrous tissues. Pauwels' conclusions are summarized in Figure 2.

In 1979, Perren first alluded to the idea of interfragmentary strain [22], which eventually led to its formal theory. The driving concept behind the interfragmentary strain theory is that a tissue cannot form in an interfragmentary region whose local strain magnitude exceeds the value at rupture for that tissue, as determined by uniaxial tests.

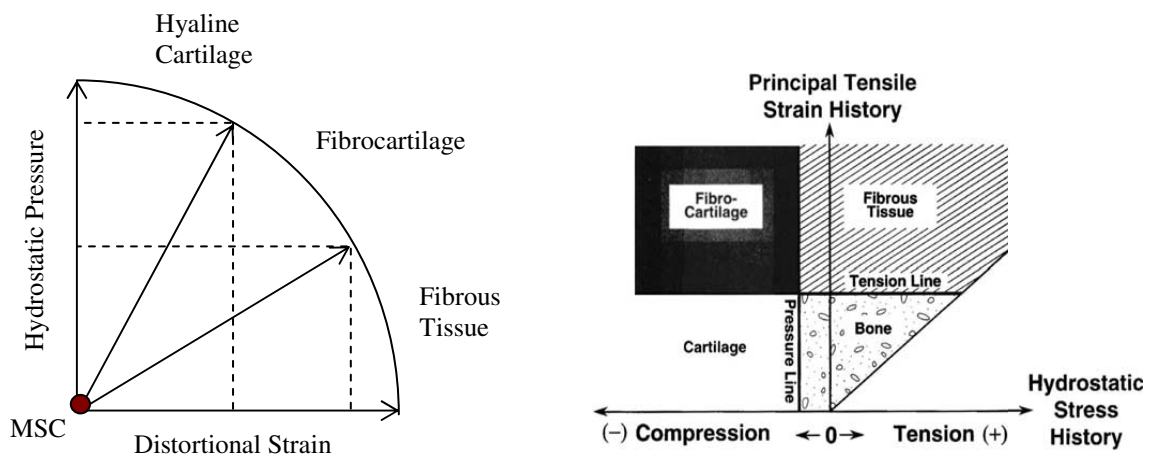


Figure 2 Left: Pauwels' theory on how mechanical stimuli induces tissue differentiation. Right: theory proposed by Carter et al. includes stress and strain histories [2]

He reported that the strain tolerance of granulation tissue is at +100%, cartilage at +10% and bone at +2%. In contrast to Pauwels, Perren focused his studies on strains as opposed to stresses since strains describe the actual physical phenomenon occurring in the tissue and its subsequent damage [2].

A combined approach (see Figure 2) that includes the effect of stresses and strains was developed by Carter et al. [2, 3]. A combination of low hydrostatic pressure and low principal tensile strain is required for the production of bone. When compared to bone, fibrous tissues require higher strains while cartilage formation requires higher hydrostatic pressures. With a combination of both high stress and strain histories, fibro-cartilage develops. Claes and Heigele proposed similar stimuli for tissue differentiation in response to stresses and strains [4], but were able to quantify the magnitudes of stress and strain needed to form certain tissues while Carter et al. only provided qualitative descriptions of tissue distributions.

Prendergast and Lacroix completed some of the first biphasic mechanoregulation studies (see Figure 3) for tissue differentiation [16, 17, 23]. They proposed that differentiation was based on shear strains in the solid matrix and by shear stresses created

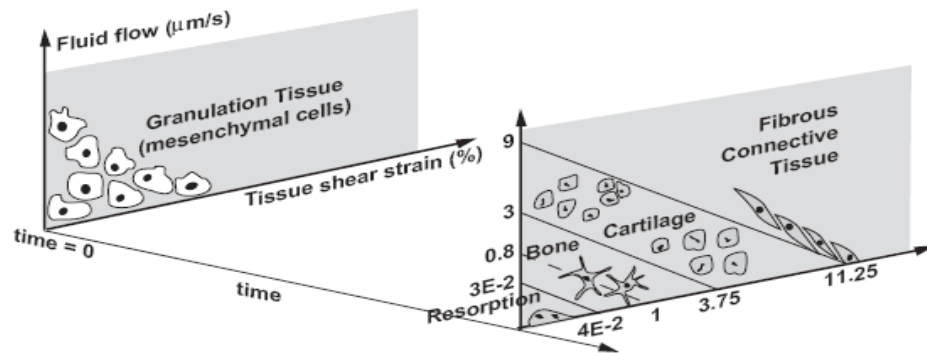


Figure 3 Biphasic mechnoregulation model developed by Pendergast et. al [21]

from interstitial fluid flow. In particular, octahedral shear strains and relative fluid velocity magnitudes are normalized to constants ($a = 0.0375$, $b = 3 \mu\text{m/s}$), as derived in Prendergast et al. [23]. These normalized values are then summed to calculate a stimulus value, S (see Equation 1) to determine if the local tissue can differentiate [14]. A high stimulus leads to the formation of softer tissues while lower levels support the formation of bone. It was determined that $S > 3$ is the stimulus for fibrous tissue formation, $1 < S < 3$ is the stimulus for cartilage formation, and $S < 1$ is the stimulus for the formation of bone. Note that conceptually, this agrees with the interfragmentary strain theory.

$$S = \gamma / a + v / b \quad (\text{Equation 1})$$

In an attempt to compare the theories in Carter et al. (1998), Claes and Heigele (1999), and Lacroix and Prendergast (2002), Isaksson et al. created one geometrically similar model and applied each of the mechanoregulation theories with its corresponding material law (ie. linear elasticity or poroelasticity) to study the predictive capabilities [15]. In the discussion, the authors admit that the model omitted a number of important biological processes (this will be reviewed further in section 1.5). In general however, the three models studied by Isaksson et al. produced accurate temporal and spatial distributions of differentiated tissues.

Because of the similarity in results among the three algorithms compared in Isaksson et al., one could make the argument that for this current thesis, the implementation of any mechanoregulation model would be valid. Though partially true, a mechanoregulation model governed only by phenomena occurring in the solid phase fails to consider the importance of fluid-related shear stresses, which has direct effects on cell function and pressurization in the tissue due to fluid, which acts in coordination with

the solid phase to resist stresses. Additionally, the existence of the fluid phase is one of the reasons why biological tissues – which are often described as being viscoelastic or poroelastic – differ from traditional engineering materials in their physical behavior. For this reason the biphasic mechanoregulation model presented by Lacroix and Prendergast is believed to be the most versatile model that best captures the mechanical stimuli that can be of significant importance to bone fracture healing.

1.5 Limitations of Current Models

Bone is a highly regenerative system and as such, the original anatomy of the fractured bone can be fully restored in children, while mechanically stable lamellar structures develop in mature adults through remodeling processes [7]. In agreement with this idea, Isaksson et al. writes, “Healing of an osseous fracture is a unique process where the result is not a scar but a regeneration of injured tissue” [15]. To elaborate further, Perren in his 1979 paper concluded that, “through a sequence of changes of tissue development and geometry, the original structural integrity is restored” [22]. Take note of Perren’s mention of geometry as being important process for bone fracture healing.

To date, most simulations [2, 4, 11, 14, 15, 16 17] have only studied tissue differentiation under simple diffusion models and have neglected to consider the transient callus growth and subsequent remodeling-mediated geometric changes as major factors that affect bone stability. The best of these studies assume a fixed, idealized bone and soft tissue geometry that has the appearance of a “typical” fracture callus; when beginning those simulations, the soft tissue is homogeneously given the material properties of granulation tissue and throughout the simulation, the properties of the soft tissue region change as cells diffuse and differentiate.

There are several problems with the methods used in the aforementioned studies. Most notably, confining the fracture callus to a specific shape throughout the entire simulation is not realistic of actual healing processes. The callus will experience drastic shape and size changes throughout the course of healing and these changes directly affect the mechanical environment of the bone fracture site. Another problem with the methods is that the simulations do not provide a beginning-end picture of bone fracture healing since the starting point of the simulations begin with an assignment of 100% granulation tissue for the callus. The events that occur prior to the formation of the granulation tissue are absolutely critical to the latter stages in the healing process and therefore, simulating the pre-granulation stages of healing is also important. Moreover, it is not necessarily correct to assume that there is ever a point in the course of healing where the fracture callus will consist of 100% granulation tissue.

Yet another problem is related to the neglect to simulate cell division and cell death. These cell processes are factors that heavily influence the concentration of cells and their corresponding extracellular matrix, which influences the local and global material properties of the fracture callus. An additional concern is the axisymmetric assumption used in the models. Making this assumption is not realistic for two reasons: (1) bone is not axisymmetric and (2) tissue distributions within a fracture callus are heterogeneous and even slight asymmetries might cause differences in the mechanical stability of a fracture, which should be captured in simulations.

A series of recent publications from Doblare M, Garcia-Aznar JM, Gomez-Benito MJ, and Kupier JH [10, 12, 13] attempts to address the issue of callus shape in bone fracture healing. It is the only series of studies (to the author's knowledge) that takes into consideration dynamic geometric parameters for the callus growth and remodeling. Their

computational studies employ a complex diffusion-based model that considers changes in cell concentrations due to migration, mitosis and apoptosis. The mechanical analysis was performed in a commercial finite element package: (1) a poroelastic analysis determined the stresses and strains in tissues, which are evaluated under an equation to determine differentiation, (2) a diffusion analysis determined the direction of cell migration and (3) a thermoelastic analysis as an analogy to determine tissue growth. Although the results from their analyses look promising, it is believed that improvements can be made. Consider the following key points that were not considered in their analyses: 1) cell migration can go against concentration gradients; 2) biological systems are not always deterministic; 3) cell distributions are not always smooth.

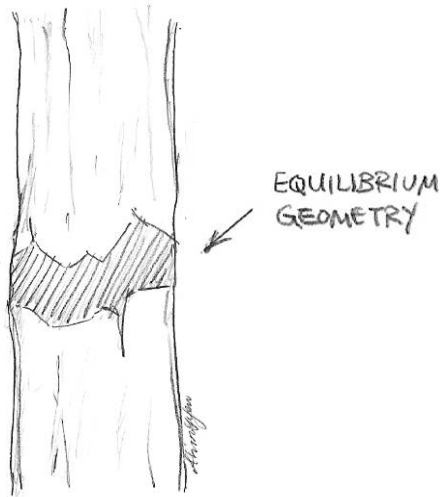
To solve these problems, Perez and Prendergast suggested a different method for modeling cell dispersal [21] by studying a simple 2D bone and implant interface. A more detailed discussion of the methodology will unfold in the next chapter. In summary, their implementation of the random walking of cells can result in a non-deterministic, though stable solution. Cell migration can also be programmed for each cell so that it will allow cells to move against concentration gradients. They use the term “anisotropic” migration to indicate that a cell has a preferred direction of movement as opposed to “isotropic” migration to indicate purely random migration. Mitosis and apoptosis are also considered in their analyses. Although their study was able to address the probabilistic nature of biological systems, their rule for anisotropic migration was simplified; their simplification is sufficient for a simple 2D, infinite plane problem but would need refinement in a complex 3D problem.

Chapter 2: Model Development

2.1 The Equilibrium Geometry Theory

It is clear that there that throughout history, models describing tissue growth and remodeling have progressively moved from the continuum-based, phenomenological approach to ones that are more mechanistic. The phenomenological approaches are convenient, but what they sacrifice is a true linking between the precise mechanical stimuli for inducing a given biological response. Further, Cowin (2006) explains that the bijective (one-to-one) mapping used in continuum models does not fit well with biological systems. He writes, “Cells move around like guests circulating at a cocktail party, they replicate themselves with some ease and they produce new material for the tissue of which they are a part” [5]. In this way, new regions of tissue appear, others vanish, and tissue regions separate and coalesce. These events are difficult to capture using continuum mechanics. On the other hand, ascertaining the exact mechanism that elicits a biological response is not any easier, making continuum mechanics attractive.

The shortcomings from the studies described in Chapter 2 is the motivation for the development of a novel theory to address both the function and form in bone fracture healing by using a combination of the phenomenological and mechanistic approaches. The Equilibrium Geometry Theory (EGT) postulates that for an instantaneous configuration of a bone fracture environment, there is a unique spatial distribution of bone cells within the interfragmentary region that establishes the equilibrium state for the system. The equilibrium geometry is defined as the geometric domain that contains all of the mature bones cells needed to define this equilibrium state (see Figure 4). While the healing process is taking place, the equilibrium geometry is not yet saturated with bone



“For an instantaneous configuration of a bone fracture environment, there is a unique spatial distribution of bone cells within the interfragmentary region that establishes the equilibrium state for the system.”

Figure 4 Depiction of the equilibrium geometry (shaded) occupying the interfragmentary region

cells and because the system is mechanically and geometrically unstable, the rates of cell dispersal at the fracture site (migration, mitosis and apoptosis) are in constant flux. Thus, through the equilibrium geometry, one can employ a way to capture a quantitative measure of instability and relate it to rates of cell dispersal.

For this current study, we simplify the fracture healing process and postulate that under the EGT, healing can be divided into two phases, (see Figure 5). Phase I is the growth and strengthening stage where cell dispersal is heavily influenced by the degree of mechanical stability at the fracture site. In Phase II (reshaping and remodeling), cell processes are dominated more and more by geometric considerations since the formation of a fracture callus has already provided mechanical stability for the system, but not geometric stability (i.e. has not attained equilibrium geometry).

Although in this study the quantitative effect of the equilibrium geometry on cell dispersal is phenomenological (discussed further in section 2.2), there is a real, physical basis to the geometry’s existence; recall that if the bony fragments in a bone fracture are placed in their pre-fractured configuration, the structural integrity of the bone is

<u>Phase I</u> Mechanical Stability: % error in displacement		<u>Phase II</u> Geometric Stability: % error in # of bone cells in EG	
100%	25%	100%	10%
<i>Simulation Start</i>		<i>Threshold</i>	
		<i>Complete</i>	

Figure 5 Two types of stability criterion are used to specify the progress of healing. Bone fracture healing must satisfy both criterions to heal properly.

reestablished during the healing process and the healed bone does not result in a scar, but resembles the original tissue [7, 15, 22]. The EGT ultimately seeks to find a way to model how a fractured bone returns to its original form. Moreover, the EGT can be used to characterize bone healing in a fracture site for a wide variety of system configurations. Note that because the EGT only drives cell dispersal processes, it is intended to work in conjunction with any of the viable mechanobiological rules for differentiation.

2.2 Implementation of the EGT

2.2.1 Convergence Criteria

In the previous section, there was a brief mention of system stability and how cellular processes vary according to the degree of stability. It was also proposed that mechanical stability proceeds geometric stability in bone fracture healing (function before form). By establishing two independent stability criteria (thereby defining two phases within the simulation), it becomes possible to specify a convergence criterion for each phase of the simulation and to later implement mathematical models to direct each cell process in accordance with the stability.

In Phase I, the mechanical instability is a measure of any current kinetic or kinematic quantity that is divided over the initial measure. For example in this study, the

quantity used for the mechanical instability criterion, $error^{mech}$ is the maximum axial displacement experienced within the domain of a fracture site after a loading cycle.

$$error^{mech} = displ^{current} / displ^{initial} \quad (\text{Equation 2})$$

When $error^{mech}$ gets smaller, the system becomes more mechanically stable. When the current displacement divided by the initial displacement crosses an established criterion (here, that value is set to be 0.25, which means that the current displacement is 25% of the initial displacement when exposed to the same magnitude of loading), the cellular processes become dominated by geometrical considerations and the simulation moves into Phase II. In Phase II, two quantities are needed in order to pinpoint the error in the geometric stability: (1) $equil^{sat}$ is the number of total cells needed to saturate the equilibrium geometry, (2) $equil^{bone}$ is the number of bone cells currently in the equilibrium geometry. Thus,

$$error^{geo} = 1 - equil^{bone} / equil^{sat} \quad (\text{Equation 3})$$

When $error^{geo}$ gets smaller, the system becomes more geometrically stable. When $error^{geo}$ crosses an established criterion (here, the convergence value is set to be 0.02, which means that 98% of the equilibrium geometry must be saturated by bone cells), the simulation is complete.

For modeling cell dispersal (migration, mitosis and apoptosis), the random walk model employed by Perez and Prendergast [21] was seen as a versatile platform that could be modified for implementing the EGT. All cells in their random walk simulation can occupy and move about discrete positions, whose points make up a pre-defined

lattice. By simulating cell processes within a lattice, it becomes possible to track the spatial and material characteristics of the cell over time and to be able to simulate its birth and death. The following paragraphs will describe how this is done in the context of the EGT. Note that the methods employed in this particular study is the suggested way of interpreting the EGT, though there may certainly be other viable rules and protocols for simulating cell behavior in the vicinity of the equilibrium geometry.

2.2.2 The Random Walk

In general, random walks are stochastic processes that have been used to model a wide variety of non-deterministic systems and whose applications can be readily seen in modeling biological systems. In the opening chapter of his book [1], Berg explains how simple diffusion can be related to the random walk. Consider a cluster of small particles confined and suspended in an aqueous solution; when these particles are released, they are free to wander about in all directions and spread out – this is called diffusion. When

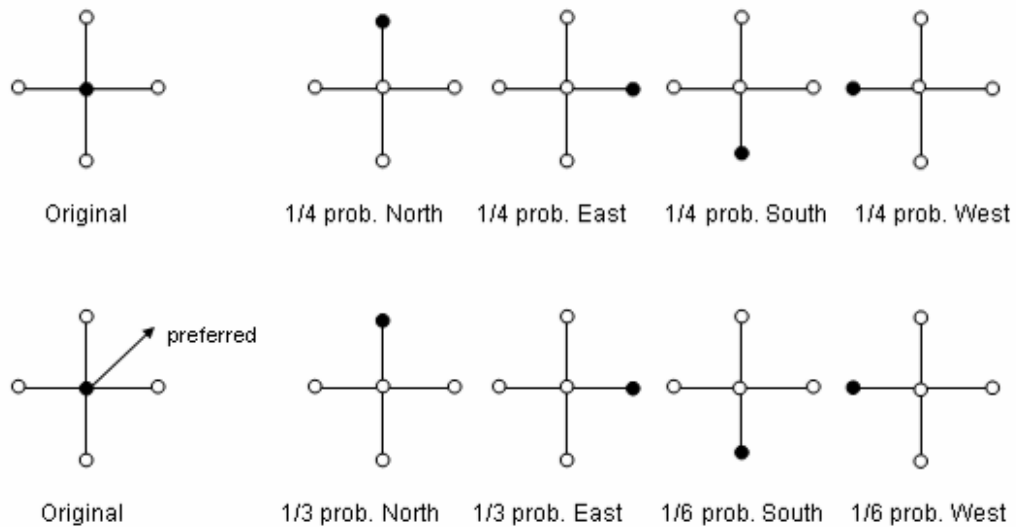


Figure 6 Top: two-dimensional isotropic random walk. Bottom: anisotropic random walk - a cell has a higher probability of migrating into preferred lattice spaces.

characterizing diffusion in one dimension for a single particle, the particle can either move to the right or to the left of its position for a time increment. The one-dimensional probability that a particle will occupy a space to either the left or the right of its position is one-half. This idea can be extended to two and three dimensions. The tracking of movement that this particle makes over time is the random walk.

Random walks can have a preferred orientation (see Figure 6 for a 2D example). In one dimension, this means that a particle will have a greater probability of moving to the left as opposed to the right, or vice versa. The influence of gravity on a system of particles for example, is a random walk with a preferred orientation. This phenomenon can also be called a random walk with drift (as opposed to simply, random walk), a biased random walk (as opposed to unbiased random walk), or an anisotropic random walk (as opposed to isotropic random walk).

2.2.3 Cell Dispersal: Migration

Under the EGT, migration is anisotropic. This means that if a cell is surrounded by unoccupied lattice spaces, there is a stronger tendency for the cell to move into spaces that are closer toward the direction of the equilibrium geometry. Anisotropy of migration can be supported on the basis of chemotaxis since the equilibrium geometry may contain a high concentration of nutrients. The strength of this tendency is calculated as a probability. The two factors that determine that probability are: (1) the proximity that the cell is to the equilibrium geometry and (2) the mechanical stability – if in Phase I – or geometrical stability – if in Phase II – of the fracture site. The second of these two factors essentially places a limit on the probability that a cell will travel in the preferred direction. This limit varies according to the system stability and will be scaled with a

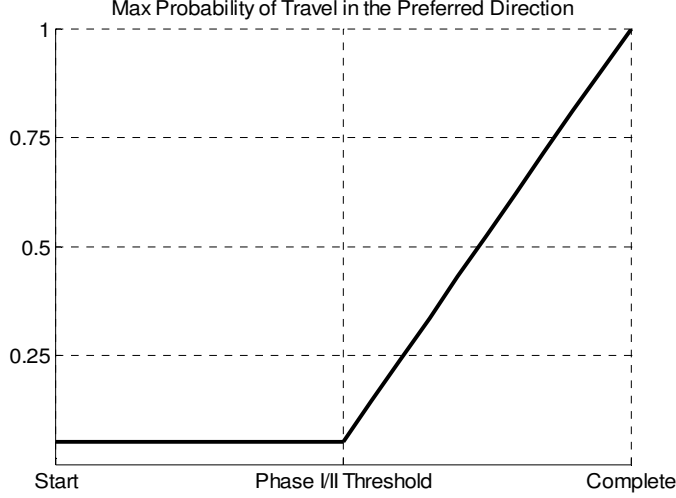


Figure 7 Mathematical model for the maximum probability of traveling in the preferred direction

proximity calculation. In this study, a piecewise linear function is used to model the maximum probability that a cell can travel in the preferred direction (see Figure 7).

The probability that a cell will travel in a particular direction (six possibilities in total, $i = \{x, y, z\}$) is therefore, a combination of an isotropic and anisotropic component for the preferred direction of the $\{x, y, z\}$ components; for the non-preferred direction of the $\{x, y, z\}$ components the probability is solely a function of the isotropic component.

$$\begin{cases} prob_i^{preferred} = prob_i^{anisotropic} + prob^{isotropic} \\ prob_i^{not-preferred} = prob^{isotropic} \end{cases} \quad (\text{Equation 4})$$

where the anisotropic and isotropic probabilities in Equation 4 can be expanded to

$$prob_i^{anisotropic} = prox \cdot weight_i \cdot prob^{directional} \quad (\text{Equation 5})$$

$$prob^{isotropic} = \left[prob^{random} + prob^{directional} \cdot (1 - prox) \right] \div 6 \quad (\text{Equation 6})$$

Note that $prob_i^{preferred} + prob_i^{not-preferred} = 1$ (implied sum over i), which means that the cells in the system are constantly moving. Also, $prob^{directional} + prob^{random} = 1$.

The proximity factor is calculated using the distance formulas for: (1) the cell's position relative to the center of the equilibrium geometry and (2) the nearest point to the cell on the equilibrium geometry relative to the center of the equilibrium geometry. The idea behind the proximity calculation, as it relates to migration, is that a cell closer toward the equilibrium geometry should have a higher recruitment potential for stabilizing the fracture site when compared to cells that are very far away.

$$prox = \begin{cases} dist^{cell} / dist^{EG}, & endosteal \\ dist^{EG} / dist^{cell}, & periosteal \end{cases} \quad (\text{Equation 7})$$

Finally, the weighting values in Equation 5, $weight_i$ are derived from vector quantities that determine the direction of minimum distance a cell needs to travel in order to reach the nearest point on the equilibrium geometry. These weighting values are the similar to direction cosines that are normalized from 0 to 1.

2.2.4 Cell Dispersal: Mitosis

Mitosis is modeled as an isotropic process. For specified iterations of the simulation, the surrounding lattice points for each cell are searched. If any of these surrounding spaces are unoccupied, then there is a probability that a daughter cell will bud into one of the unoccupied spaces. This probability is determined by the system stability and also through a proximity scaling factor. In this study, a piecewise linear function determines the maximum probability that a cell will undergo mitosis (see Figure 8).

An important note needs to be made with regard to the mathematical functions used to form the mitosis probability values. By intuition, one might conclude that the linear segment used in Phase II for this study is flawed. After all, during remodeling,

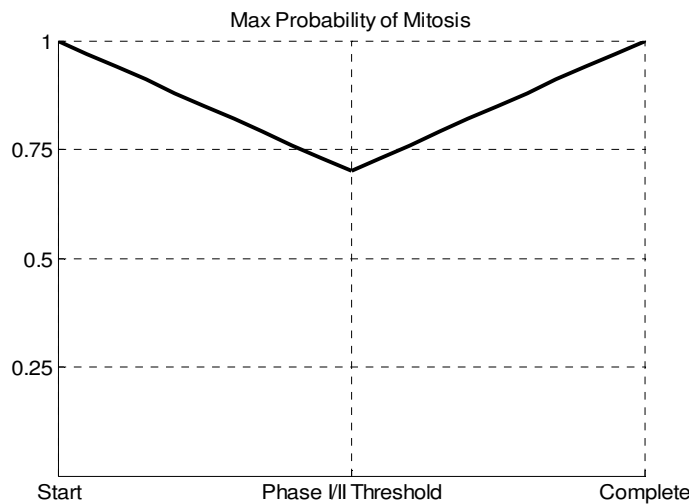


Figure 8 Mathematical model for the maximum probability mitosis

shouldn't the callus be shrinking in size as it attempts to optimize its geometry? If the callus is shrinking in size, then shouldn't rates of mitosis be decreasing? The answer to these questions lies in the fact that mitosis probabilities are intended to work in sync with apoptosis probabilities and other growth-competing factors.

Indeed, the probability of mitosis is modeled as increasing linearly through Phase II, but if the probability of apoptosis approaches the probability of mitosis, then the net effect should be a drastic slowing in growth and the eventual decline in cell population throughout Phase II. Further, one should not forget that in the latter stages of healing, many of the cells are completely surrounded by neighboring cells and thus, these neighboring cells prevent mitosis from occurring. Because of this delicate balancing effect between the cell processes, it is of utmost importance that one carefully chooses the appropriate mathematical models to simulate correctly, the desired conditions.

2.2.5 Cell Dispersal: Apoptosis

For specified iterations of the simulation, all the cells in the system undergo a check for apoptosis. If apoptosis is determined to occur, information for that cell is no longer

recorded and the cell is “deleted” from the system. Apoptosis is determined by calculating its probability of occurrence. Similar to the calculations for migration processes, the two factors that determine that probability are: (1) the proximity that the cell is to the equilibrium geometry and (2) the mechanical or geometrical stability of the fracture site. The second of these two factors, $prob^{max}$ essentially places a limit on the probability that a cell will go through apoptosis. This limit varies according to the stability of the system and a piecewise linear function is used to model the maximum probability that a cell will undergo apoptosis (see Figure 9). The probability that a cell will undergo apoptosis is calculated as

$$prob^{apoptosis} = \left(1 - prox^{\frac{4}{error-geo}} \right) \cdot prob^{max} \quad (\text{Equation 8})$$

The proximity value is calculated in the same way as in Equation 7. The proximity that a cell has with respect to the equilibrium geometry is important because it is believed that cells closer to the fracture site have a higher chance of survival since they are closer to nutrient sources and will be readily available to produce an environment suitable for bone

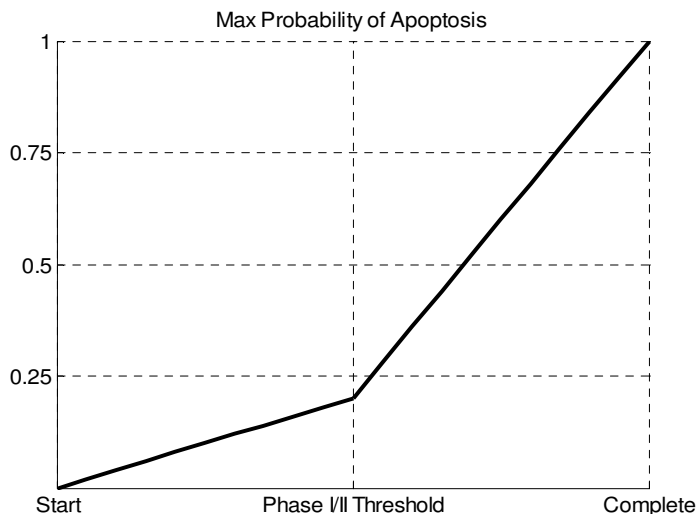


Figure 9 Mathematical model for the maximum probability apoptosis

formation. Note that $error^{geo}$ augments the influence of the proximity in Equation 8 by increasing the chance of apoptosis with increasing stability for cells that are farther from the equilibrium geometry. This derivation will be discussed fully in Chapter 3. Equation 8 also prevents cells in the equilibrium geometry from undergoing apoptosis.

Cell death by necrosis due to cells experiencing abnormal levels of mechanical stimuli have not been considered in this simulation. This is an important factor to include and will be fairly easy to implement. It is with hope, however, that the mathematical models for survivability used in this study have been able to capture the gross cell death phenomenon (to include both apoptosis and necrosis) within the system.

2.2.6 Poroelastic Finite Element Model

Every cell in the system produces an extracellular matrix (ECM). The ECM for a collection of cells essentially defines the gross mechanical properties of a tissue and it consists of a structural protein network and an amorphous ground substance (analogous to a fiber-reinforced composite). This fact is what conveniently allows one to make a continuum assumption in the finite element analysis and to apply the mechanoregulation rules for differentiation by evaluating stresses and strains in each element.

As was previously mentioned, the cells in the system exist within a cell dispersal lattice (or simply, “lattice”). A systematic grouping of finite lattice volumes is what will be used to define the finite element mesh (or simply, “mesh”). This concept is shown in Figure 10. Cell dispersal occurs in the lattice and is controlled through a comprehensive MATLAB v.7.2 (The MathWorks, Natick MA) code. The mechanical analysis (applied to the mesh) is performed using a commercial finite element software package, ABAQUS v.6.7-1 (Simulia, Providence RI).

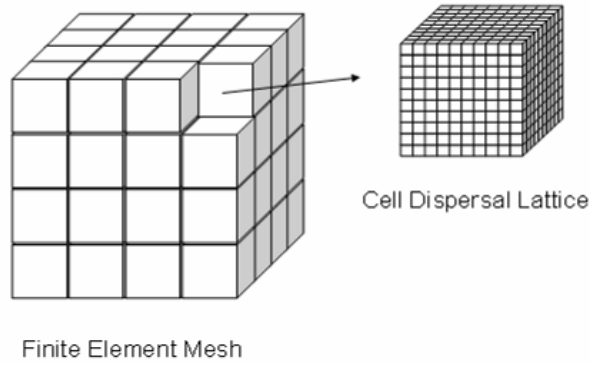


Figure 10 The cell dispersal lattice is ten times finer than the finite element mesh.

As cell dispersal is carried out, cells move constantly in and out of elements in the mesh; therefore, for each iteration of the simulation, new material properties are calculated and delicately orchestrated in MATLAB for each element based on the element's current content of cells. Since every cell produces a unique ECM, it is assumed that every cell (and its corresponding ECM) contributes a fraction of the element's material properties. For example, Young's modulus is calculated as:

$$E^{new} = \sum_t \frac{c^t}{c^{max}} E^t + \frac{c^{max} - c^t}{c^{max}} E^{void} \quad (\text{Equation 9})$$

where

- c^{max} = max number of cells allotted in each element
- c^t = number of differentiated cells of type t
- E^t = Young's modulus for differentiated cell of type t
- E^{void} = Young's modulus of the void tissue

Among other features, the MATLAB code contains a robust searching and sorting algorithm that calculates the number and type of each cell population within every element in the mesh. Note that because the mesh lies directly on top of the lattice and because cells can only exist on lattice points, an element will contain a combination of whole, half, quarter, and eighth cells (see Figure 11). Thus, cells that lie on the boundary of an element will contribute only a fraction of its material properties to an element.

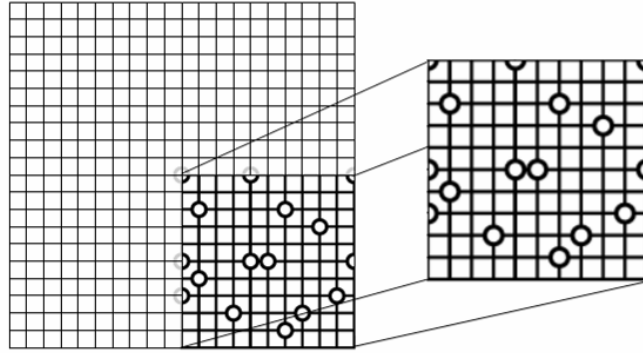


Figure 11 Cells move about in the dispersal lattice. In the magnified image, material properties for the finite element are recalculated based on the number of cells and the corresponding cell type. In this two-dimensional example, there are 2 quarter cells, 4 half cells, 9 whole cells – all of which are the same cell type.

This simulation assumes the existence of five predominate types of tissue (or more precisely, tissue composites) during bone fracture healing. At the beginning the simulation, the domain of the finite element mesh is homogeneously assigned as void tissue, which has half the Young’s modulus as granulation tissue and therefore, assumes that void tissue provides little mechanical stability to the system. At the beginning of the simulation, the void tissue is also seeded with several granulation-producing cells that support the production of granulation tissue. It is from these initial seeds that allow for the amplification of itself through mitosis and through which differentiation into more advanced tissue types will develop. Cell seeding is one of the major advantages of utilizing the random walk method within the dispersal lattice since it allows one to very easily place cells in areas of initially high immune response or nutrient supplies, which is advantageous for highly complex bone fracture geometries.

Table 1 Material properties from Perez, et al. [21]

	Void	Granulation Tissue	Fibrous Tissue	Cartilage	Immature Bone	Cortical Bone
Young’s Modulus (MPa)	0.1	0.2	2	10	1000	17000
Permeability ($m^4/Ns \times 10^{-14}$)	1	1	1	0.5	0.1	0.001
Poisson’s Ratio	0.167	0.167	0.167	0.3	0.3	0.3

The mesh is composed of 64 one-element, perfect cubes of size $n \times n \times n$ – physical dimension of $1 \times 1 \times 1$ mm – which are assembled to make a larger perfect cube of size $4n \times 4n \times 4n$ – physical dimension of $4 \times 4 \times 4$ mm (see Figure 12). Although immensely time-consuming to construct, the reason why 64 one-element parts are used as opposed to one part of 64 elements is that the former method will allow for easier material property definitions for each part. A 64 part domain is considered to be extremely coarse and not sufficient in being able to capture accurate bone geometries. Nonetheless, running simulations based on this mesh design is sufficient in being able to evaluate the overall biological trends in the system.

A $1 \times 1 \times 1$ mm element with a lattice that is 10 times as fine as the mesh will result in a lattice spacing of 0.1 mm. The resulting cell density is 100 cells/mm^2 , which is 100 times less dense than the lattice and mesh specifications used by Perez and Prendergast in their random walk study [21]. Using a denser cell packing would require significantly greater computing resources, but it is ideal to have the lattice spacing be the same as the average diameter of a cell. Making this improved modification to the current thesis is not difficult to do and it will certainly be explored at a later time.

Using 64 parts to construct the mesh requires proper definition of interaction properties between parts. These interaction properties are a unique feature in ABAQUS and in terms of transmission of forces, displacements, materials, etc., interactions generally adhere to the following analogy – Elements:Nodes::Parts:Interactions. In the tangential direction of each boundary shared by more than one part, a rough friction definition with a tolerance of 0.1 is specified. By doing this, a no-slip condition is enforced that will ideally transmit information from one part to another in much the same

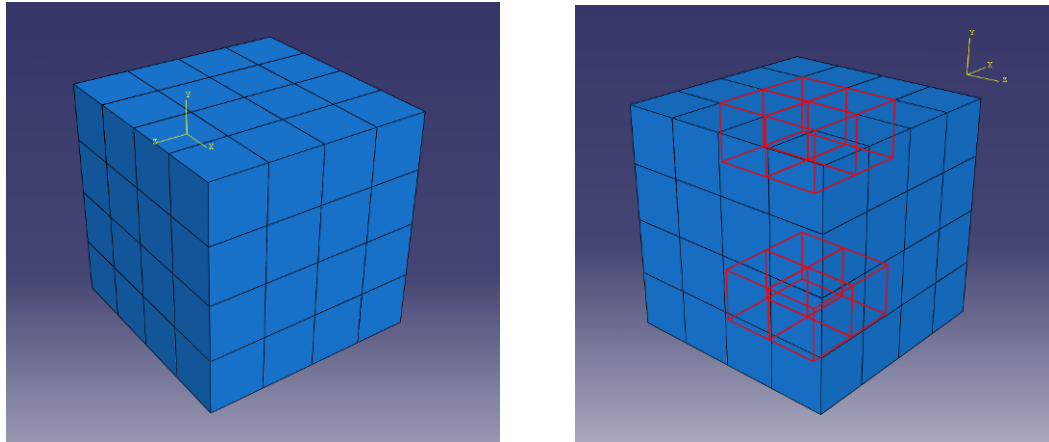


Figure 12 Left: finite element mesh. Right: highlighting the original cortical bone fragments.

way elements communicate. Used in a liberal way before in this thesis, we henceforth formally state that “elements” and “parts” are used interchangeably.

To support a poroelastic analysis, the parts are built with eight-node trilinear displacement and pore pressure elements with a reduced integration formulation. Each element has unique material properties to aid in the poroelastic analysis (Young’s modulus, Poisson’s ratio, permeability). At the start of the simulation with two tissue types being valid at the beginning: (1) the original bony fragments and (2) the void tissue. Cortical bone material properties are assigned to these bony fragments, which occupy the four, interior elements on the top and bottom surfaces (see Figure 12).

For the boundary conditions, an initial pore pressure of 0 MPa is prescribed on the boundary of the finite element domain. Also an encastre condition that restricts translations and rotations is established on the bottom surface of the bottom bony fragment, as shown in Figure 13. Loads are applied to the top surface of the upper bony fragment. Although the idea is to determine an optimal loading protocol to implement in an attempt to expedite fracture healing, only one protocol was applied in this study. Uniaxial compression under static load-control is specified. Using a Soil Consolidation

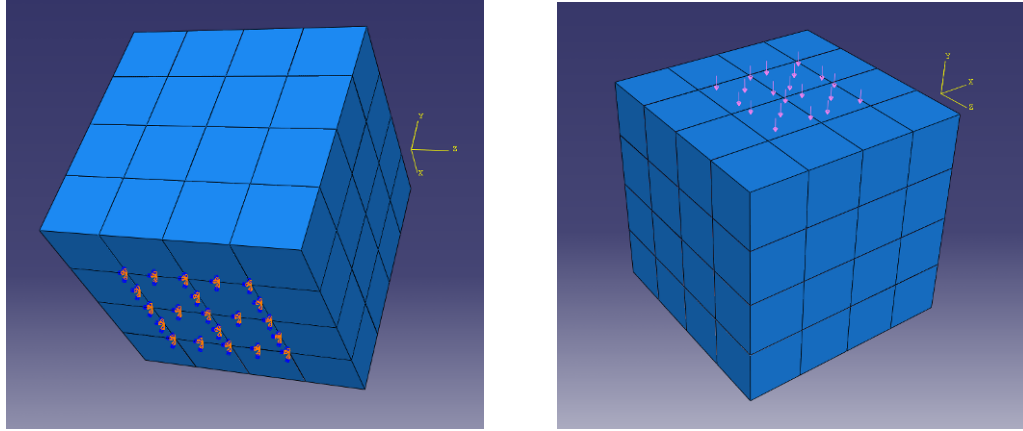


Figure 13 Left: encastre boundary condition imposed on the specified elements on the lower surface of the bottom cortical bone fragment. Right: load is applied to the top surface of the upper cortical bone fragment.

Analysis in ABAQUS, a load of 0.5 MPa is applied and linearly ramped from 0 to 1 sec. To determine the proper loading magnitude, take the case for a bone fracture that has completely healed and where the equilibrium geometry is completely infiltrated by immature bone cells. Note that the saturation of the equilibrium geometry of immature bone cells was chosen rather than cortical bone cells because for this study, no algorithm has been generated to allow for the conversion of immature bone matrix to the fully-organized, cortical bone. One-dimensional Hooke's Law is:

$$\sigma = E_4 \varepsilon \quad (\text{Equation 10})$$

where $E_4 = 1000$ MPa is Young's modulus for cell type 4, the immature bone cells. If we assume that for a healed bone, $\varepsilon = 0.0005 \ll 1$, then $\sigma = 0.5$ MPa. This loading condition is reasonable, since it represents roughly one-tenth of the physiological stresses seen in the femur of the adult human male when standing.

After applying the required stress in ABAQUS, the principal strains, fluid velocity magnitudes and nodal displacement values are appended into the *.dat file. The

MATLAB code extracts these values for evaluating the mechanical stability of the system and to determine the stimulus values for cells in an element. Thus, all cells in a single element are universally given the same stimulus value, and the probability for differentiation after experiencing that stimulus is determined by a differentiation factor, which for this study is 0.3. Besides being regulated by the differentiation factor and the stimulus value, cells can only differentiate if they meet the following two criteria: (1) if a cell must differentiate, it can only differentiate into a stiffer material and (2) differentiation can only occur if the cell meets a minimum age requirement – a cell must be at least 2 iterations old to allow for the formation of fibrous tissue, 4 iterations for cartilage, and 8 iterations for immature bone.

The idea for specifying cell-specific age requirements for differentiation is that newly formed cells need time to mature and produce the corresponding ECM before they can support the formation of other tissue types. Thus, it is postulated that with increasing levels of matrix organization, more time is needed to recruit materials and form the matrix. The age requirements described above were settled upon after performing a sensitivity analysis (results in Chapter 3).

The MATLAB code manages all of the data and initiates the execution of the ABAQUS *.inp file in an iterative loop. A high-level mechanoregulation algorithm simulates the healing process. A single iteration of the simulation represents a specific time interval, whose value is to be specified at a later time when the simulation can be calibrated with experiments. The procedure for the simulation is the following:

1. Lattice Initializations: Define the location of the original cortical bone fragments and seed cells in the lattice (MATLAB)

2. Poroelastic Analysis: Apply loading to the FEM domain and generate results in a *.dat file. (ABAQUS)
3. Data Extraction: Use octahedral shear strain and fluid velocity to calculate stimulus value in each element. (MATLAB)
4. Differentiation: Determine for each cell if the stimulus criterion is met and if it has a probability of differentiating. Execute. (MATLAB)
5. Migration: Calculate the probability of a cell moving into an adjacent lattice space as determined by the global mechanical/geometric stability of the fracture by its proximity and direction to the equilibrium geometry. Execute. (MATLAB)
6. Mitosis: Calculate the probability that a cell will divide into adjacent, open lattice spaces as determined by the global mechanical/geometric stability of the fracture by its proximity to the equilibrium geometry. Execute. (MATLAB)
7. Apoptosis: Calculate the probability that a cell will undergo programmed cell death as determined by the global mechanical/geometric stability of the fracture and by its proximity to the equilibrium geometry. Execute. (MATLAB)
8. Recalculate Material Properties: Count the number of cells and sort by type for each element in the corresponding lattice space. Regenerate the ABAQUS *.inp file. (MATLAB)
9. Check the Convergence Criterion: Determine the system stability so error quantities can be used in cell dispersal calculations and repeat the steps 2-8 (MATLAB)

Chapter 3: Simulation Results

3.1 Scope of the Studies

Some of the parameters described in Chapter 2 were a result of having gone through a rudimentary sensitivity and parameter analysis. It will be worthwhile to walk through some of these results and so, part of this chapter will be devoted to this endeavor; when showing these results however, variations in these parameters and the motivation for varying them will be explained in detail. Unless stated otherwise, all other results will be based on the parameters described in Chapter 2.

3.2 Apoptosis Proximity Scaling

Varying the proximity scaling factor in the Equation 8 strongly influences Phase II of fracture healing. Three proximity scaling modalities were studied in an attempt to reduce, what was initially observed, to be the continued growth of tissue during Phase II; this growth is contrary to the goals of bone fracture remodeling. Changing the proximity scaling does not regulate the Phase I/II threshold, which occurs at iteration 20 for all three simulations. Changing this parameter also has little effect on the time-development of tissue types; for example, osteoblasts begin to appear between iterations 28/29, 26/27 and 28/29 for each of the three variations of the proximity scaling factor.

Recall that the idea of including a proximity factor is so that the second term in Equation 8 will contribute more and more to the apoptosis probability for cells that are farther from the equilibrium geometry. When we had preliminarily used only *prox* in the mathematical model, the end result was continued tissue growth at the end of the simulation and the cell population never reached a peak (see dotted line Figure 14). From

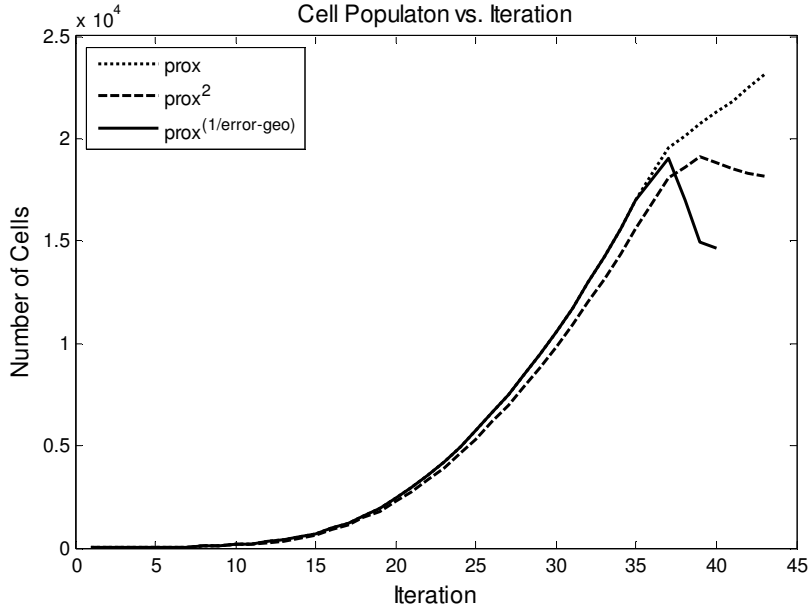


Figure 14 Cell population for the parameter study of the apoptosis proximity scaling factor.

this, it was determined that the proximity factor was not strong enough so we used $prox^2$ to scale the second term in Equation 8, hoping that augmenting the order of the proximity would strengthen its influence. The augmentation resulted in a distinguishable peak in the cell population, but a significant amount of periosteal tissue still remained at the end of the simulation (see the dashed line in Figure 14). The best variation of the proximity factor is the one that incorporates $error^{geo}$; this is represented by the solid line in Figure 14. By taking $prox$ to the inverse of $error^{geo}$, we are specifying a time-varying augmentation of the proximity which makes the proximity factor smaller and smaller as the system converges to the Phase II criterion.

From these results, the final version of the second term in Equation 8 was derived to be $prox^{4/error_{geo}}$. The constant of “4” is simply a smoothing coefficient that helps to decrease the concavity of the cell population peak by moderating the proximity scaling factor when $error^{geo}$ is still very large. Also note that these simulations were conducted under a moderate convergence criterion for $error^{geo}$ (set as 0.1), which means that after satisfying the mechanical stability convergence criterion, only 90% of the equilibrium

geometry needs to be saturated with bone before the simulation is complete. The moderately high value for $error^{geo}$ explains why the cell population is still relatively large at the end of the simulations.

3.3 Age Requirement for Differentiation

In another sensitivity analysis we considered varying the age that newly formed cells need to have before they can support the formation of more advanced tissues. Three scenarios were explored in an attempt to determine the set of parameters that best simulates tissue development in fracture healing: (1) a two iteration requirement for all cell types {2 2 2}; (2) 2 iterations old to allow for the formation of fibrous tissue, 3 iterations for cartilage, and 4 iterations for immature bone {2 3 4}; (3) 2 iterations for fibrous tissue, 4 iterations for cartilage, and 8 iterations for immature bone {2 4 8}.

Scenario 3 (solid line in Figure 15) produces a more sustained cell population peak than the other two scenarios, which show more immediate declines in cell population after reaching their peaks in cell population. Further, convergence of the

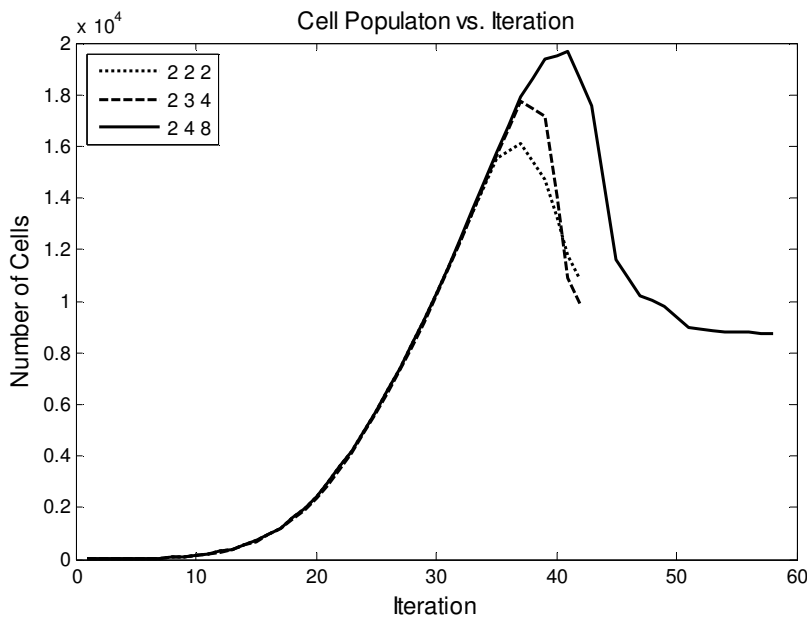


Figure 15 Cell population for the sensitivity study on the age requirements for differentiation.

system to the final cell population shows a more gradual post-peak reduction in scenario 3 when compared to the other two scenarios, which do not show this “easing effect.”

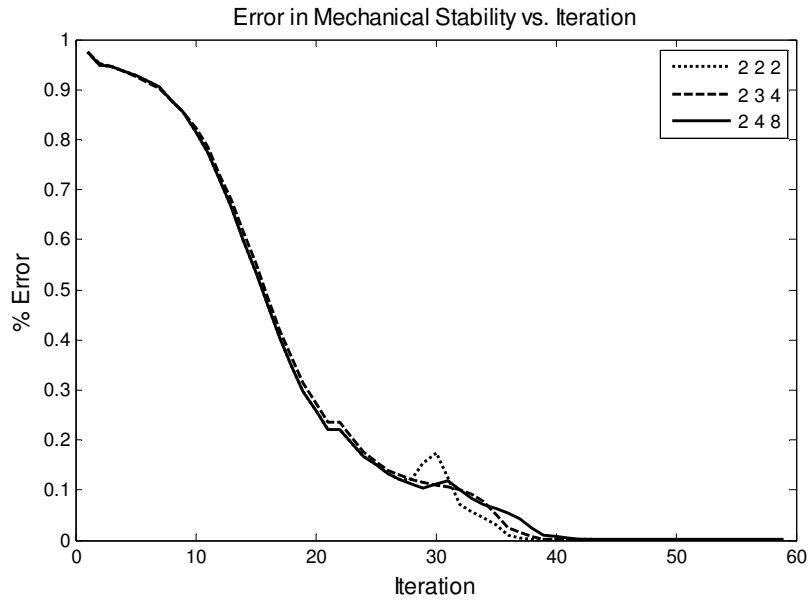


Figure 16 Error in the mechanical stability for the sensitivity study on the age requirements for differentiation.

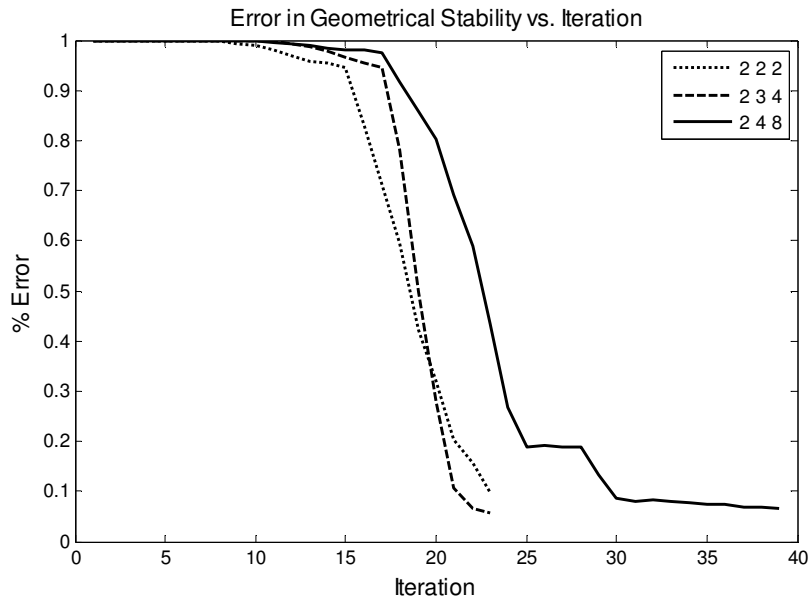


Figure 17 Error in the geometrical stability for the sensitivity study on the age requirements for differentiation.

There is not a significant effect on the trends in percentage error for the mechanical stability among the three scenarios (see Figure 16). It is believed that this is due to the fact that most of the variation among the three scenarios occur during the remodeling phase; but since the fracture site is already mechanically stable in the latter stages due to the presence of stiffer tissues (correlating to a higher Young's modulus), the increased differentiation of more compliant tissues produce less and less of an effect on the mechanical stability as the effective Young's modulus for the entire system converges towards a limit. The results for the geometrical stability show a different story. In Figure 17, we see that by implementing the age requirements in scenario 3, the system convergence is pushed out to almost 50% more iterations than in scenarios 1 and 2. As predicted, this observation makes sense since we have indirectly stunted the rate at which bone cells proliferate by imposing lengthier age requirements in scenario 3.

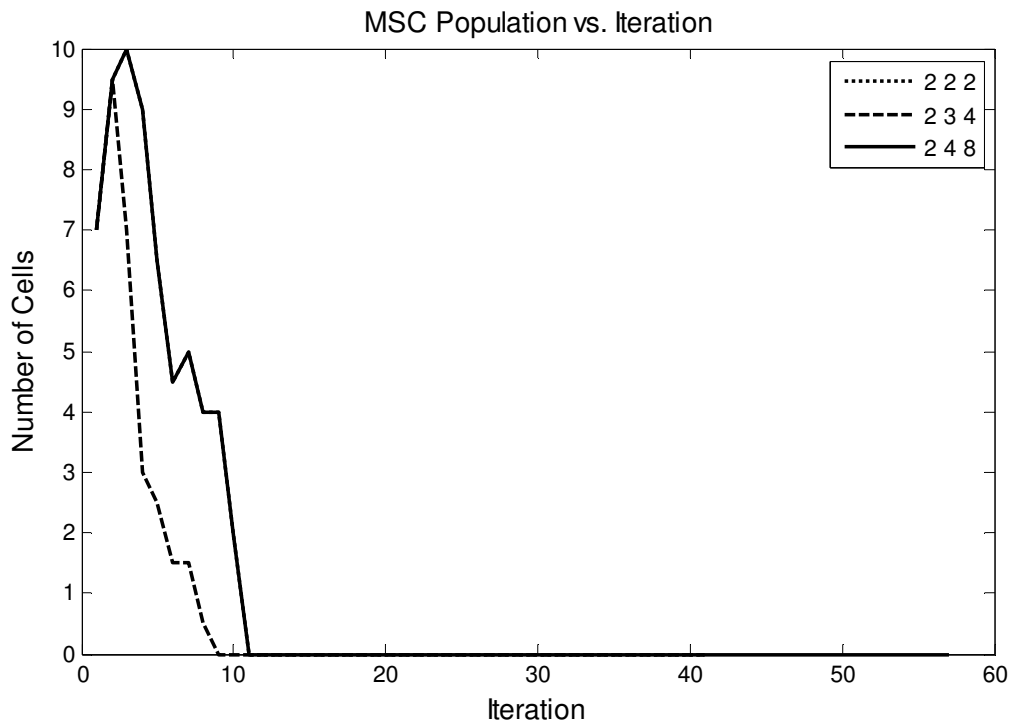


Figure 18 MSC population for the sensitivity study on the age requirements for differentiation. Scenarios 1 and 2, or {2 2 2} and {2 3 4} overlap.

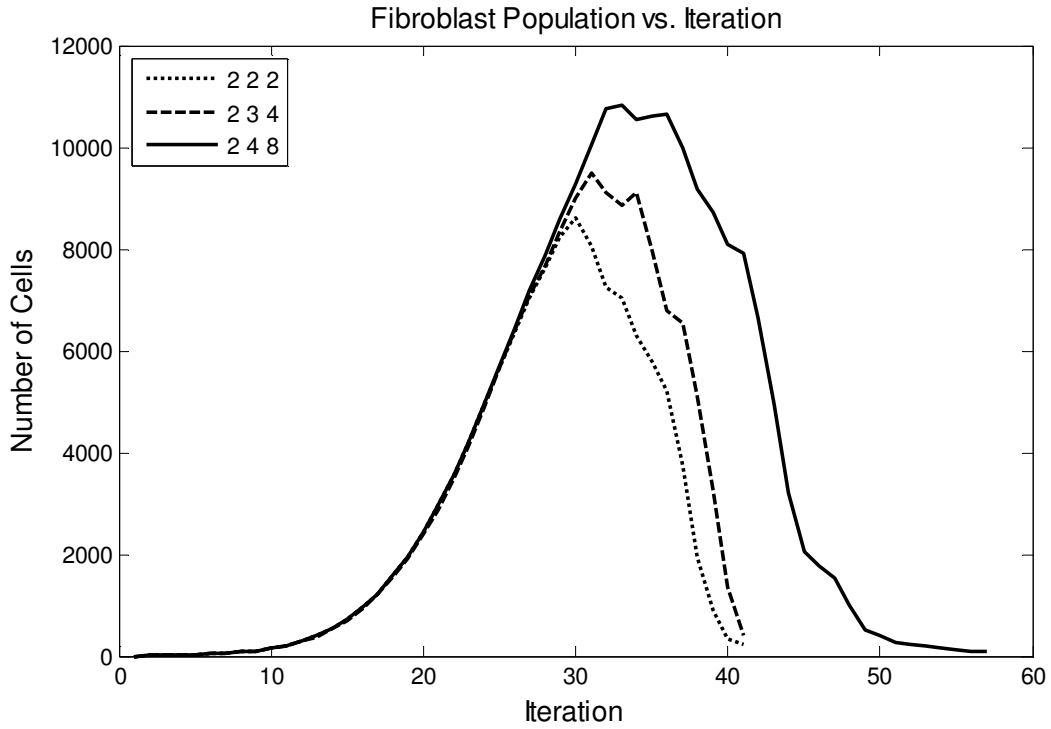


Figure 19 Fibroblast population for the sensitivity study on the age requirements for differentiation.

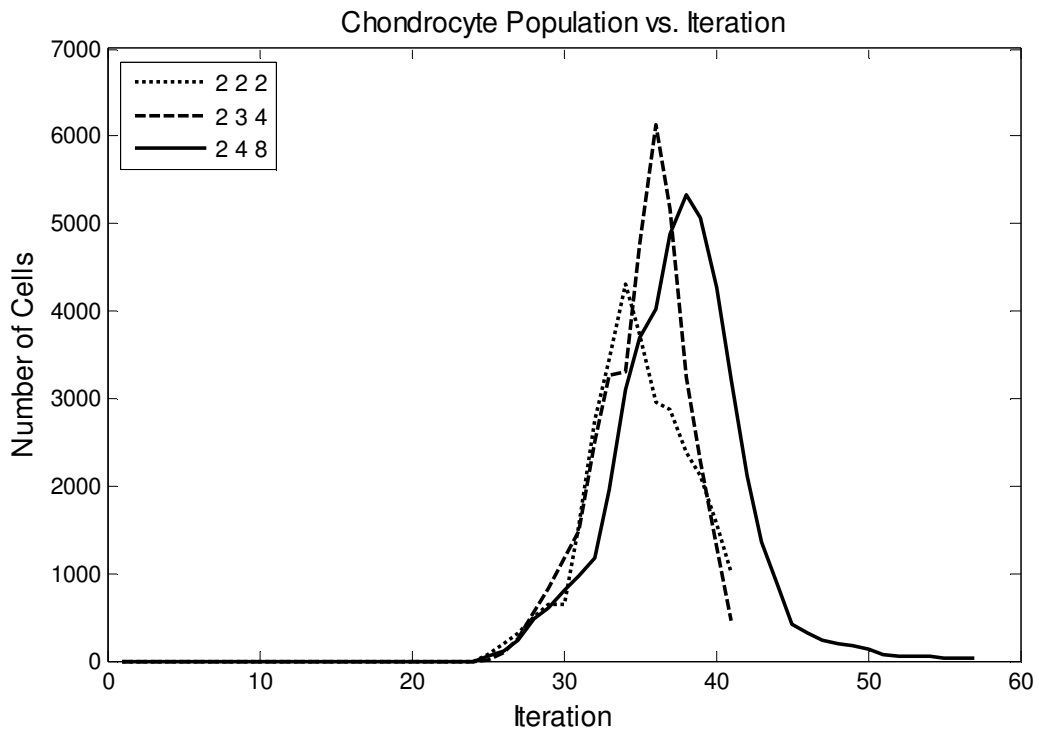


Figure 20 Chondrocyte population for the sensitivity study on the age requirements for differentiation.

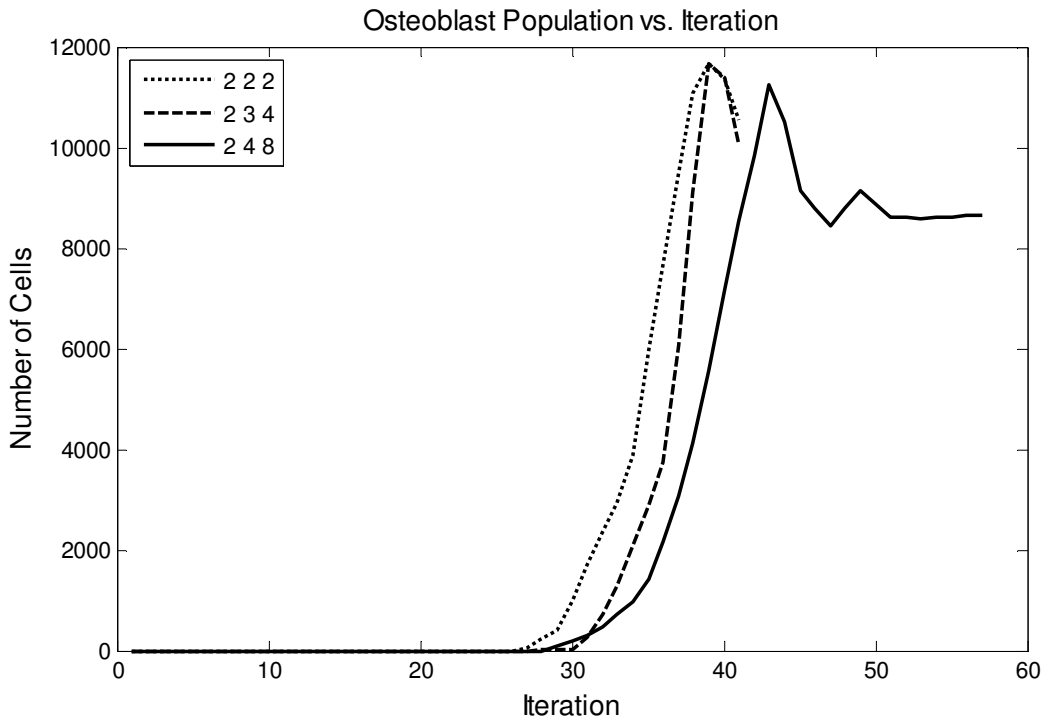


Figure 21 Osteoblast population for the sensitivity study on the age requirements for differentiation.

The trends for the tissue-specific populations throughout the simulation can lead to a number of exciting interpretations (Figures 18-21). All scenarios show immediate declines in MSC population from their starting values (see Figure 18). We are not certain if our simulation of MSC behavior is correct, for it is believed that MSCs will continue to infiltrate the fracture site throughout the course of healing. Thus, it may be worthwhile to constantly introduce a fresh batch of MSCs at specified iterations in the simulation.

At the end of fracture healing for all scenarios, there are insignificant amounts of fibrous tissue and cartilage tissue remaining at the fracture site, which is consistent with expectations (see Figures 19 and 20). With regard to bone formation, Figure 21 shows that that bone population reaches a peak before settling into a steady-state value; this phenomenon is especially vivid in scenario 3. Because there is a peak in the bone

population, it can be inferred that a small number of bone cells were formed outside of the equilibrium geometry and that these cells were eventually eliminated. It is known in skeletal biology that the process of bone removal is carried out through osteoclasts, which are bone removing cells. The results from this sensitivity study show that the mathematical models for cell dispersal can simulate the effect of specific processes (e.g. bone removal through osteoclasts) without incorporating the processes directly into the development of the code. We conclude that results from scenario 3 are ideal.

3.4 Mechanical Loading Protocols

We studied the effect of varying the static load magnitudes on cell dispersal during bone fracture healing. This sub-study is a demonstration of how we could methodically determine the optimal mechanical protocols for expediting the healing process. Loads of monotonically increasing magnitudes (0.125, 0.25, 0.375, 0.5, 0.625 MPa) were applied in uniaxial compression to the top surface of the upper bony fragment.

Cell population is directly proportional to the load magnitude (see Figure 22). Figures 23-26 show the tissue-specific cell populations. From these Figures, it can further be deduced that the fibrous tissue formation constitutes much of the increase in overall cell population. The higher rates of fibrous tissue formation for increased load magnitudes agree with preliminary experiments conducted in our lab. With increasing loads, cartilaginous tissue and bone also generally saw an increase in population – though not as significant as that seen with fibrous tissues.

An interesting phenomenon was observed for the production of osteoblasts (see Figure 26). The growth and remodeling of the bone matrix displayed behavior typical of step responses for second-order control systems with various degrees of damping.

Increasing the load magnitude for the fracture healing protocols seem to be analogous to increasing the damping ratios in a control system. The 0.125 MPa case is analogous to a critically damped system, 0.25 MPa to a slightly underdamped system, 0.5 MPa to an underdamped system, and 0.5-0.625 MPa to a very underdamped system with a large percent overshoot. It is not certain if bone remodeling actually displays this oscillatory behavior, so part of selecting the optimal protocol will also be to select one that best represents the physical processes.

The tissue-specific population trends seen in the 0.25 MPa load scenario produce optimal results. First, the population profile for osteoblasts is slightly underdamped, which agrees with intuition about bone remodeling. Second, the production of fibrous tissues (see Figure 24) is very low, almost matching the production seen in the 0.125 MPa scenario; this is good because the growth of fibrous tissue is thought to slow down the healing process. Third, the 0.25 load scenario produced unusually high volumes of cartilage relative to fibrous tissue formation (see Figures 24-25), which does not follow the general trend of cartilage population for the various load magnitudes; significant amounts of cartilage are usually thought to proceed bone formation in fracture healing.

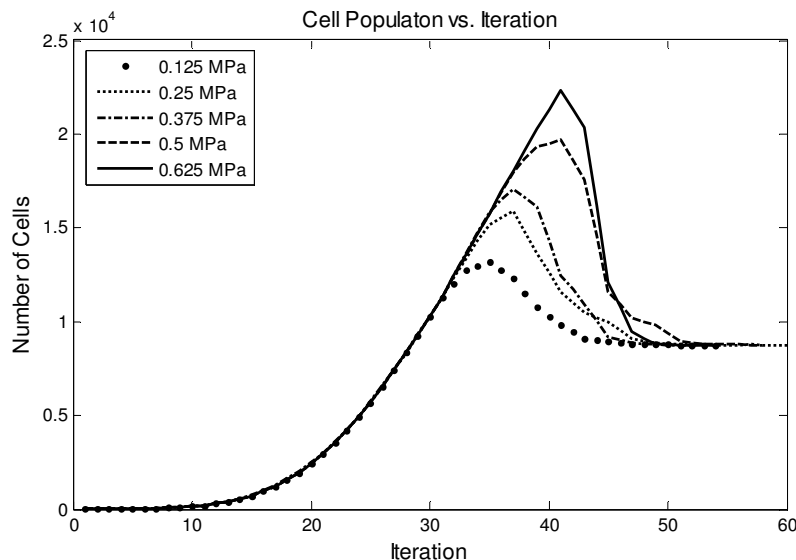


Figure 22 Cell population for the study on mechanical loading protocols.

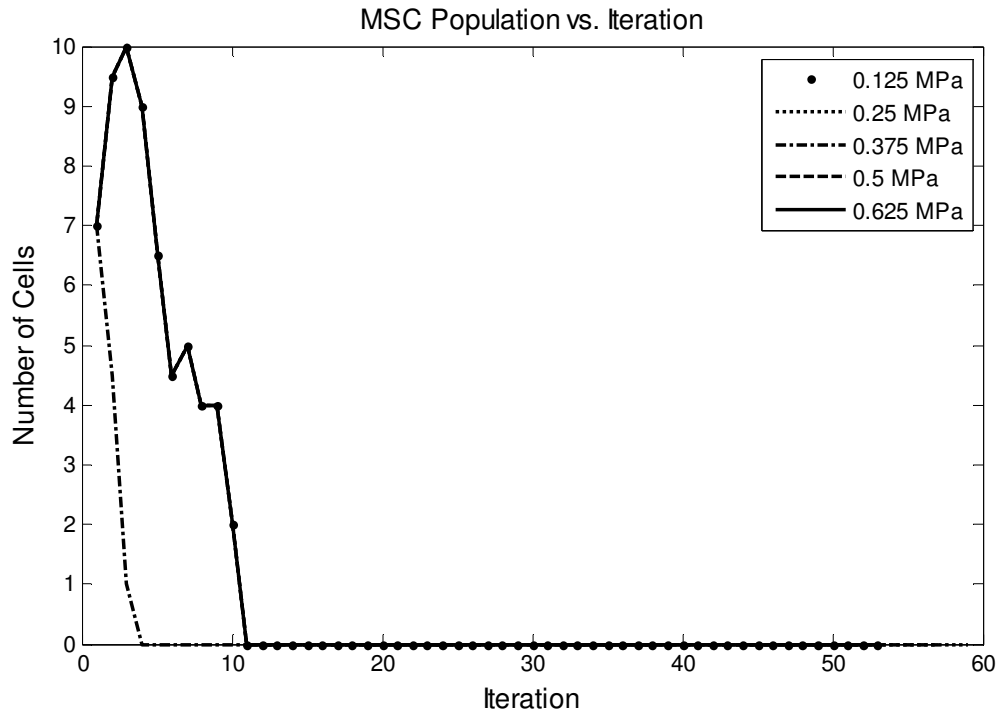


Figure 23 MSC population for the study on mechanical loading protocols. There are overlapping results.

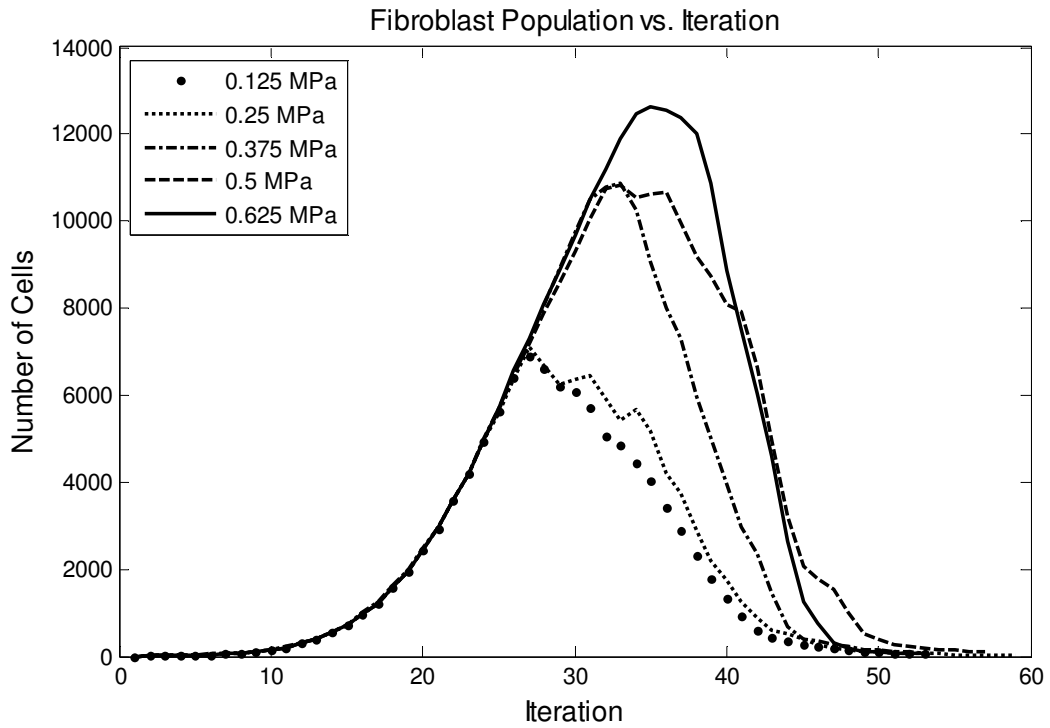


Figure 24 Fibroblast population for the study on mechanical loading protocols.

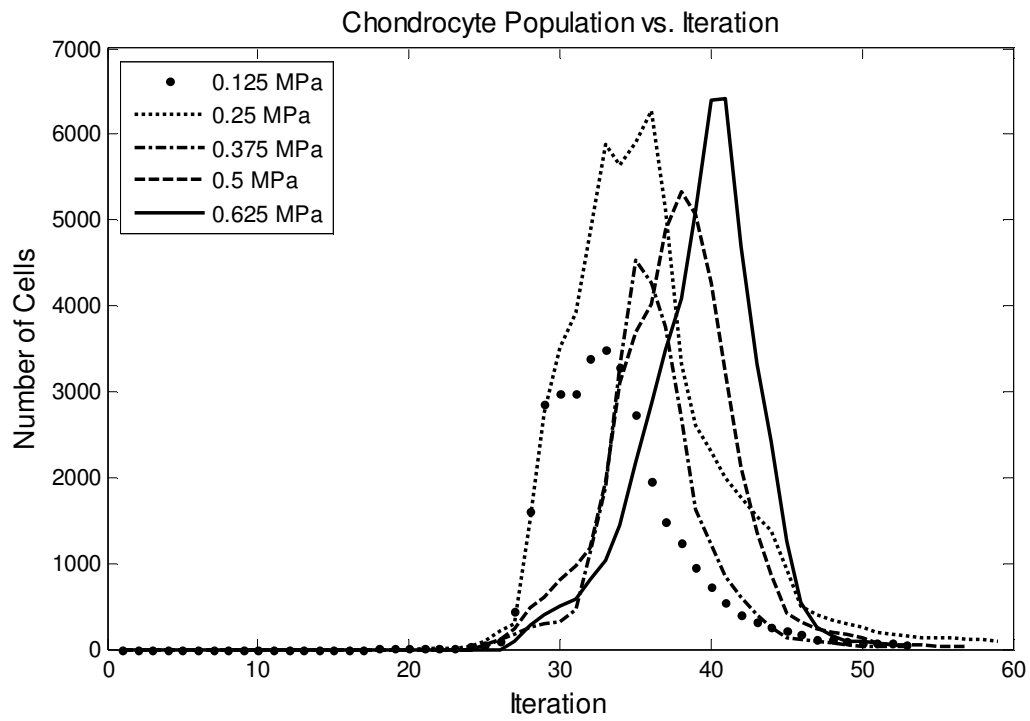


Figure 25 Cartilaginous tissue population for the study on mechanical loading protocols.

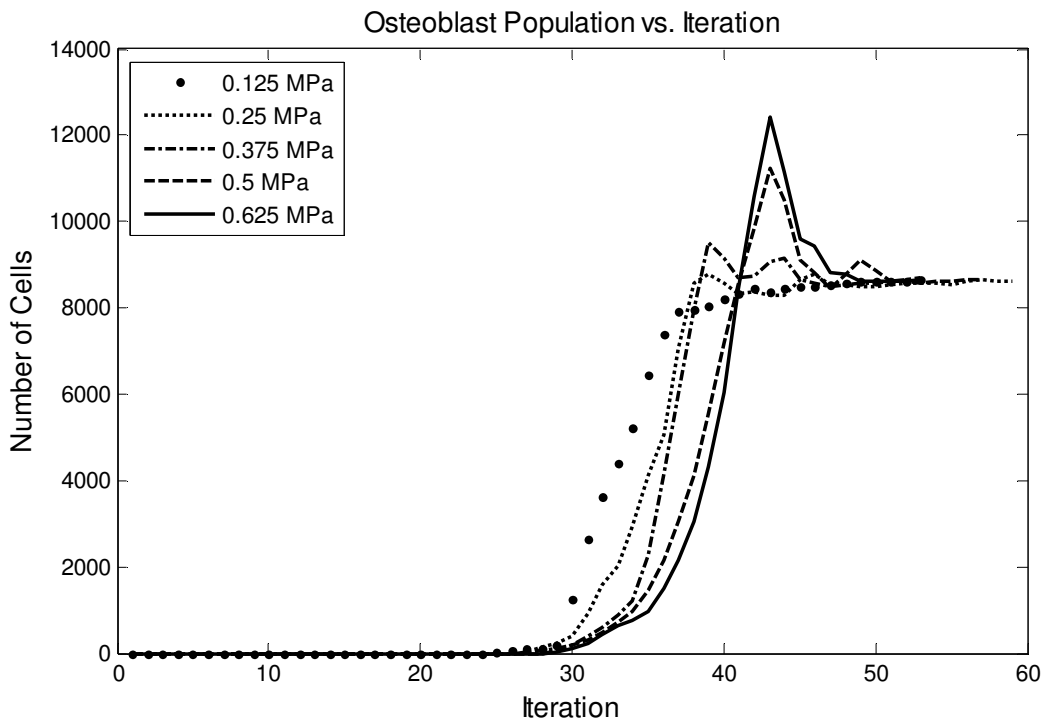


Figure 26 Bone population for the study on mechanical loading protocols.

3.5 Computational Histology

One of the advantages of using the computational platform developed in this study over existing methods is that it provides a way to see clearly, the morphology of the callus. While many of the other methods may require examining the callus morphology indirectly (by looking at tissue-specific concentrations and extrapolating the shape), our platform allows one to visualize and operate directly on the callus, in the same way a surgeon would if he could excise a section of tissue and bone at the fracture site.

In Figure 28, a series of plots at different time points is assembled, which depict the callus (red) with respect to the original bony fragments (blue). From these successive plots, it is evident that the entire course of healing is captured in the simulation. The callus begins with a relatively spherical shape and slowly envelops the fracture site. When the callus has stabilized the mechanical environment and the equilibrium geometry begins to saturate with bone cells, the callus volume decreases. What remains at the end is mostly immature bone in the equilibrium geometry.

It should be noted that the beginning stage of the healing process does not necessarily produce a callus of such “perfect” spherical shape as we see in Figure 28. There is most certainly tissue proliferating directly from the surfaces of the bone fragments and from the periosteum as well. This is very easy to produce in our simulations and would simply require seeding cells directly at the bony surfaces (as opposed to only placing seven seeds at the origin and its surrounding lattice spaces). The effect of seeding cells in such a manner would result in a callus that spans the entire interfragmentary gap instead of originating from the middle.

A close examination of the three-dimensional plots (and of the raw data) makes it clear that the callus size exceeds the finite element domain. Recall that the finite element mesh is $4 \times 4 \times 4$ elements and that the cell dispersal lattice is 10 times finer than the mesh, which means that if $(0,0,0)$ is the origin, then the lattice can only intersect the mesh in the range of $[-20:20, -20:20, -20:20]$. In this simulation, the larger callus is not a major concern because the cells that do exceed the boundary are not very far from the domain. The cells that are outside of the boundary simply do not contribute significantly, to providing mechanical stability to the system nor do they differentiate (since no stimulus value can be calculated for the cells); they do however, follow all the cell dispersal rules. In any case, these results show that a thorough boundary study must be conducted for each specific set of simulations.

Mid-femur sections (thin slices of tissue) were taken in the coronal and sagittal planes (see Figure 27; Appendix A). The tissue-specific cells were stained in different colors. Examining these tissue distributions reveals a couple of interesting findings. First, as we hypothesized, the axisymmetric assumption that many studies have been accustomed to taking is not valid. Tissue distributions (especially those occupying the equilibrium geometry) are not symmetrical. Thus, three-dimensional models for bone fracture healing would provide a more accurate picture of the process.

Second, based on an examination of the tissue distributions at the equilibrium geometry, it is apparent that the cell populations differentiate in groups based on the coarse discretization of the finite element mesh. This isn't true in regions outside of the equilibrium geometry where differentiation patterns seem more random. In fact, large square-like regions of similar tissue types (with only small amounts of other tissue types

infiltrating those regions) clearly outline how the mesh was constructed. This type of behavior was not expected.

Although all cells within the same finite element experience the same stimulus level, the differentiation rate for the cells is 0.3, which means that even if cells experience the magnitudes of stimulus needed to differentiate, only 30% at best, would differentiate. Along with the rate of differentiation, there is an age-criterion for newly formed cells that decreases the probability of differentiating, as described in section 3.1. It is believed that two modifications to the simulation design will help to alleviate this problem: (1) include the rule of mixtures into the calculation of current material properties (i.e. the average of the material properties over previous iterations) so that the properties of an element do not change drastically from one iteration to the next and (2) use a finer mesh discretization for the finite element domain.

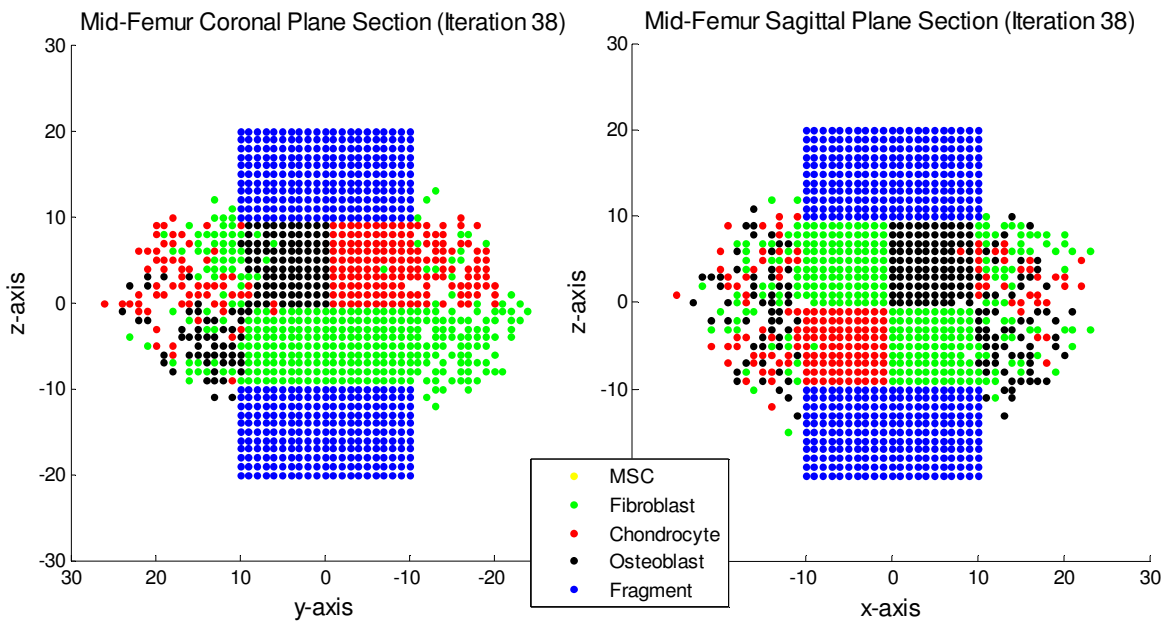


Figure 27 Mid-femur sections showing cell types in produced at iteration 38.

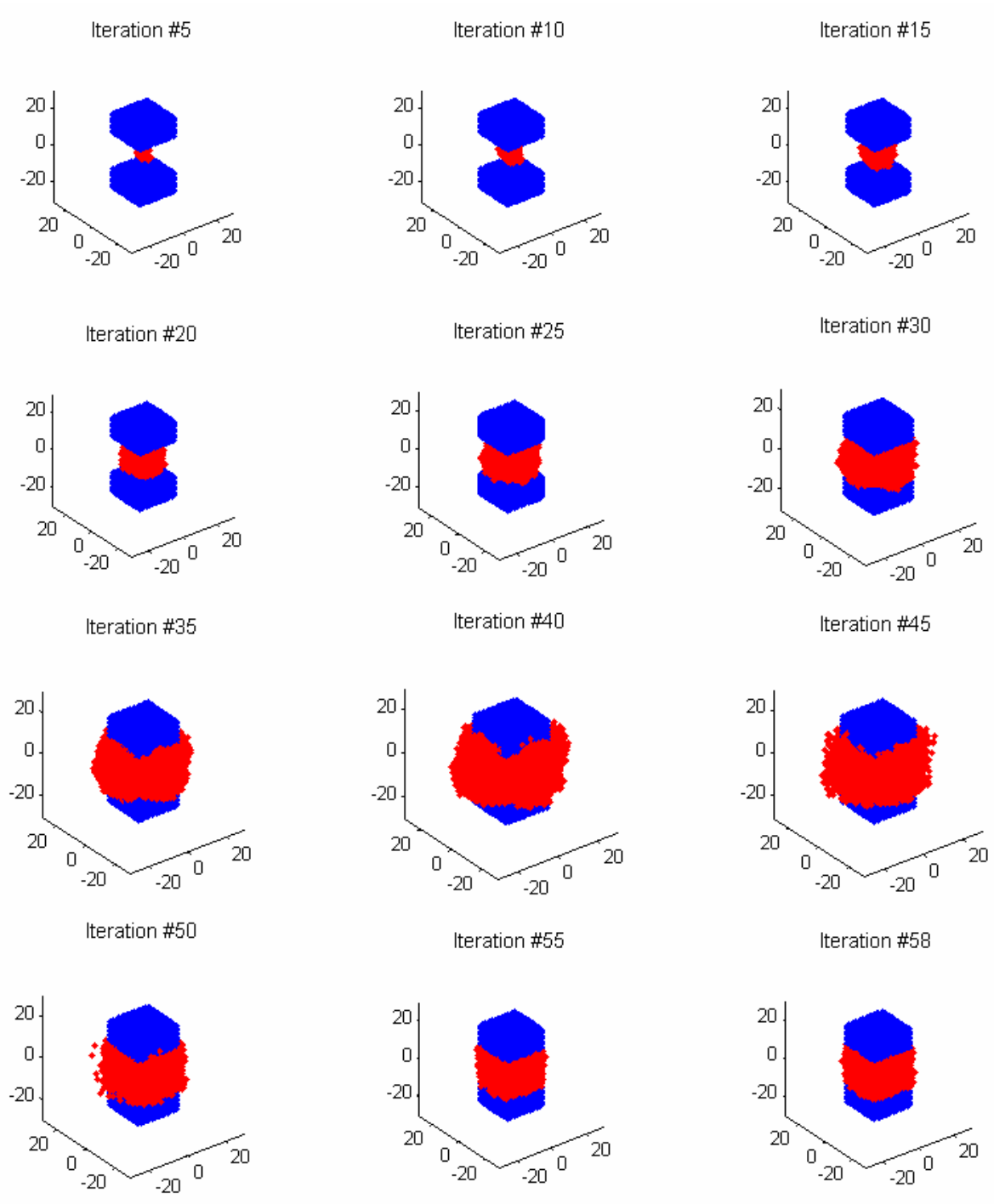


Figure 28 3D visualization of the formation of callus (red) between the original bony fragments (blue)

3.6 Statistical Analysis

The goal is to perform a descriptive statistical analysis to show that simulations behave in a probabilistic manner. Results are collected for $n=7$ runs of a simulation. The average time to completion is 60.43 iterations with a standard deviation of 2.23 iterations. The Phase I/II threshold occurs at 20.14 ± 0.38 iterations. Figure 29 shows the mean cell population for each iteration with error bars for one standard deviation.

The largest variations generally occur with increasing average cell populations (see Figure 30). There is a time lag however, between the average peak in cell population and iterations where the largest variations occur. Computationally, the time lag is believed to be an artifact of the remodeling algorithm as it attempts to deal with higher cell populations by increasing the apoptosis probabilities; it is not certain if such a pattern exists physiologically. However, the more cells that are present in the fracture callus, the less available nutrients become, potentially leading to a higher rate of apoptosis. Such biological phenomena would require some lag time to take effect.

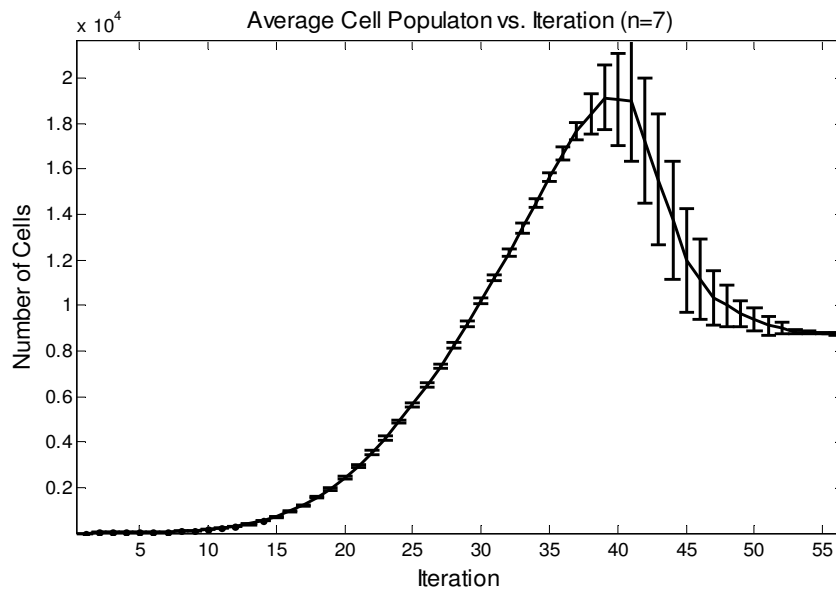


Figure 29 Average cell population to show probabilistic behavior of the simulations

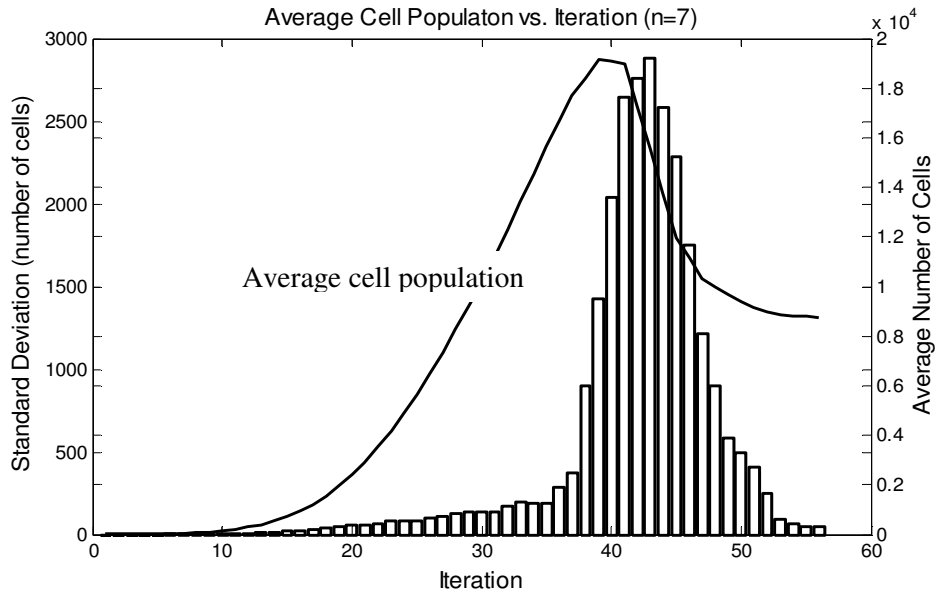


Figure 30 Same information as in Figure 29, but the average population and standard deviations are overlaid to emphasize the peak offset between the population and the variance.

Chapter 4: Conclusion

4.1 Summary of Results and Future Work

The Equilibrium Geometry Theory (EGT) for bone fracture healing was used in conjunction with a biphasic mechanoregulation rule for tissue differentiation and applied to a random walk model, whose 3D lattice exists in an adaptive finite element framework. This theory arose from the neglect of previous studies to directly take into consideration, the geometric form of a fracture callus when modeling the transient changes in the callus morphology. The unique platform from which the simulation was developed (i.e. random walk dispersal lattice in an adaptive finite element domain) provides a novel way to address other problems with current modeling techniques. In particular, the ability to control cell processes is an advantage to using the platform. Note that in this thesis, two cell processes were not considered: (1) the maturation of immature bone cells into fully-organized cortical bone and (2) the necrosis of cells due to over/under-stimulation by mechanical stress; these cells processes are important considerations in the biological development and response of tissues and they will be incorporated in future work.

It was demonstrated that using the random walk model resulted in non-deterministic solutions. This means that the probabilistic behavior of biological tissues is successfully mirrored when using the platform developed in this study. Besides having the ability to perform more complex statistical analysis (e.g. the Monte Carlo method, multi-factor ANOVA for developing an optimal protocol, etc.), the results highlight an important point that is often overlooked in current studies – it is worth investing time into developing 3D models as opposed to using the axisymmetric assumption. Not only are

bone fractures inaccurately represented as being axisymmetric in most other studies, but our results indicate that tissue distributions are irregularly dispersed throughout the callus, which may result in asymmetric load-bearing capacity at the fracture site.

Although an extremely coarse lattice and mesh were used in the study, we believe that trends in tissue formation are generally consistent with histological observations. One minor discrepancy however, is observed in the simulation results and does not jive with expectations – for most loading conditions, we saw the lack of significant populations of cartilaginous tissue development prior to the appearance of bone. Modifications to the MATLAB program are currently being made, but it is believed that this discrepancy is a result of the instantaneous changes in the material properties of the finite elements within a single iteration. These drastic changes do not occur in real biological systems and other studies have proposed using the rule of mixtures for an average of the material properties over previous iterations of the simulation. Once a smoothing of the transient changes in material properties is implemented, the development of a small population of cartilage will not immediately stiffen the tissue enough to result in the – almost immediate – formation of bone, thus allowing a greater fraction of cartilage to develop in the callus. The rule of mixtures may also help to solve problems regarding groupwise differentiation patterns based on the mesh discretization.

The convergence criteria in this study have provided a great deal of flexibility in controlling cell dispersal. Convergence criterion 1, which concerns mechanical stability of the fracture site, is seen as being a very effective tool for monitoring the progress of fracture healing for the first phase of the simulation. In the future, it will be desirable to impose a wide variety of loading configurations, which may require using a different kinetic or kinematic quantity for determining mechanical stability of the system, such as

angular displacement or energy dissipation. The platform that has been developed easily allows for exploring this area of study.

Convergence criterion 2 has consistently been a challenging aspect of the simulation to refine. Simulating the remodeling process is difficult, which involves developing a realistic algorithm to address the innate desire for bone to maintain an efficient geometric form. We know that a fracture in a bone, when completely healed, resembles the configuration of the original, pre-fractured bone (again, this is a fundamental basis behind the EGT). Applying this idea to Phase II in the simulation proves to be rather difficult. Nevertheless, we have shown through 3D plots that through the use of the proximity calculation, it is possible to create a stronger impetus for cells to coalesce and thrive in the region containing and surrounding the equilibrium geometry, which is important during the latter stages in the healing process. Regardless of whether or not we decide to exploit the proximity calculation further, it will be worth the effort to find better mathematical models to represent cell processes in future studies.

An end application is for this simulation platform to be used to help with patient-specific treatments for bone fractures. We ultimately seek to answer the question: given a patient's unique physiology and fracture characteristics, what mechanical protocols can be best implemented to expedite the healing process? To accomplish this task, the ability to support the analysis of more complex fracture geometries is needed. The platform from which this simulation is based on easily accommodates for this requirement. By using advanced imaging techniques, one can employ grey-scale thresholding to reconstruct 2D layers of images for a 3D finite element model. The multi-part domain from which the finite element framework is built upon provides easy correlation between individual pixels in an image and the material property definitions for finite volumes for

the mesh. Without belaboring the point further, it is worth mentioning one final time that the results from this thesis were based on an extremely coarse mesh and lattice and that more realistic results can be obtained by using a finer discretization. To do this, there is need to create an algorithm for the independent and external generation of an ABAQUS *.inp file, with the ability to take input for specifying the mesh details.

Qualitatively, the transient morphology of the fracture callus is consistent with experimental studies. Using a finer mesh, we will be able to provide improved correlations with experiments since cells in the simulation will experience more localized strains and fluid behavior as opposed to experiencing a more regional, larger-scale phenomenon. Currently, animal experiments are being conducted in our lab, and it is with hope that we will be able to calibrate our simulation platform with the experiments. Specifically, we will need to develop techniques that will provide a quantitative assessment of the callus and the distribution of its various tissue types; this is easily done in the simulations but more difficult in the animal models.

A full parameter and sensitivity study still needs to be conducted to assess the dynamics of the computational platform. The preliminary analysis that we have conducted so far (for proximity scaling in the apoptosis probabilities and for differentiation age requirements) show the immense latitude we have in modeling bone fracture healing. As a whole, the EGT is seen as a compliment to mechnoregulation models for differentiation and it addresses the much needed issue of callus geometry as being a significant factor in stabilizing the fracture site during healing. The platform that was developed in this thesis is designed to accommodate simulations for varying levels of complexity and its fully-automated protocols and self-maintaining, data manipulation algorithms make it an attractive platform for continued study.

4.2 Philosophical Implications of the EGT

Despite the EGT's ability to accurately predict the callus morphology in fracture healing, the theory is for the most part, phenomenological, capturing what has been observed in nature. Using the computational platform as a means to carry out the EGT however, we see that there is a clear yearning to move toward a mechanistic approach; for example, great care was taken to simulate various cellular processes. Even so, other details were ignored. Where are the osteoclasts? The macrophages and inflammatory cytokines? Why wasn't the vascular system nor the immune responses directly modeled? It is with hope that the gross behaviors of the various phenomena are captured in the mathematical models developed for migration, mitosis and apoptosis.

When explaining the EGT to my piano teacher several weeks ago, she asked me if it was even scientific. I responded by telling her that the science is definitely there in the computational platform, but buried under layer upon layer of algorithms lies the philosophy of the EGT. As such, the EGT is a unifying idea that ties together individual cell processes and like all philosophy, it tells us, 'why'. Science only tells us, 'how' and so without philosophy, science is meaningless.

Let's take a step further. Recall that according to the EGT, by means of changes in the cell processes at a fracture site (as influenced by its surrounding environment and through the appropriate mechanical stimuli), a unique equilibrium state is obtained when the bone is completely healed. Through the computational platform, we have seen the aforementioned cell processes modeled in a way that results in cells coalescing and thriving in the region containing and surrounding the equilibrium geometry. Is this 'flocking' phenomenon also not observed in most higher order systems? Do ants in a

colony not migrate together in order to achieve a unified goal? Does a zebra not stand a greater chance of survival when in close proximity to its herd? Here, I've provided support for the EGT by demonstrating its tendencies and nuances in other natural systems, but the development of the theory has even deeper roots.

My advisor once referred to the EGT as the creationist theory. I told him that his conclusion was only an interpretation. Perhaps he drew his idea from the fact that with the EGT, we predefine an equilibrium state, a desired end condition. Certainly, I had no intention for the EGT to be interpreted as support for creationism. Nonetheless, hearing him mention this idea left me surprised. Was my advisor able to unravel all of the 'secrets' hidden within the EGT without even knowing at that particular time, all of the gritty details? I am not certain if he still holds his interpretation but without embarrassment, I testify that the EGT and its computational platform as having been inspired by general Christian philosophy. I emphasize however, that the EGT is not Christian philosophy, only inspired by it. Moreover, the EGT does not necessarily derive from a creationist perspective, but can come from general observations about the highly regenerative nature of bone, as many authors have elegantly described.

Without delay, I march forth with explaining the EGT in the context of Christianity. The fracture site represents the world, broken and in pain. The equilibrium geometry is the world, as God intended it to be and represents a state of grace. But in this broken world, "We all, like sheep, have gone astray, each of us has turned to his own way" (Isaiah 53:6). And so, like people who are wandering in spirit, the cells at the fracture site also wander, which is modeled as the probability of isotropic migration.

There is however, an innate desire in all people to seek grace. Acts 17:26-27 states, "From one man he made every nation of men, that they should inhabit the whole

earth; and he determined the times set for them and the exact places where they should live. God did this so that men would seek him and perhaps reach out for him and find him, though he is not far from each one of us.” To continue with the analogy, cells (which again, represent people) near the fracture site also have a drive to migrate toward the equilibrium geometry, which is modeled as the probability of anisotropic migration.

James 1:13-15 says, “When tempted, no one should say, ‘God is tempting me.’ For God cannot be tempted by evil, nor does he tempt anyone; but each one is tempted when, by his own evil desire, he is dragged away and enticed. Then, after desire has conceived, it gives birth to sin; and sin, when it is full-grown, gives birth to death.”

Now recall that according to the EGT, cells wandering far from the equilibrium geometry will have a greater potential of moving even farther (“dragged away and enticed”) when compared to cells closer to the equilibrium geometry. Further, through the proximity scaling in the apoptosis probability, a cell that is farther from the equilibrium geometry has a greater chance of undergoing apoptosis (“evil desire . . . gives birth to death”).

For cells that are able to make it into the equilibrium geometry, they cannot die since the mathematical model for apoptosis prevents death from occurring for these cells. In the same way, all men who have come into grace – who have accepted Jesus as their Lord and Savior – are granted everlasting life. Ephesians 1:13-14 says, “And you also were included in Christ when you heard the word of truth, the gospel of your salvation. Having believed, you were marked in him with a seal, the promised Holy Spirit, who is a deposit guaranteeing our inheritance until the redemption of those who are God's possession – to the praise of his glory.”

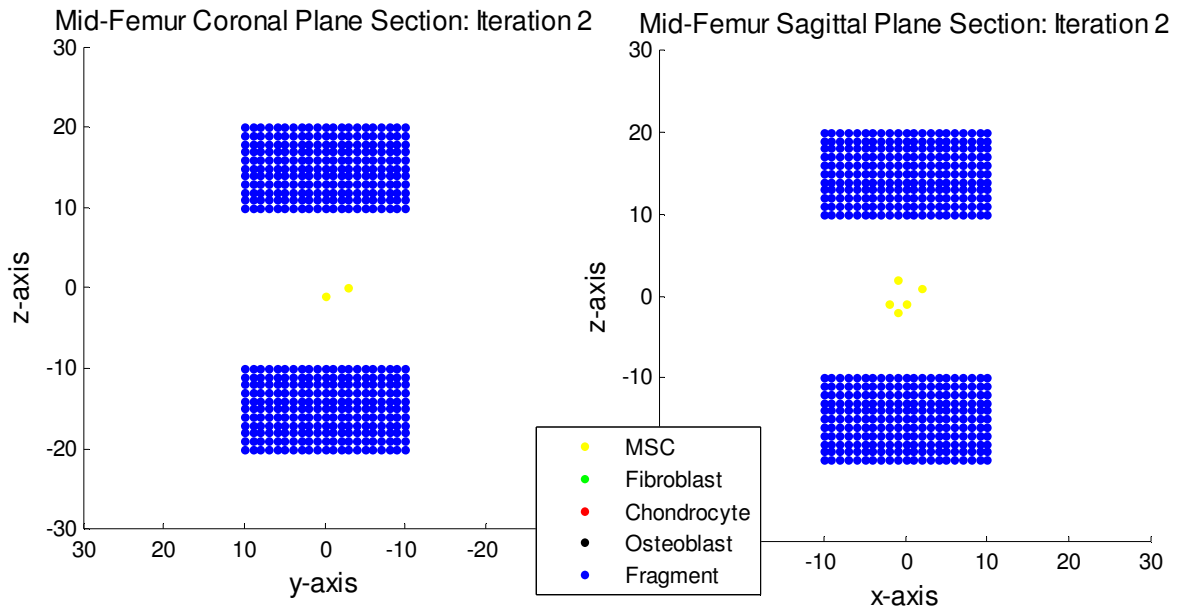
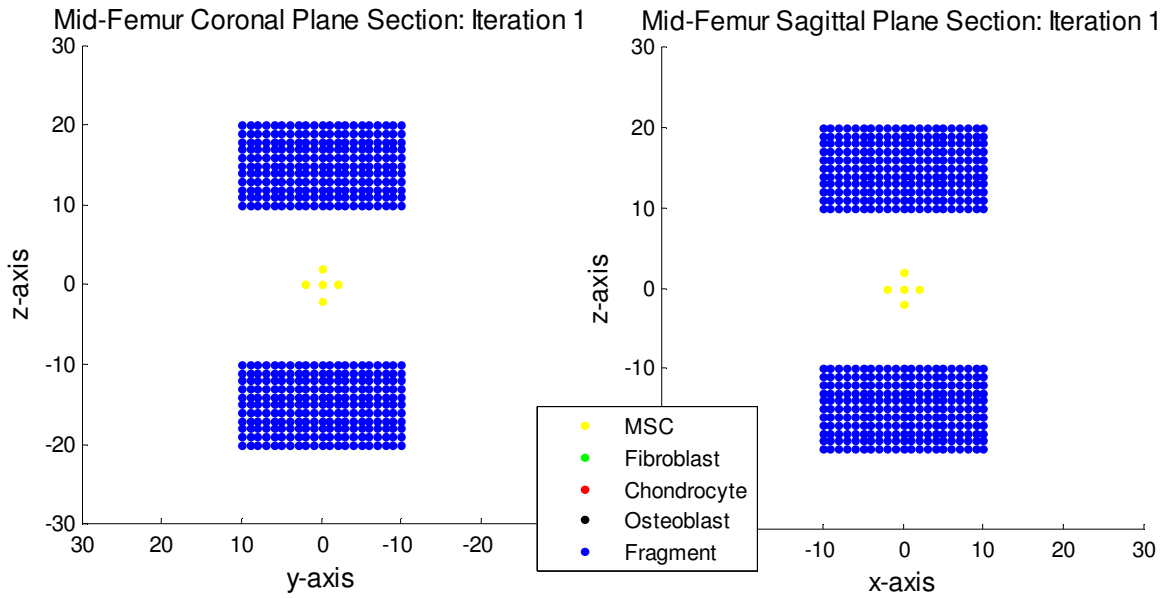
When the world, as we know it, comes to an end there will be a new earth. “But in keeping with his promise we are looking forward to a new heaven and a new earth, the

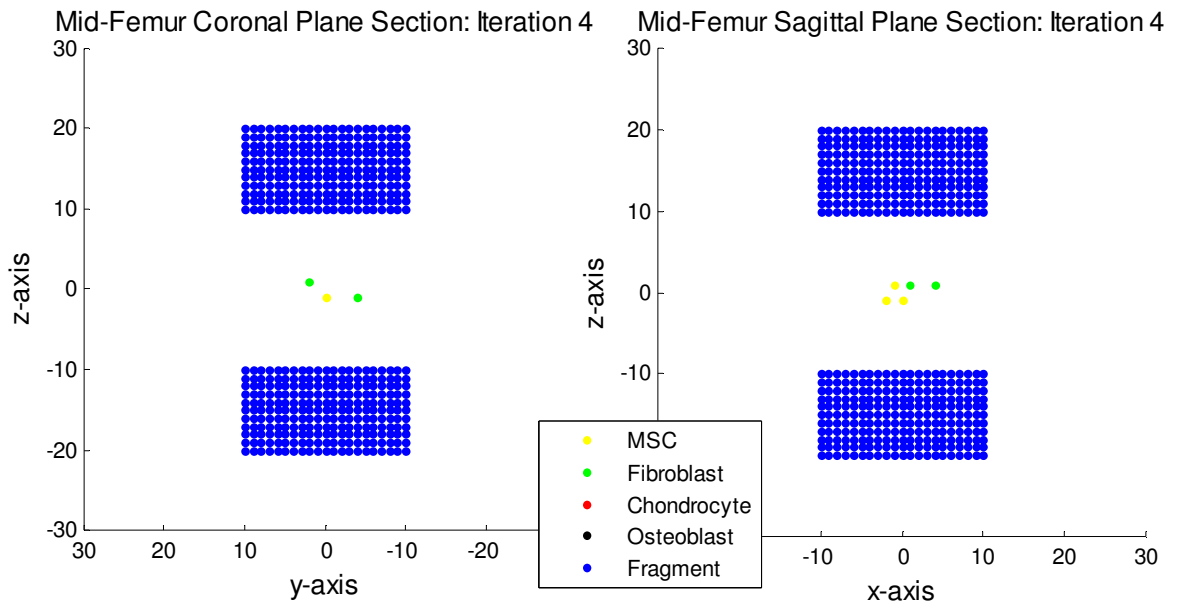
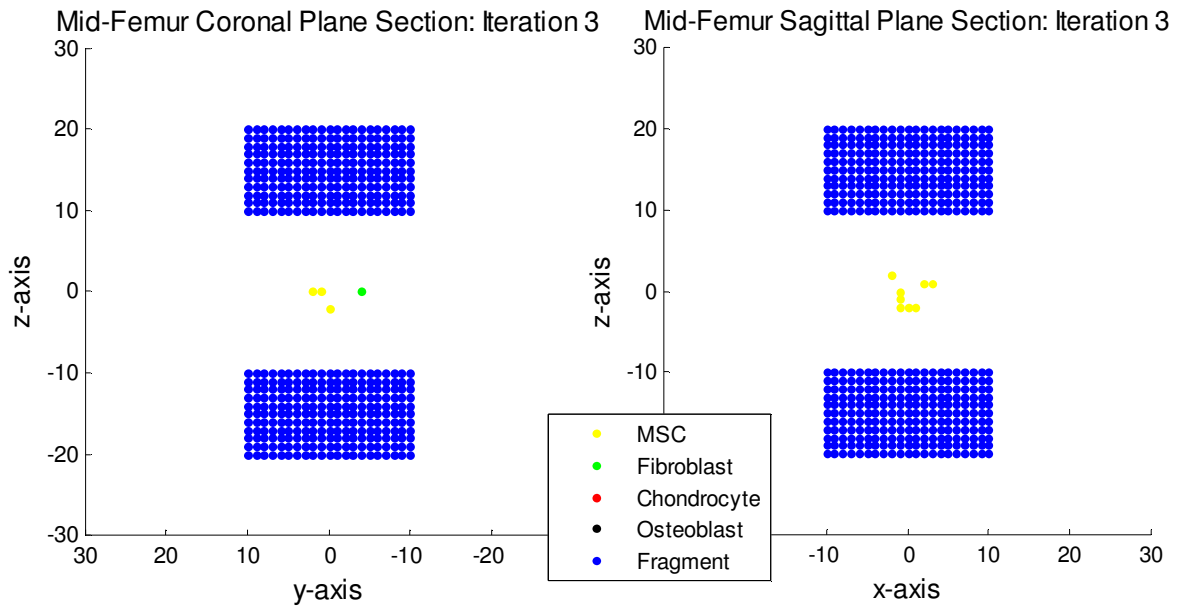
home of righteousness.” From 2 Peter 3:13 it is clear that all that only a remnant, those who have come into grace, will inhabit the new earth. This is analogous to cells in the equilibrium geometry at the end of the simulation. These cells will be all that that is left at the bone fracture site.

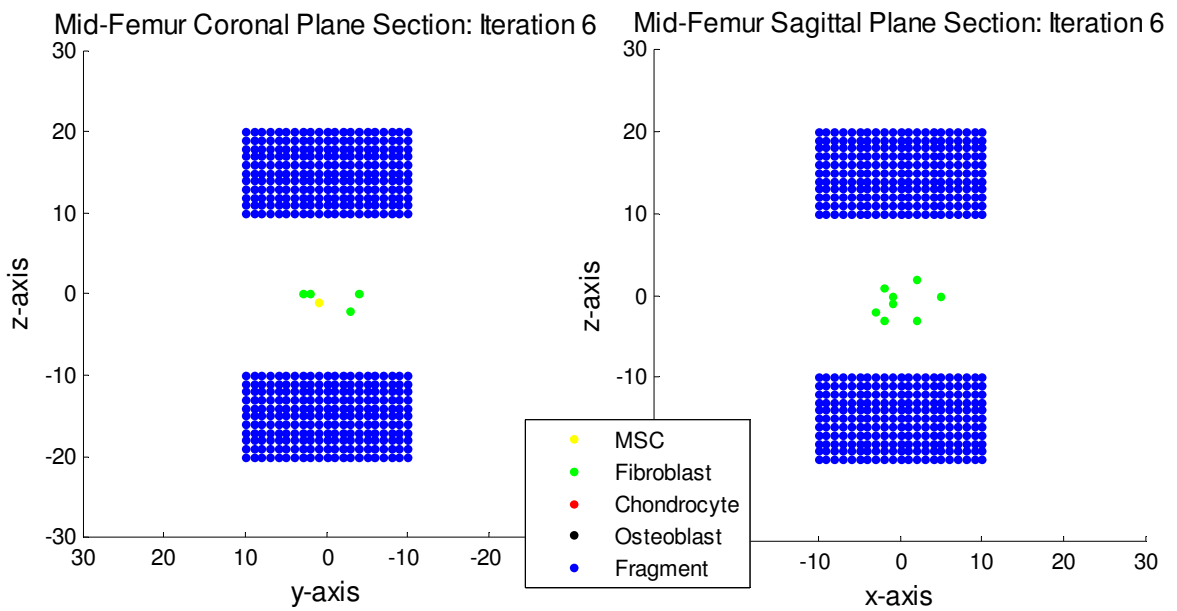
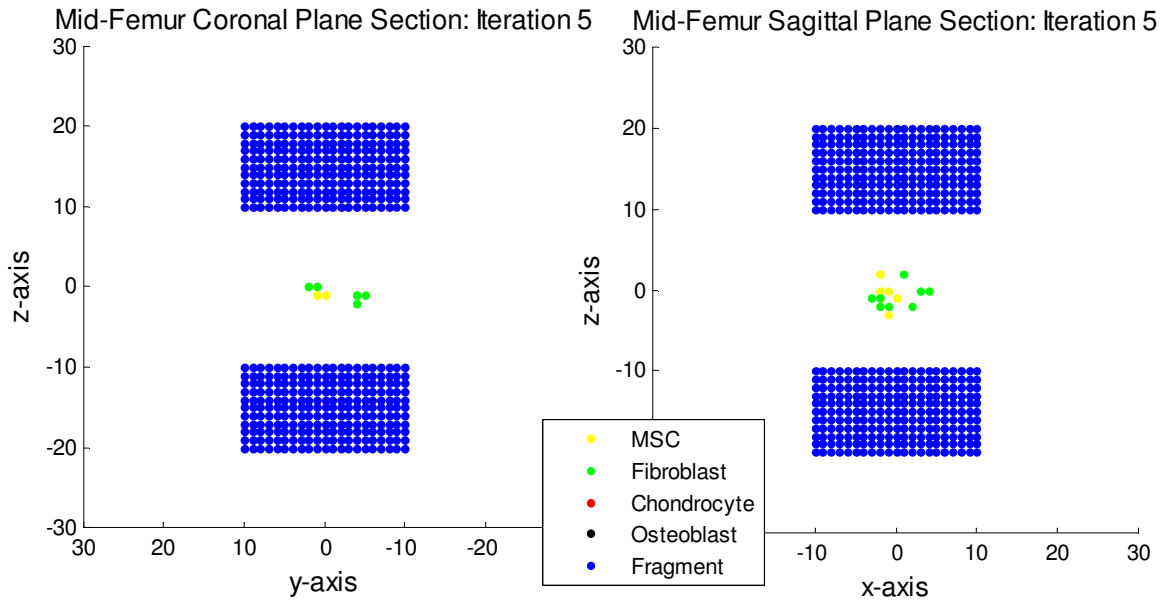
In these few paragraphs, the EGT has been described in parallel with Christian philosophies. In no way was there an attempt to misplace Christian scriptures; rather, there was an attempt to show in as much brevity as possible, the origins of the EGT and the computational platform developed to support the theory. Having said this, an important question must be asked. Do the origins of a scientific theory matter? Is it important for science to give birth to science or can theology give birth to science? I believe that the origin of any scientific theory is irrelevant as long as it is practical and only if the theory does not violate any of the laws of nature.

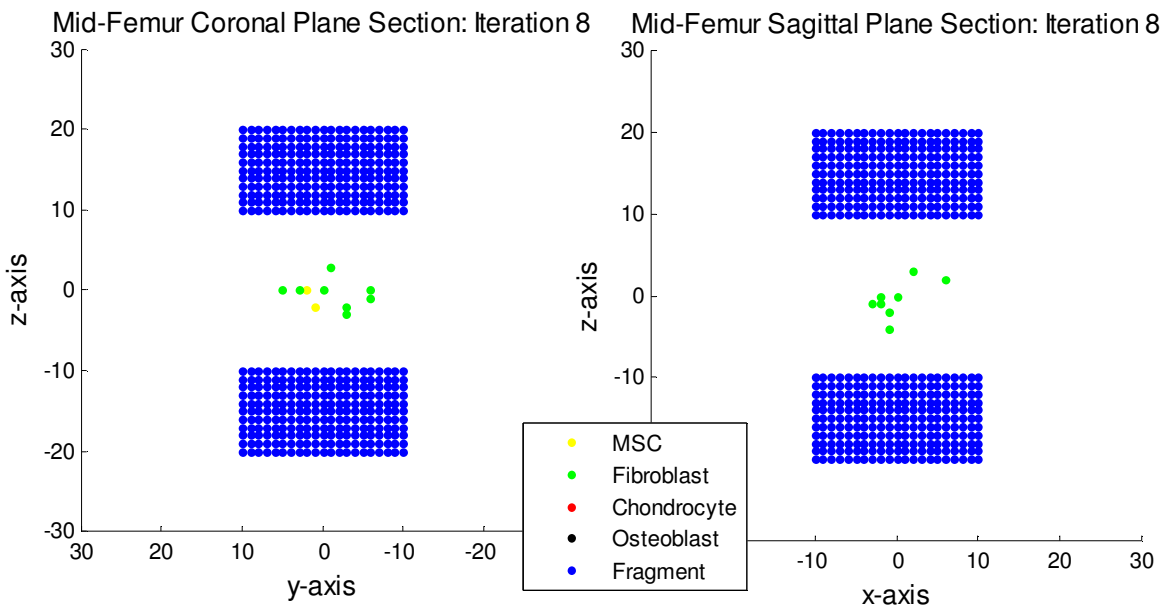
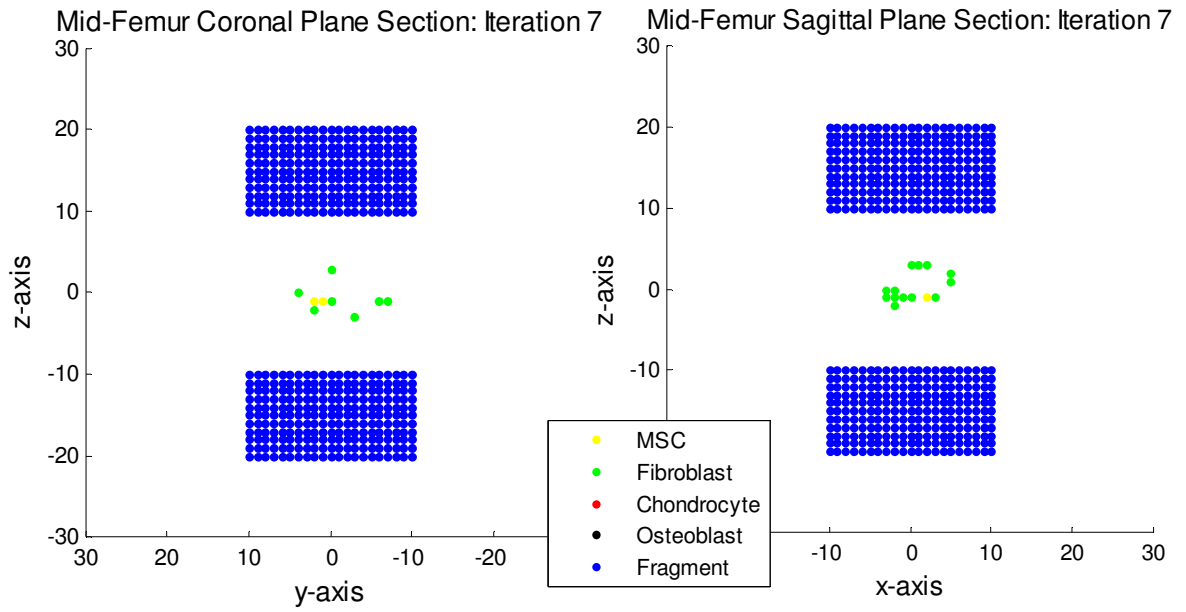
In engineering, many scholars who attempt to derive a mathematical model to describe a scientific phenomenon do so from basic principles. Others have derived their models from empirical data, of which some are later verified through basic principles. Still, there are some who develop a model on the basis of logic, an idea, or by intuition and whose ideas can also be verified from basic principles. The EGT is a theory of the third type. So, the next step in justifying the theory will be to confirm it with the laws of thermodynamics and to compare it with experimental studies.

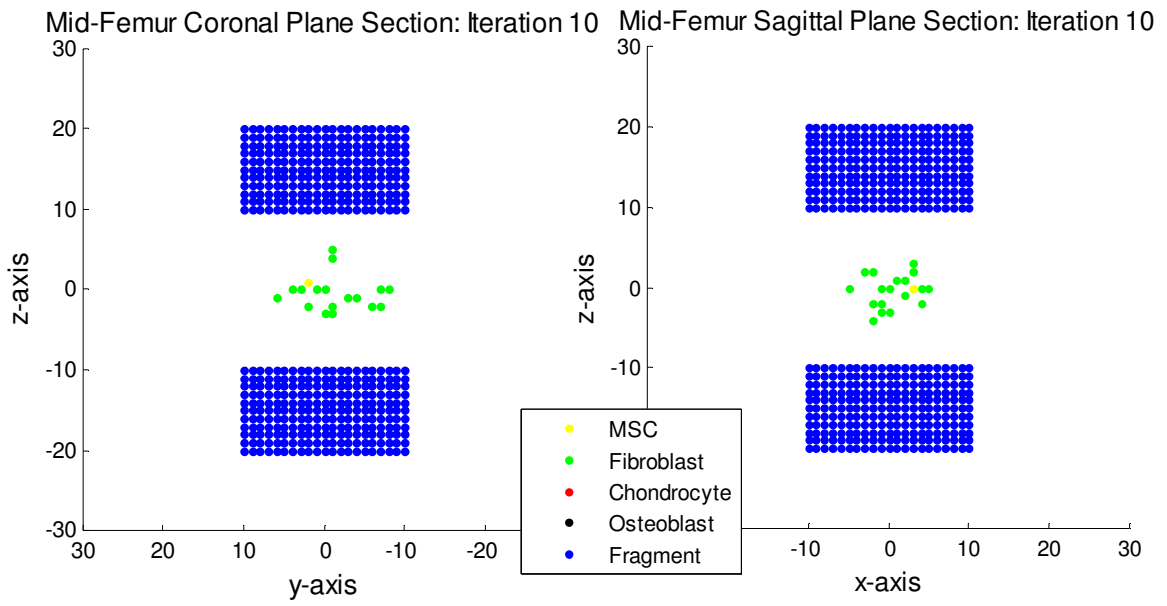
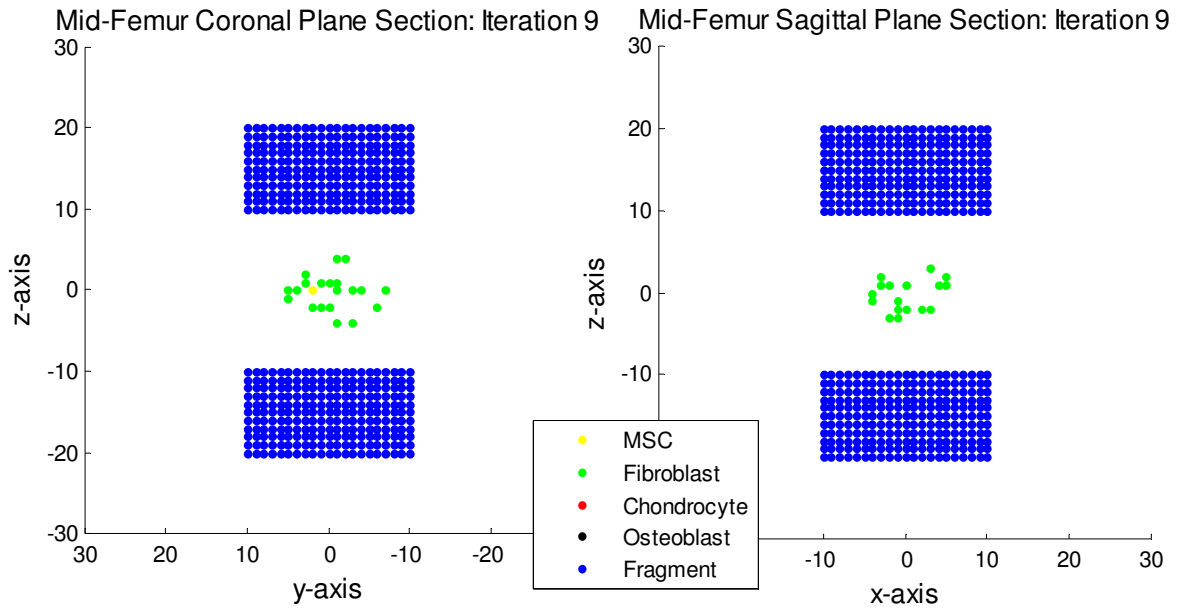
Appendix A

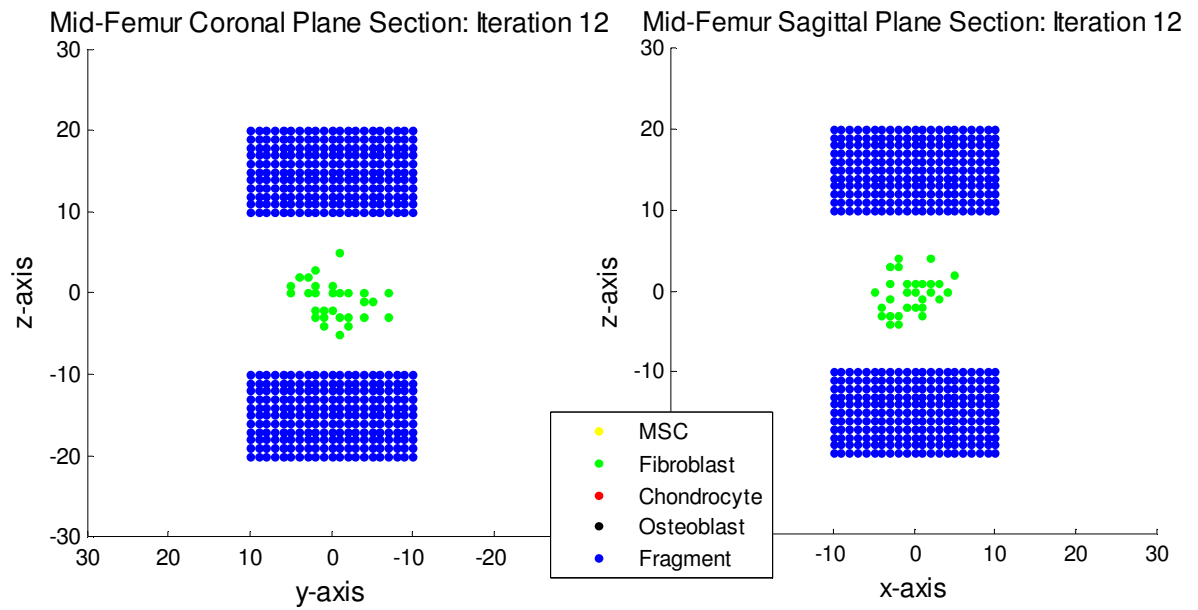
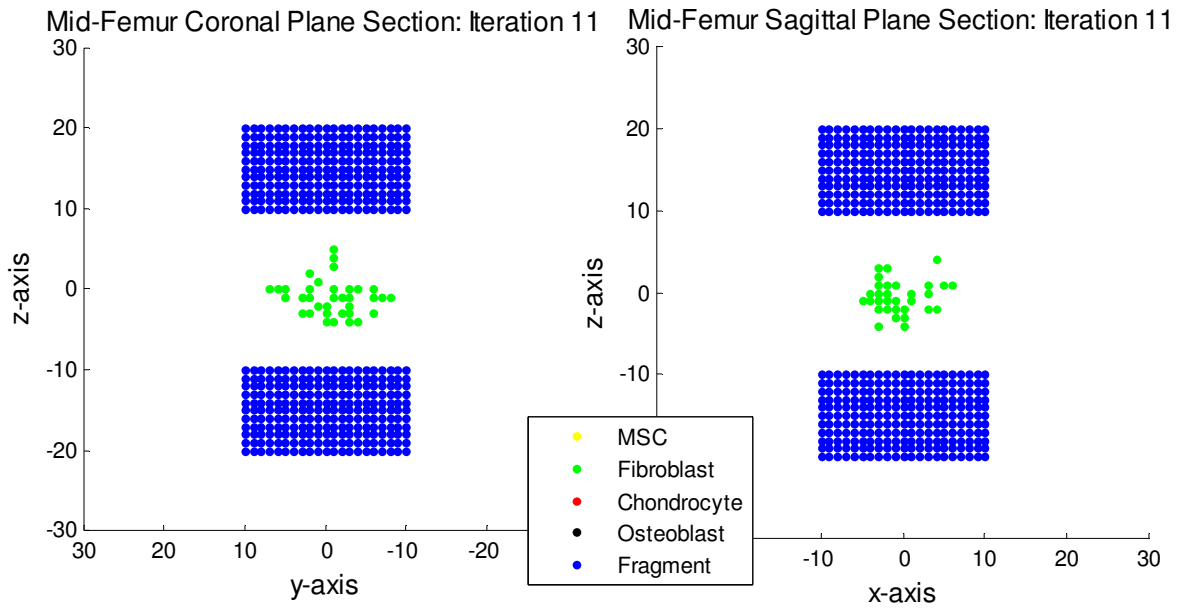


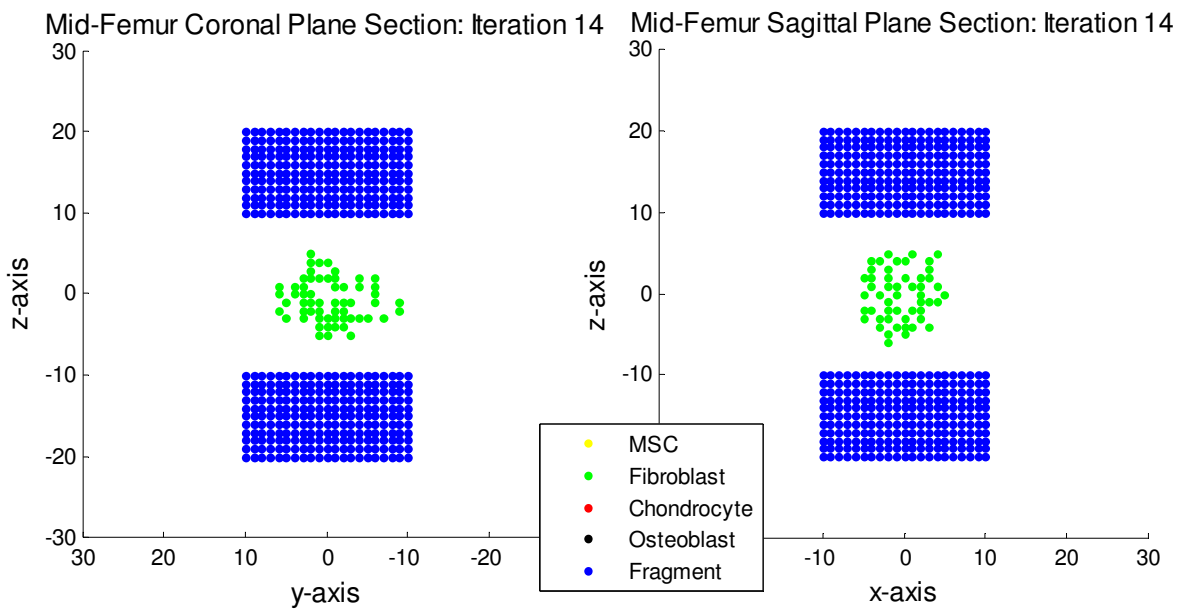
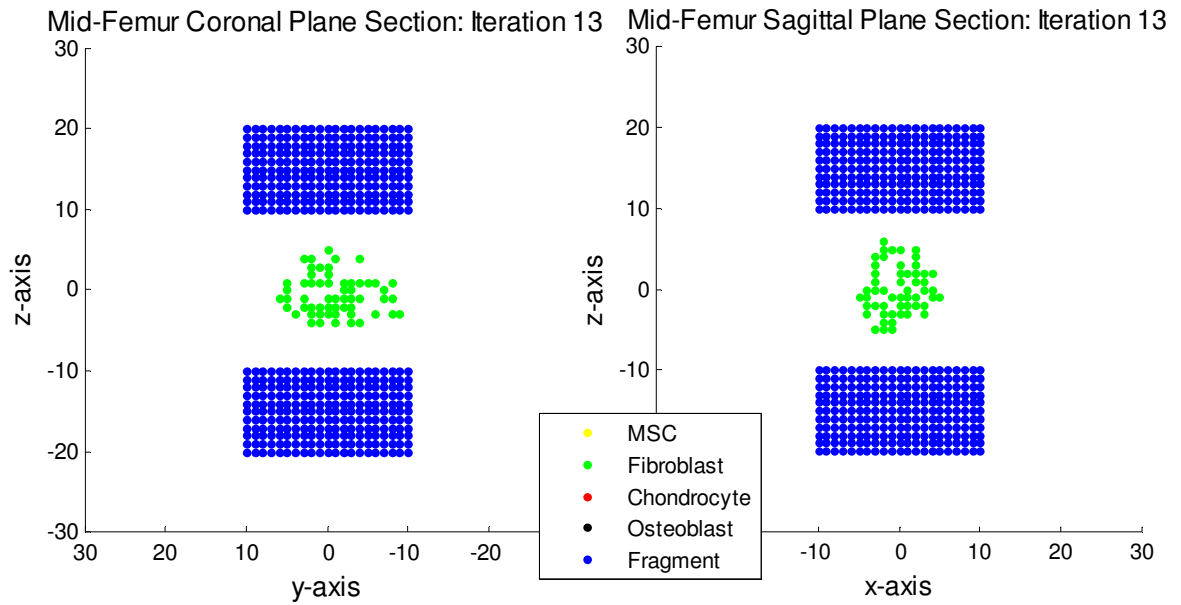


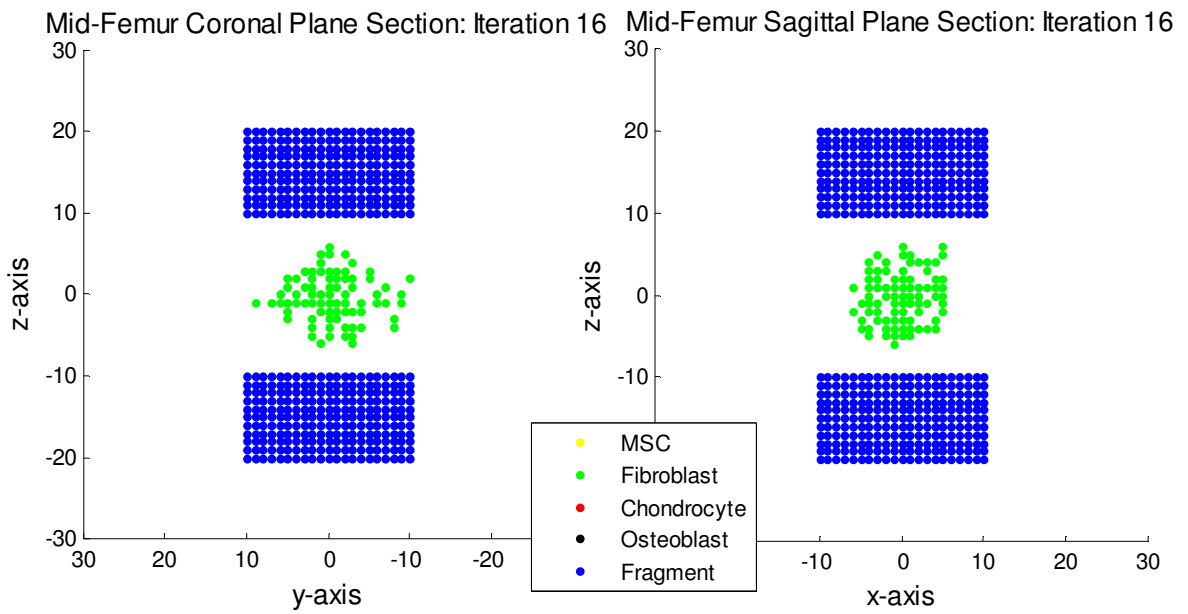
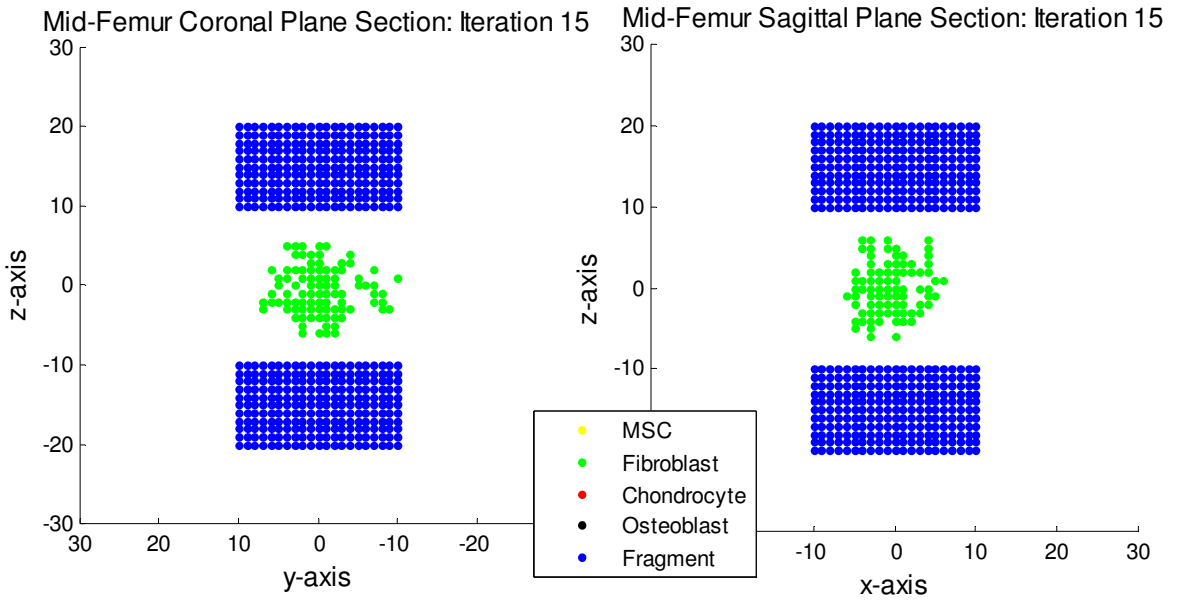


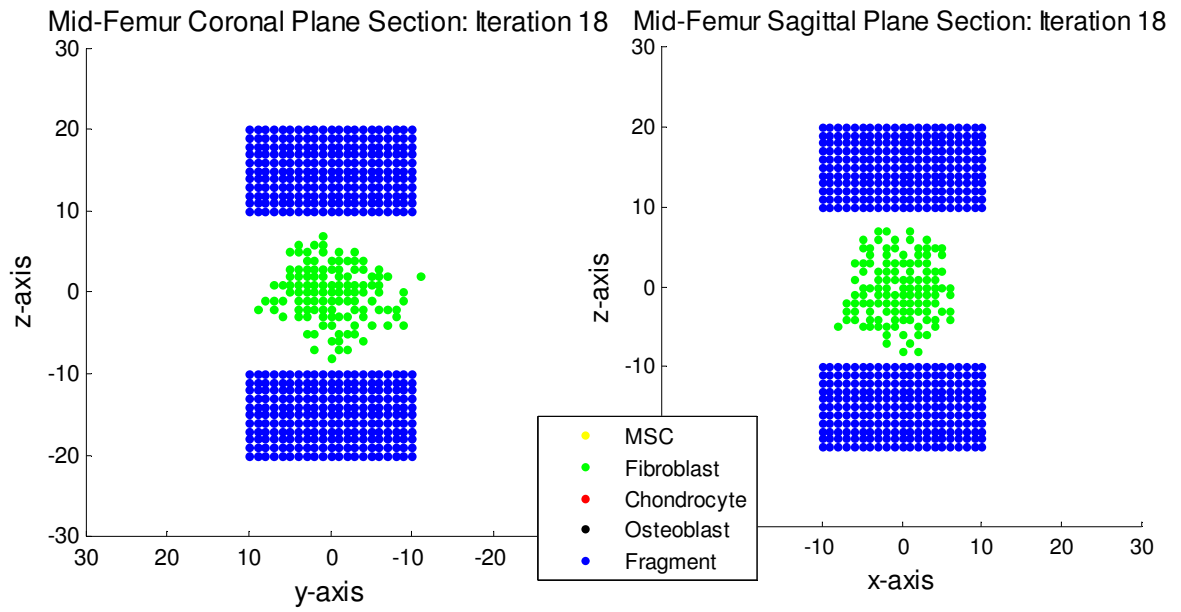
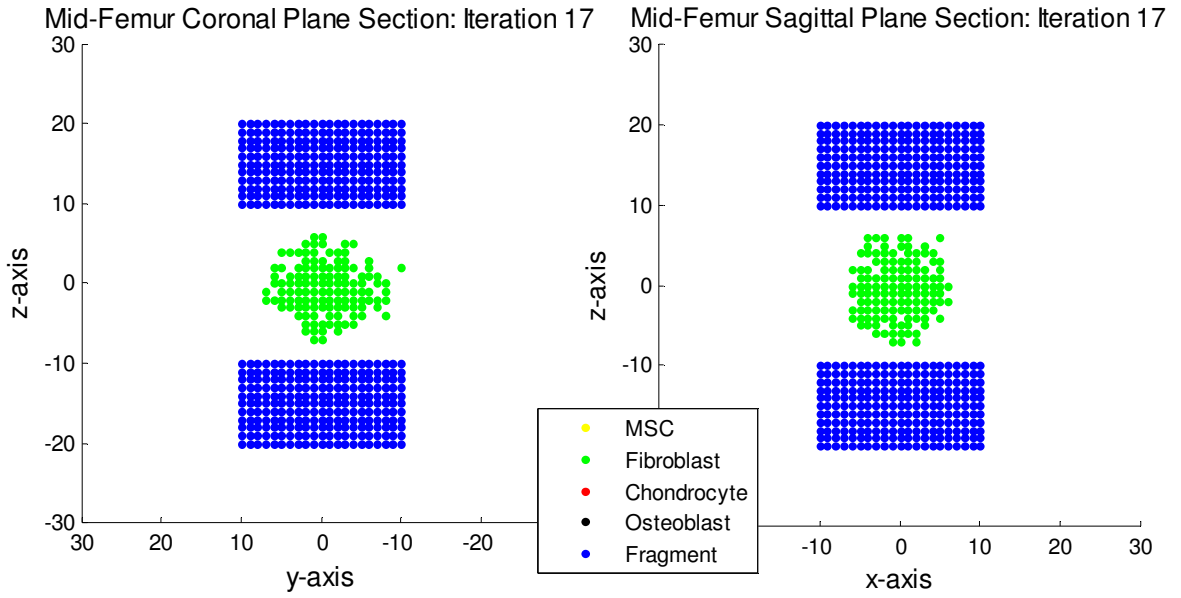


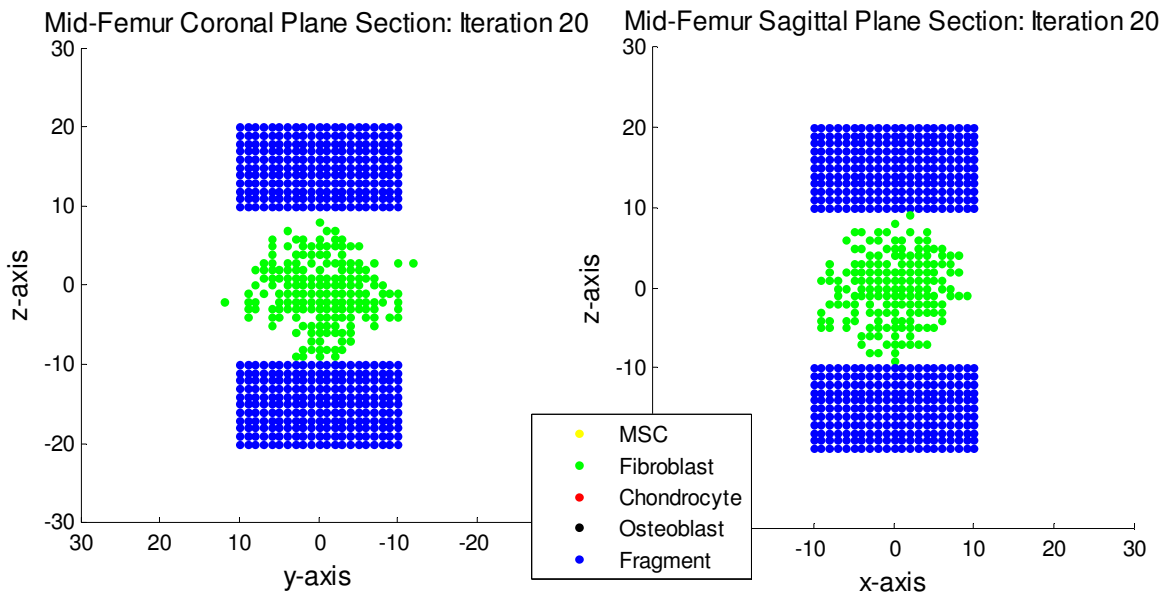
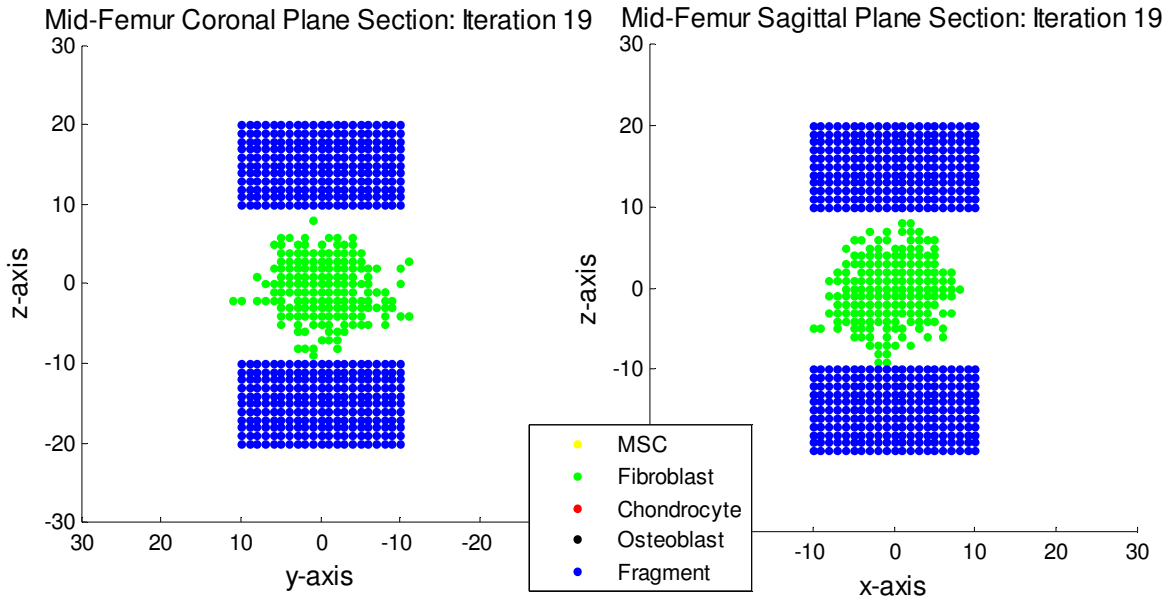




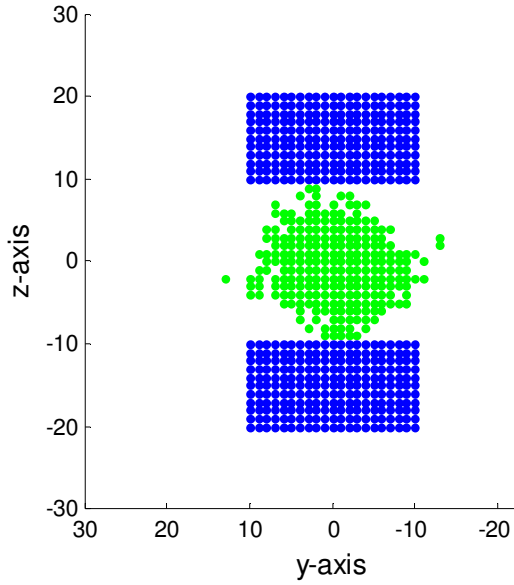




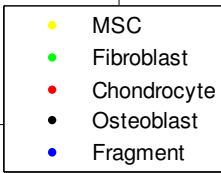
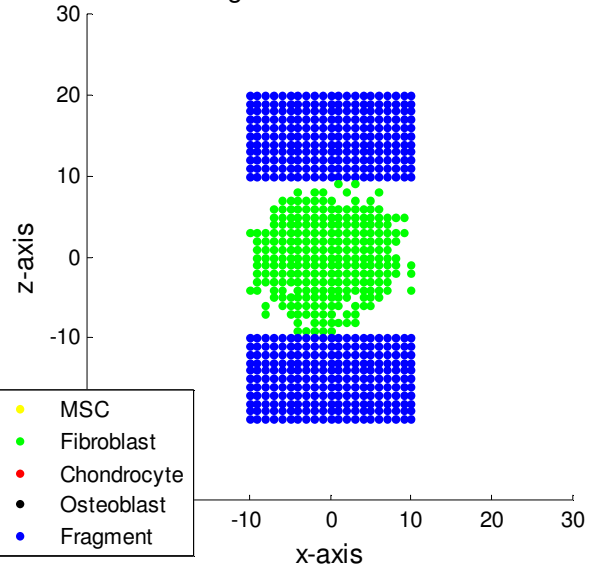




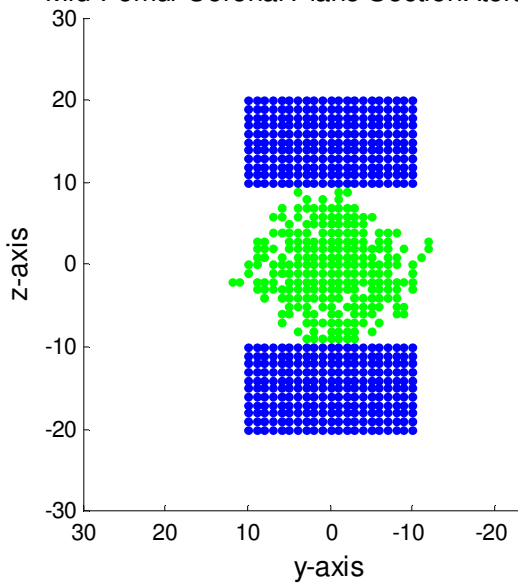
Mid-Femur Coronal Plane Section: Iteration 21



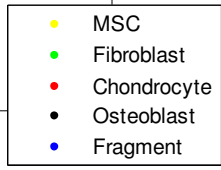
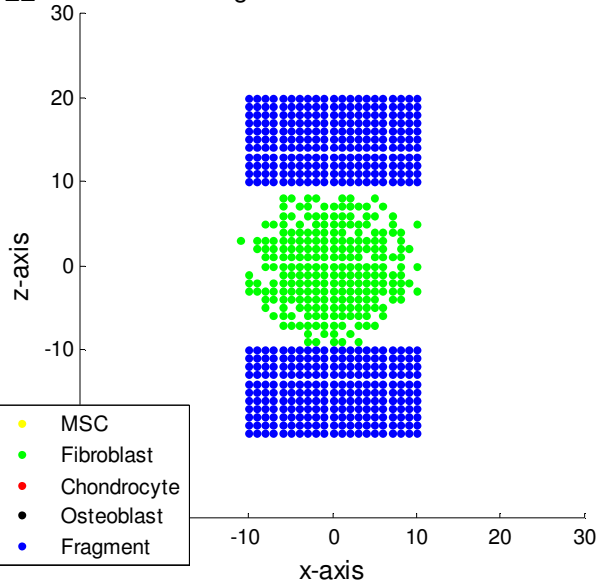
Mid-Femur Sagittal Plane Section: Iteration 21

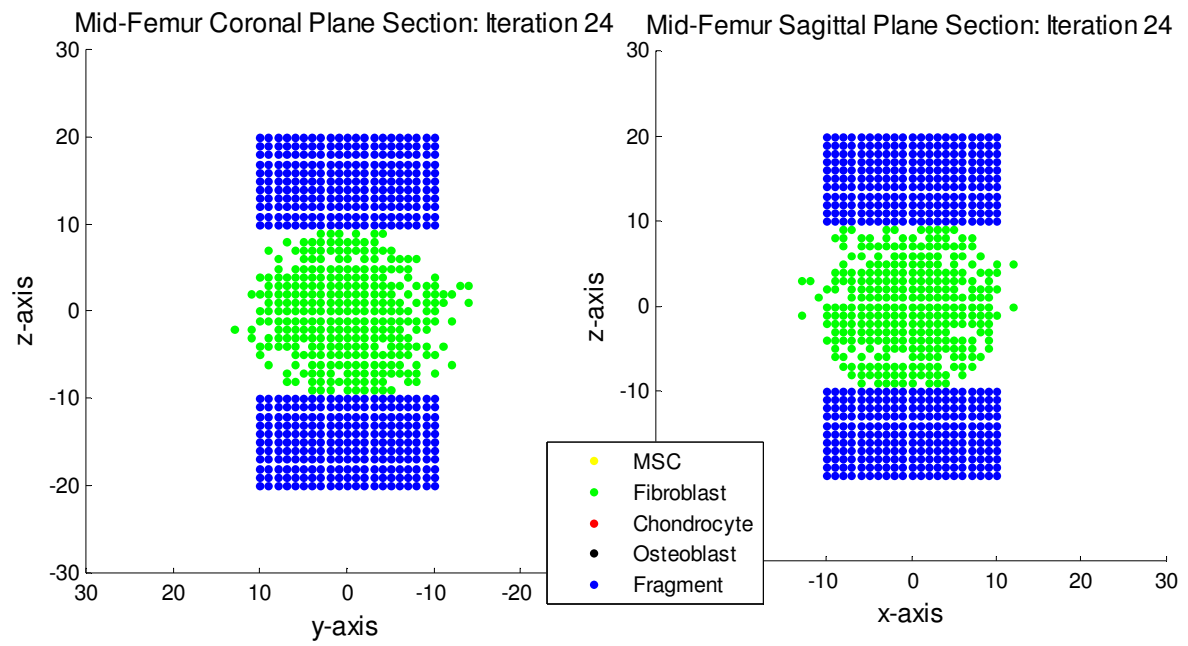
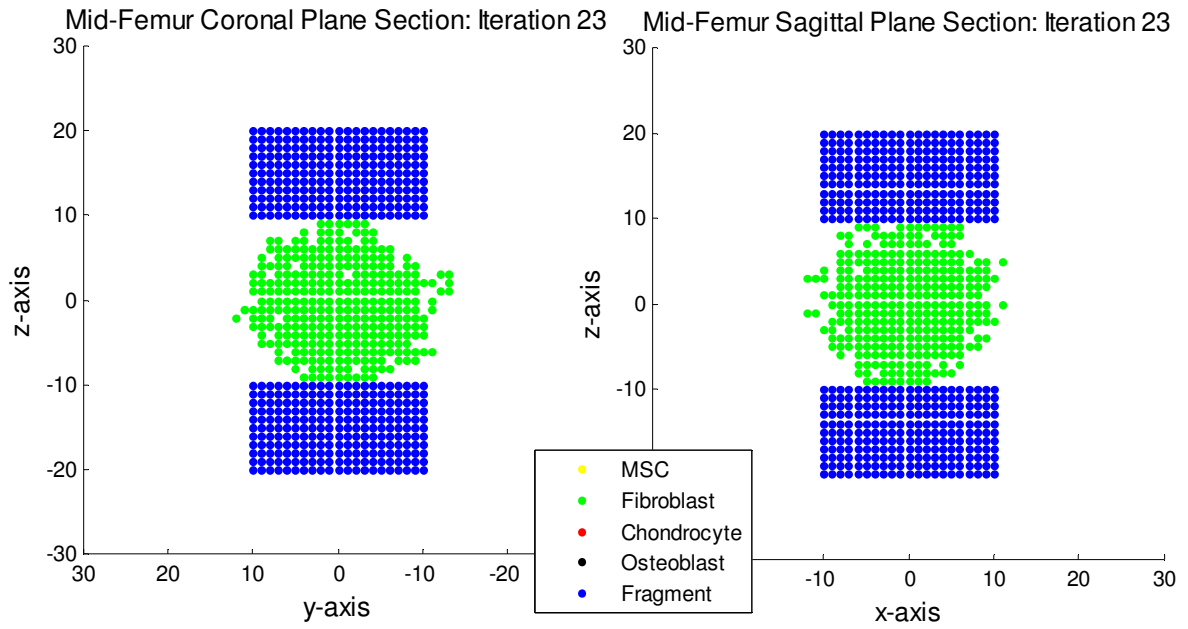


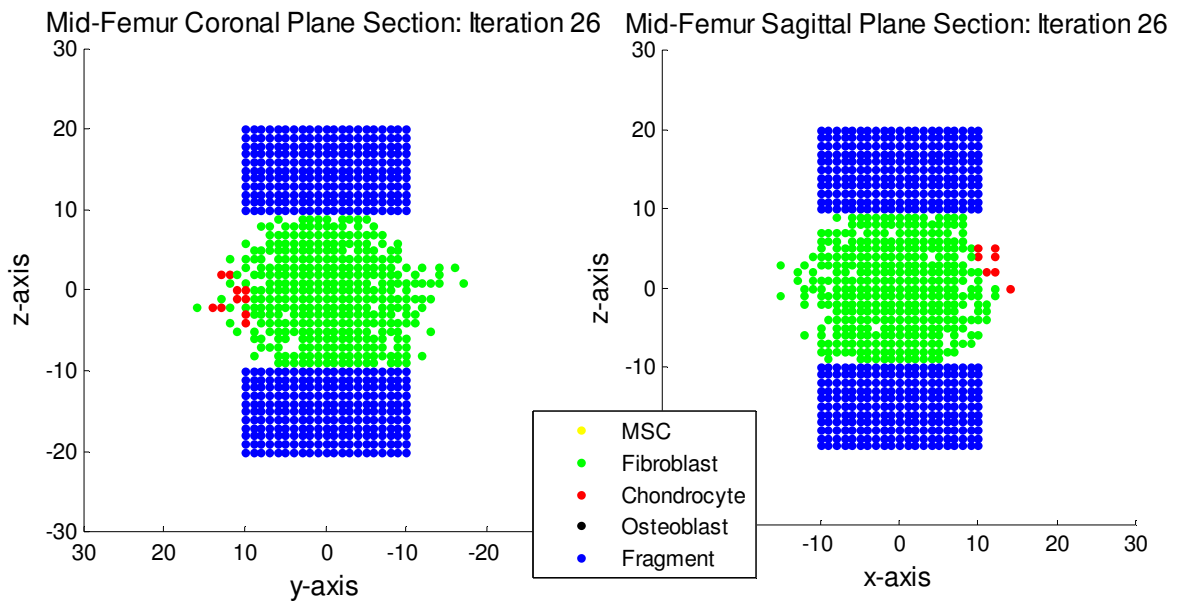
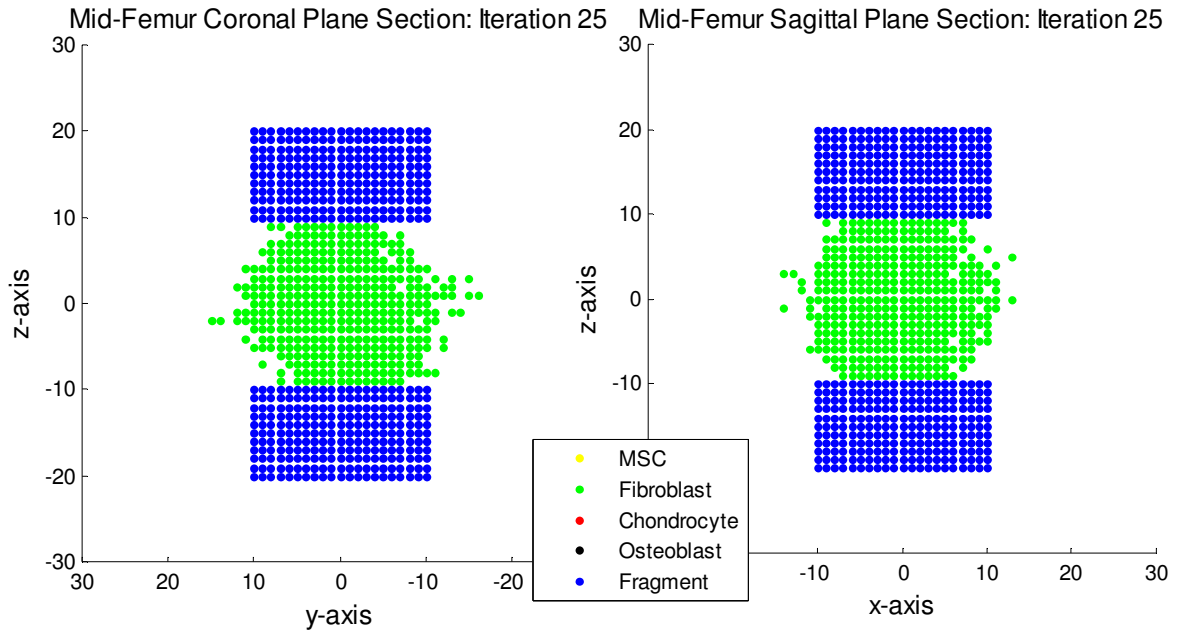
Mid-Femur Coronal Plane Section: Iteration 22



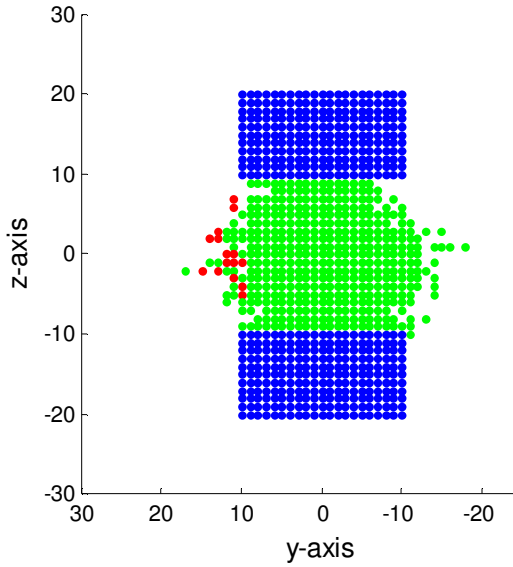
Mid-Femur Sagittal Plane Section: Iteration 22



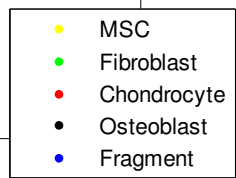
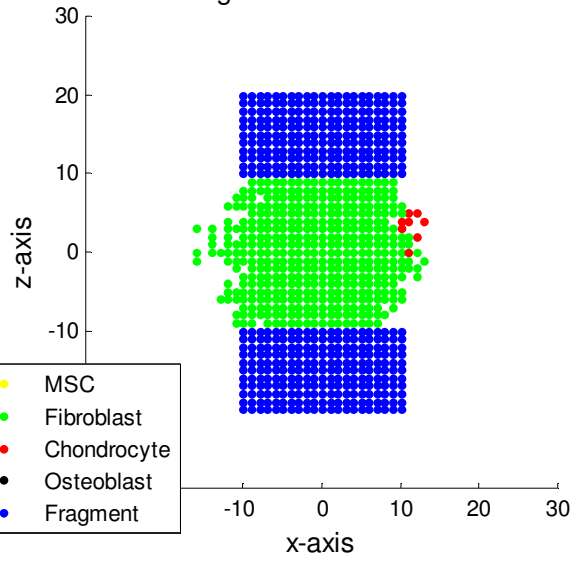




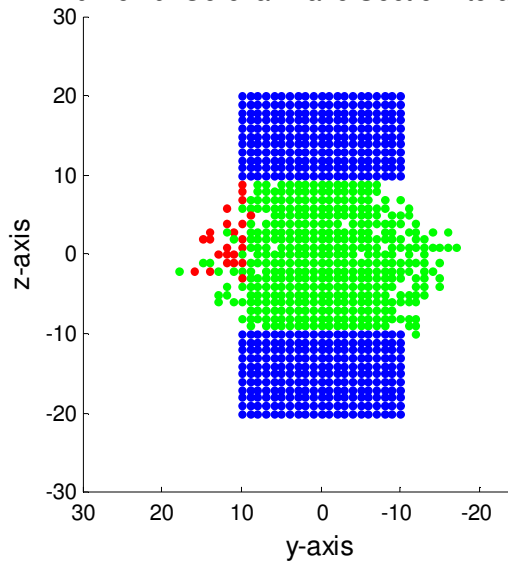
Mid-Femur Coronal Plane Section: Iteration 27



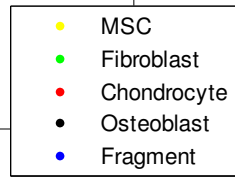
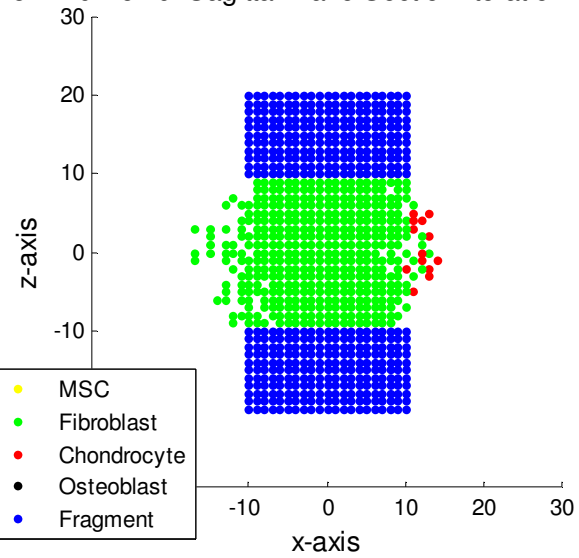
Mid-Femur Sagittal Plane Section: Iteration 27

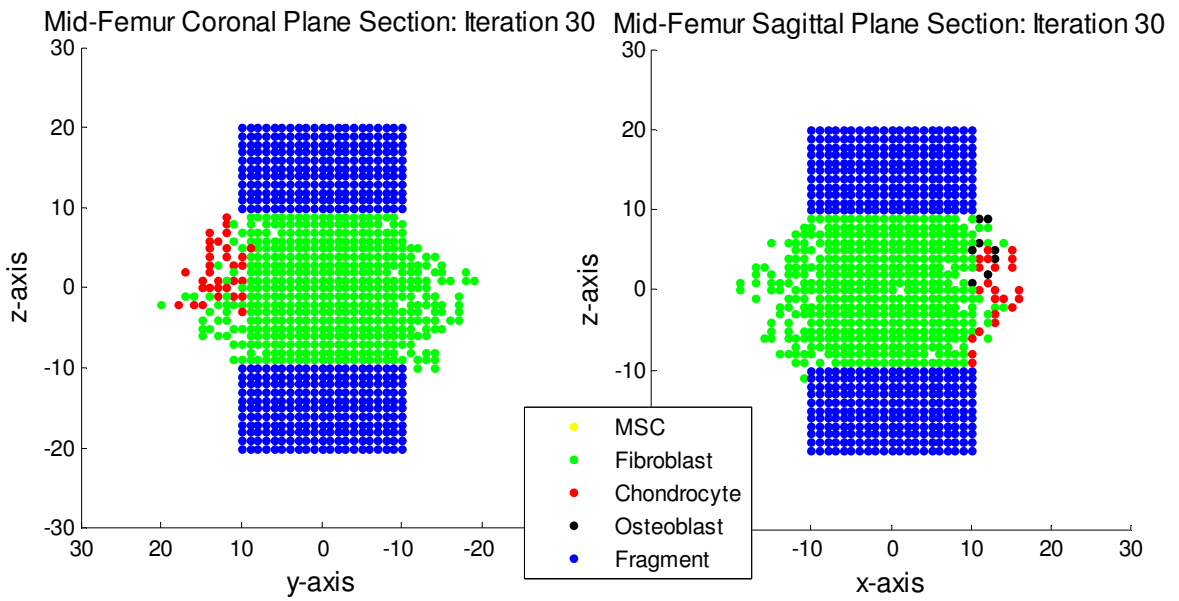
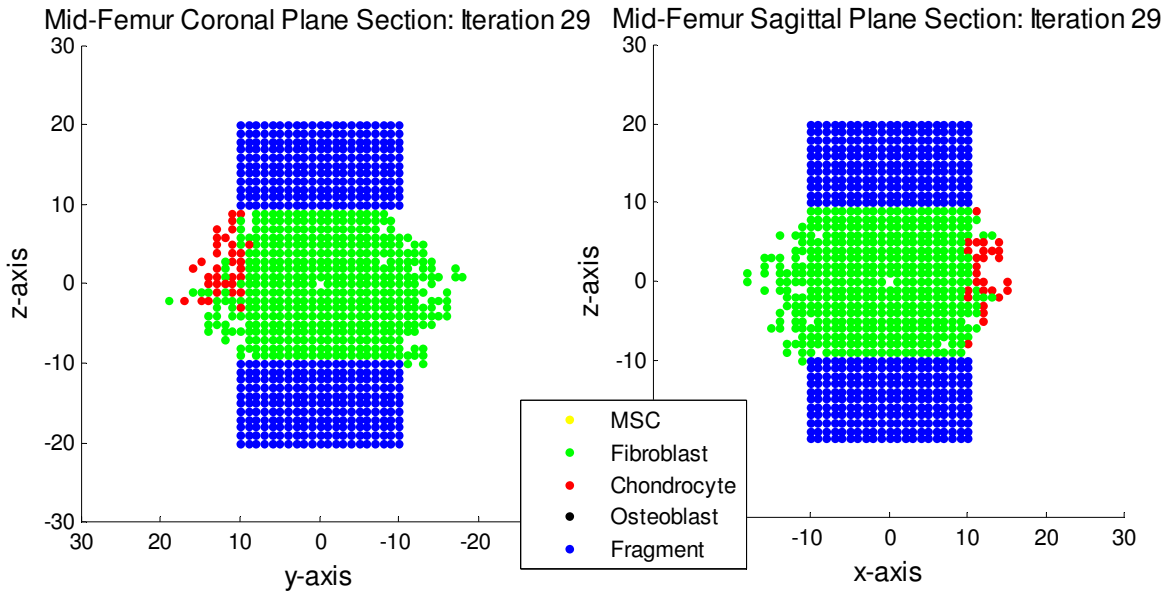


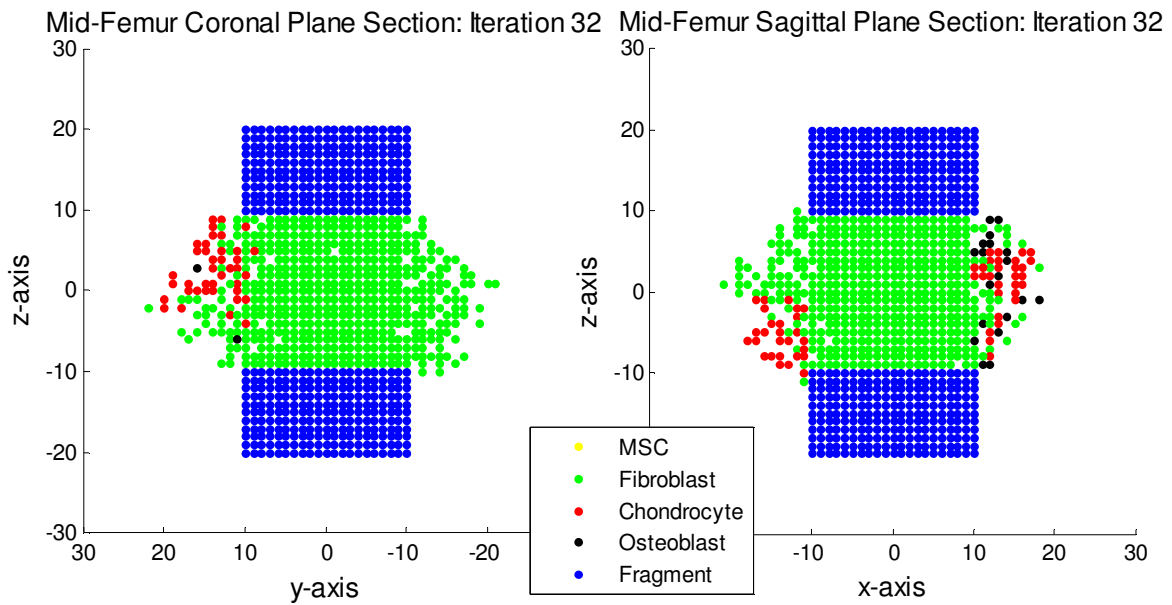
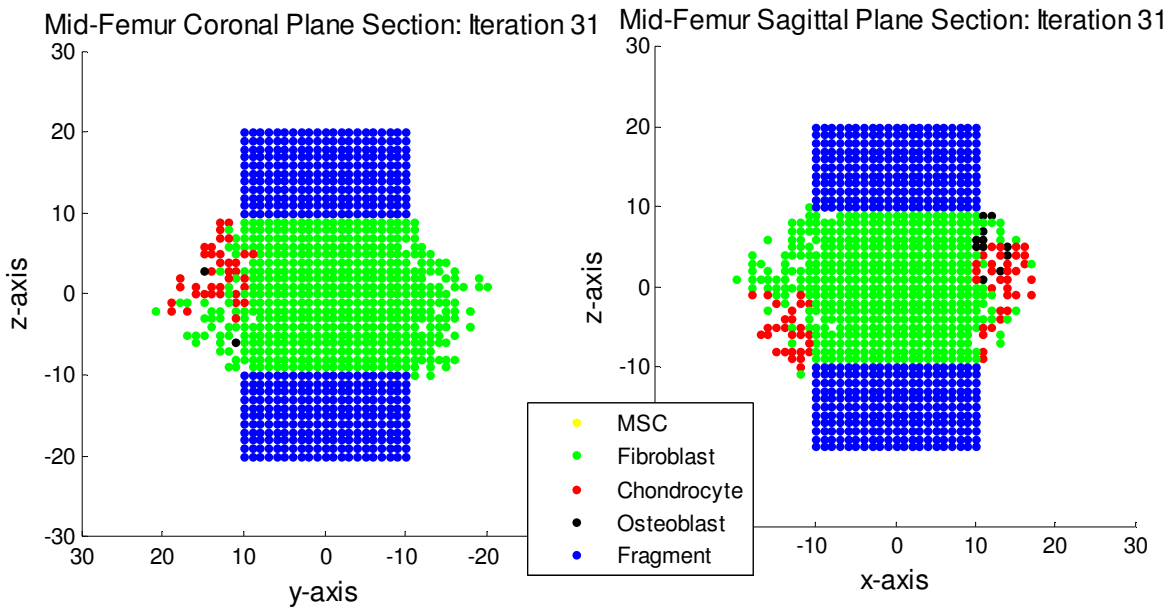
Mid-Femur Coronal Plane Section: Iteration 28



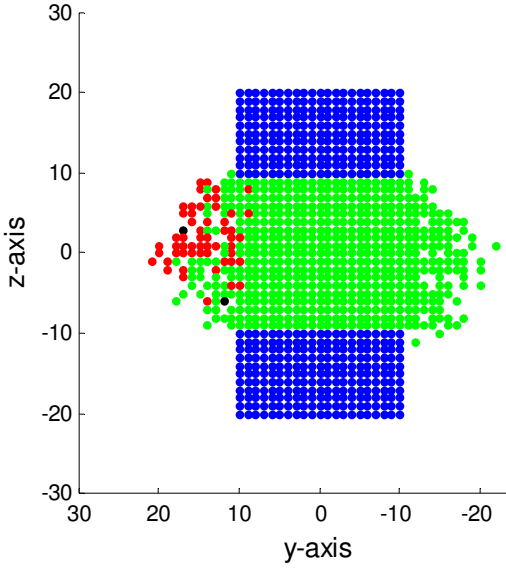
Mid-Femur Sagittal Plane Section: Iteration 28



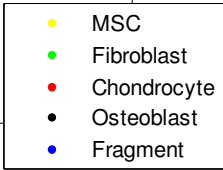
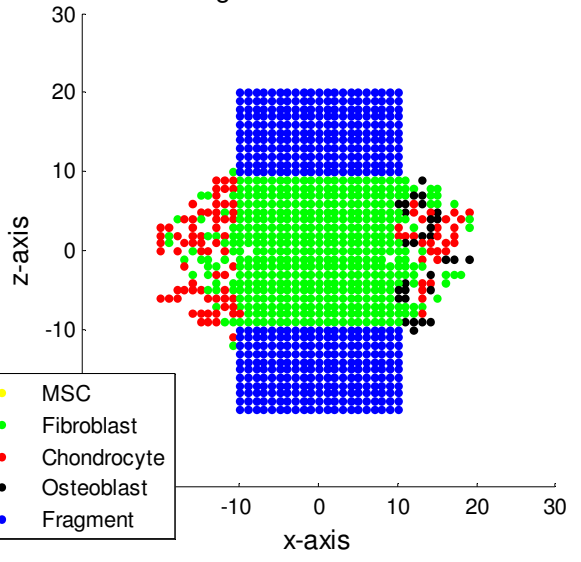




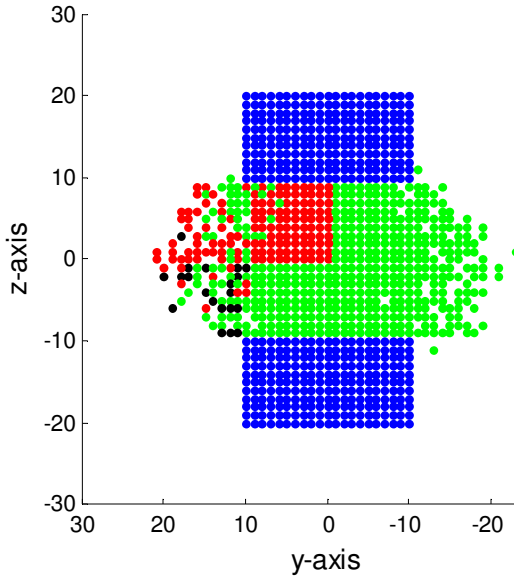
Mid-Femur Coronal Plane Section: Iteration 33



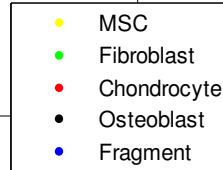
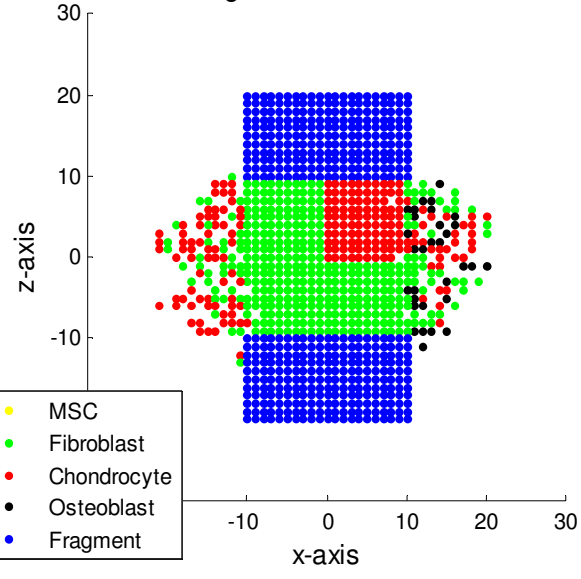
Mid-Femur Sagittal Plane Section: Iteration 33

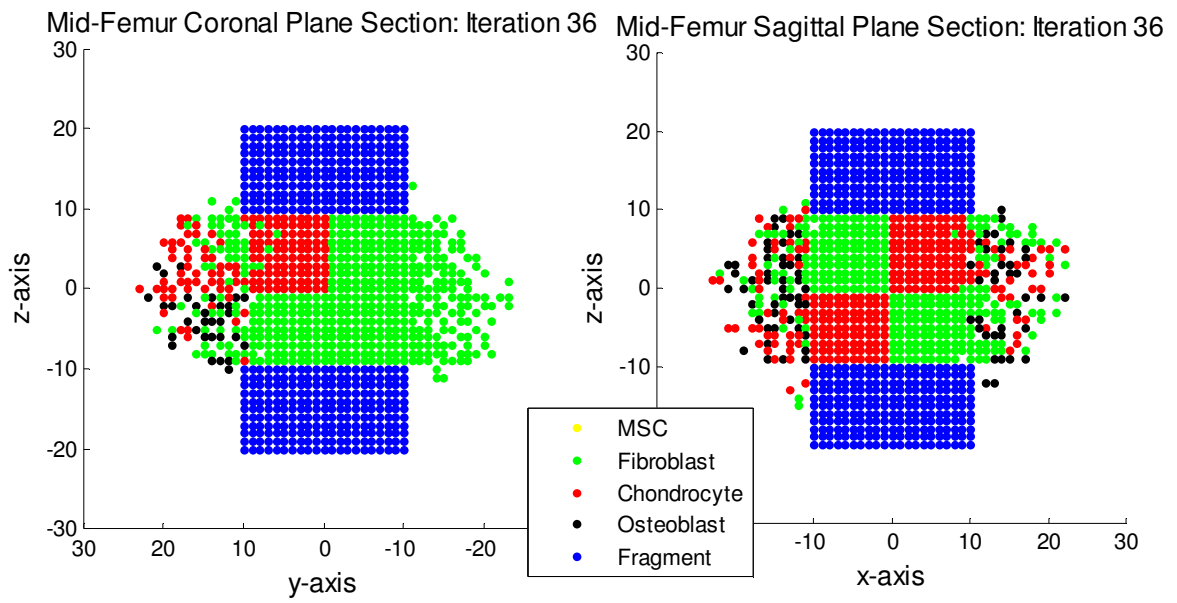
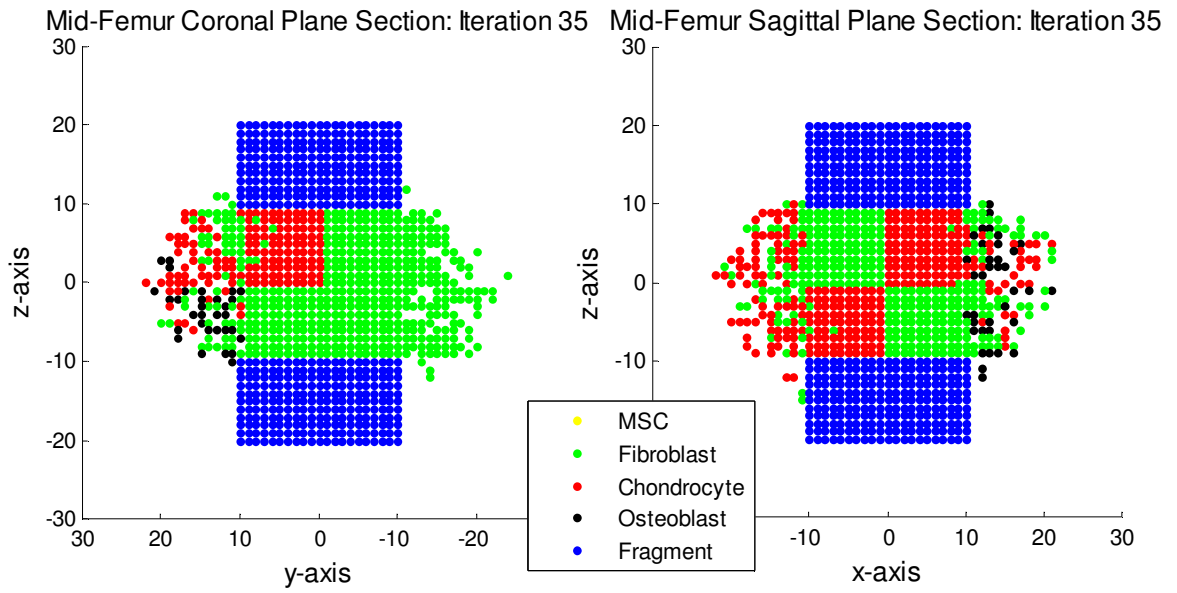


Mid-Femur Coronal Plane Section: Iteration 34

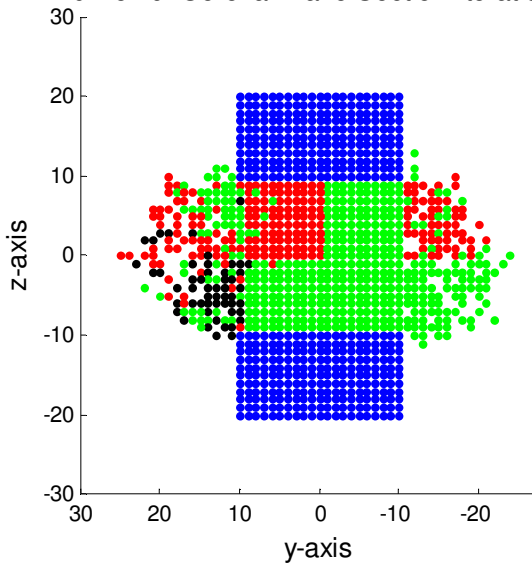


Mid-Femur Sagittal Plane Section: Iteration 34

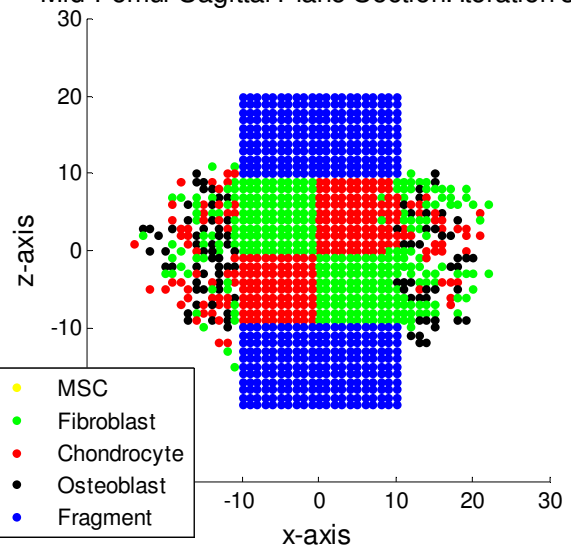




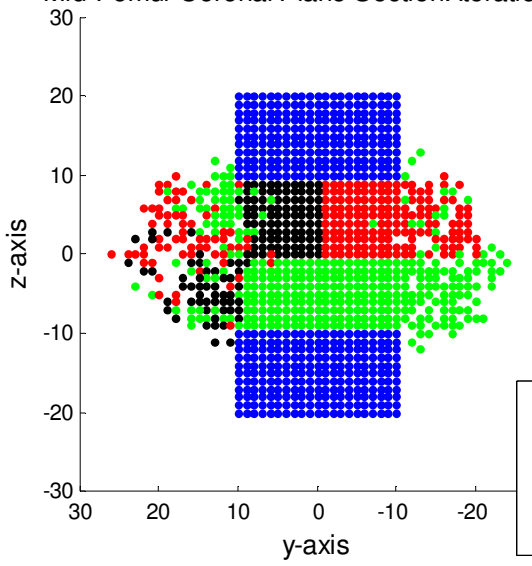
Mid-Femur Coronal Plane Section: Iteration 37



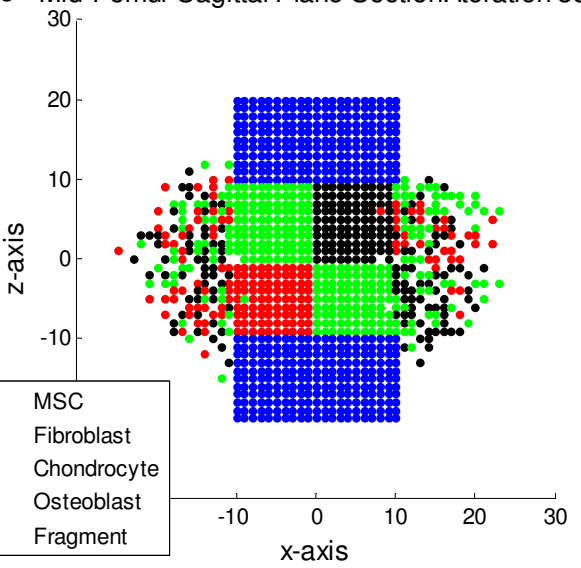
Mid-Femur Sagittal Plane Section: Iteration 37



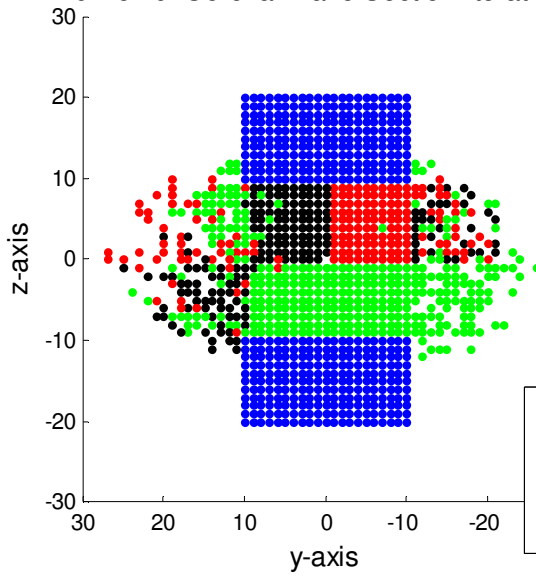
Mid-Femur Coronal Plane Section: Iteration 38



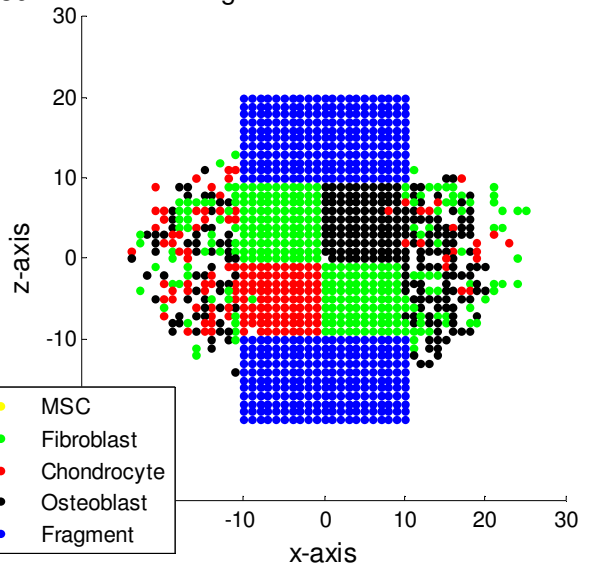
Mid-Femur Sagittal Plane Section: Iteration 38



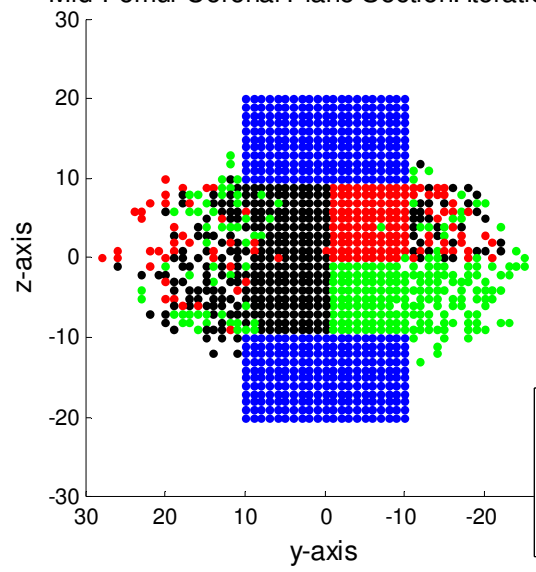
Mid-Femur Coronal Plane Section: Iteration 39



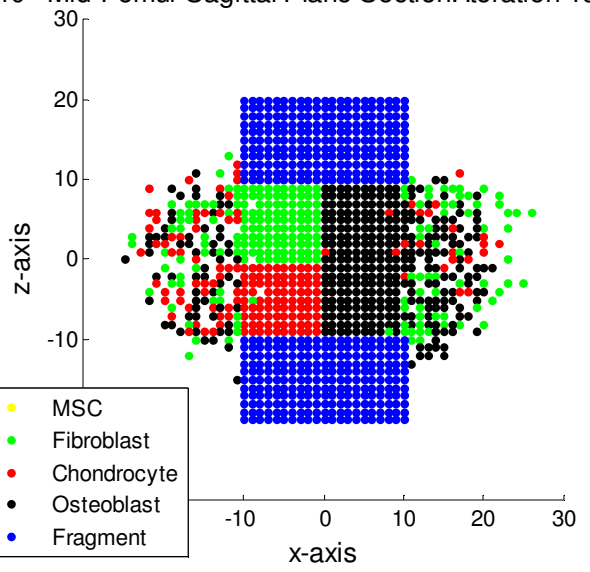
Mid-Femur Sagittal Plane Section: Iteration 39



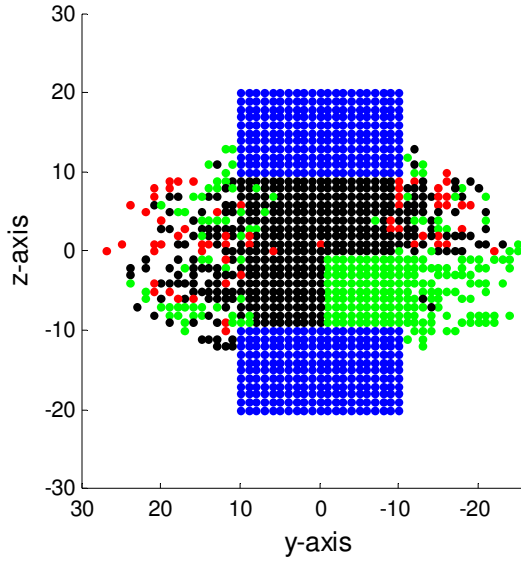
Mid-Femur Coronal Plane Section: Iteration 40



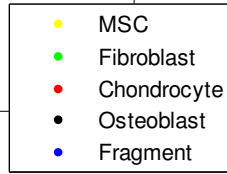
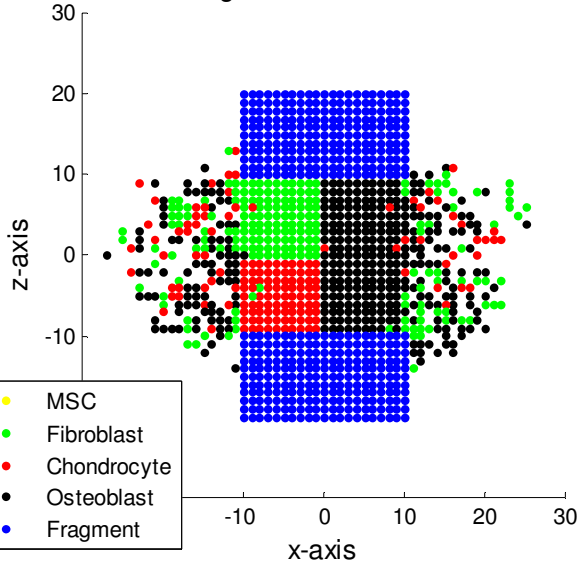
Mid-Femur Sagittal Plane Section: Iteration 40



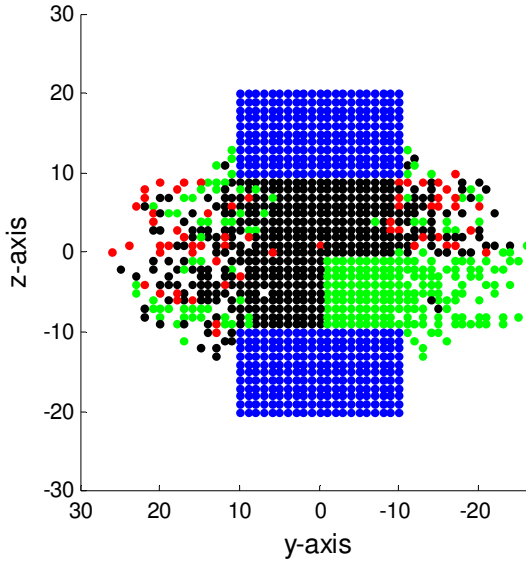
Mid-Femur Coronal Plane Section: Iteration 41



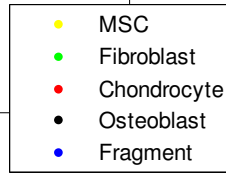
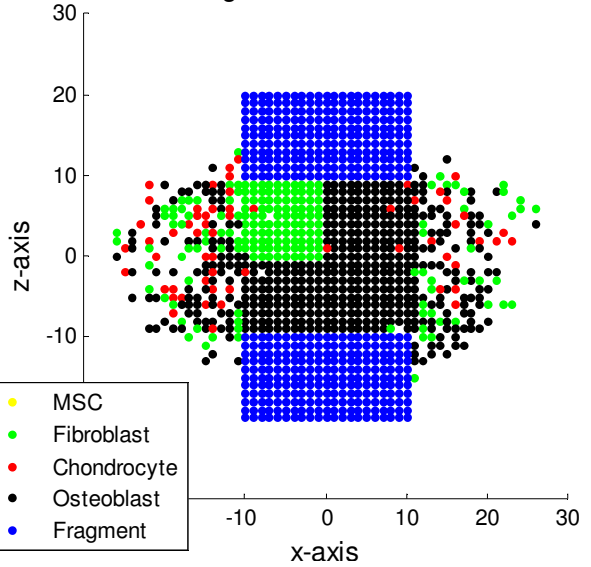
Mid-Femur Sagittal Plane Section: Iteration 41



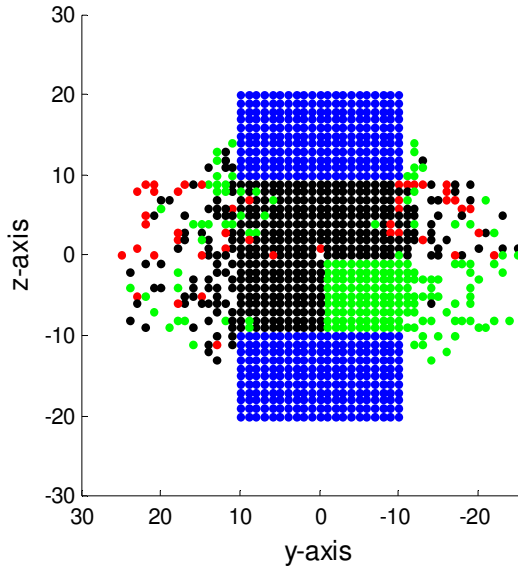
Mid-Femur Coronal Plane Section: Iteration 42



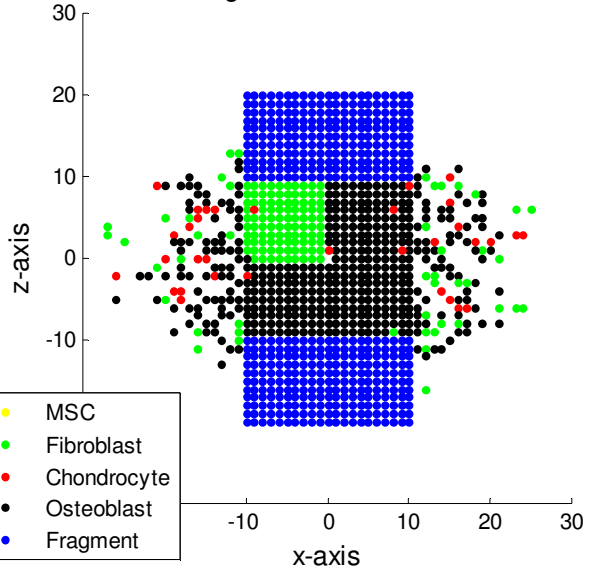
Mid-Femur Sagittal Plane Section: Iteration 42



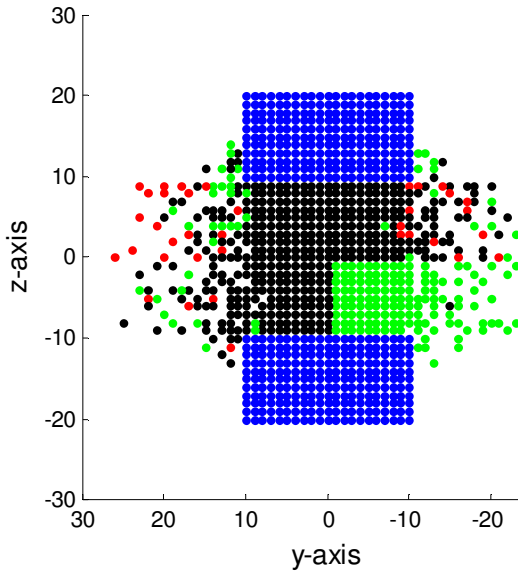
Mid-Femur Coronal Plane Section: Iteration 43



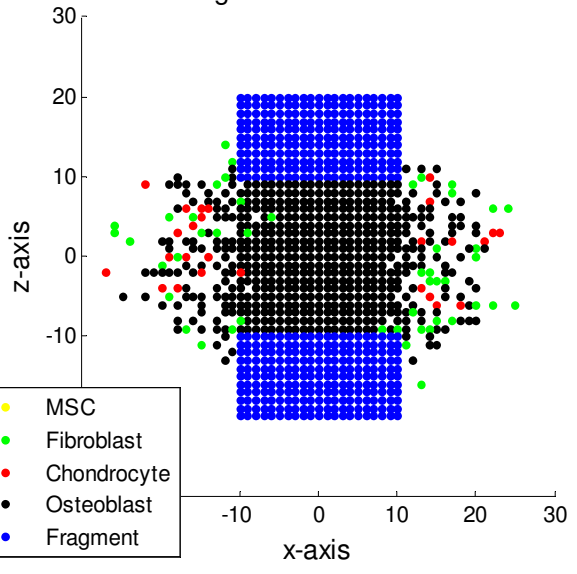
Mid-Femur Sagittal Plane Section: Iteration 43



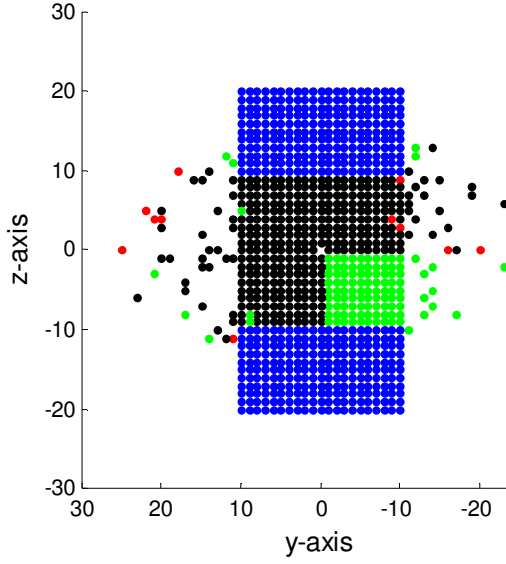
Mid-Femur Coronal Plane Section: Iteration 44



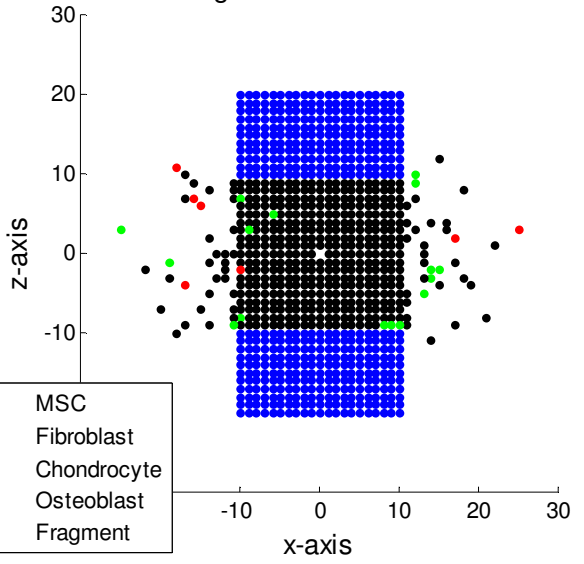
Mid-Femur Sagittal Plane Section: Iteration 44



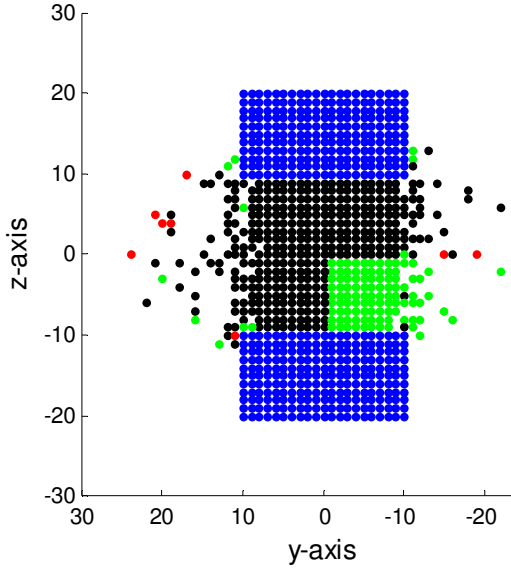
Mid-Femur Coronal Plane Section: Iteration 45



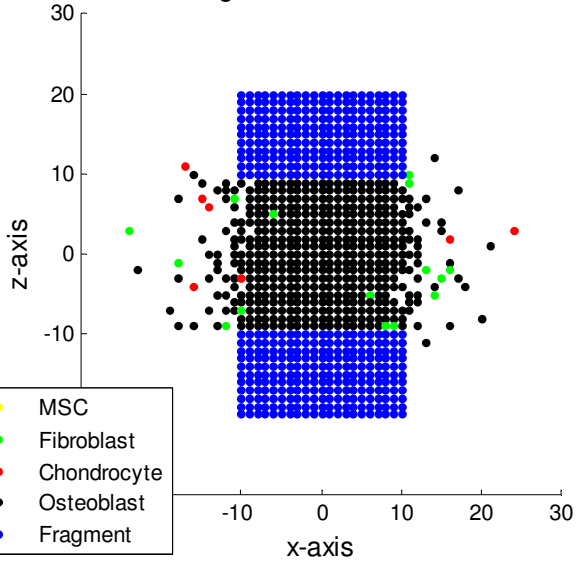
Mid-Femur Sagittal Plane Section: Iteration 45

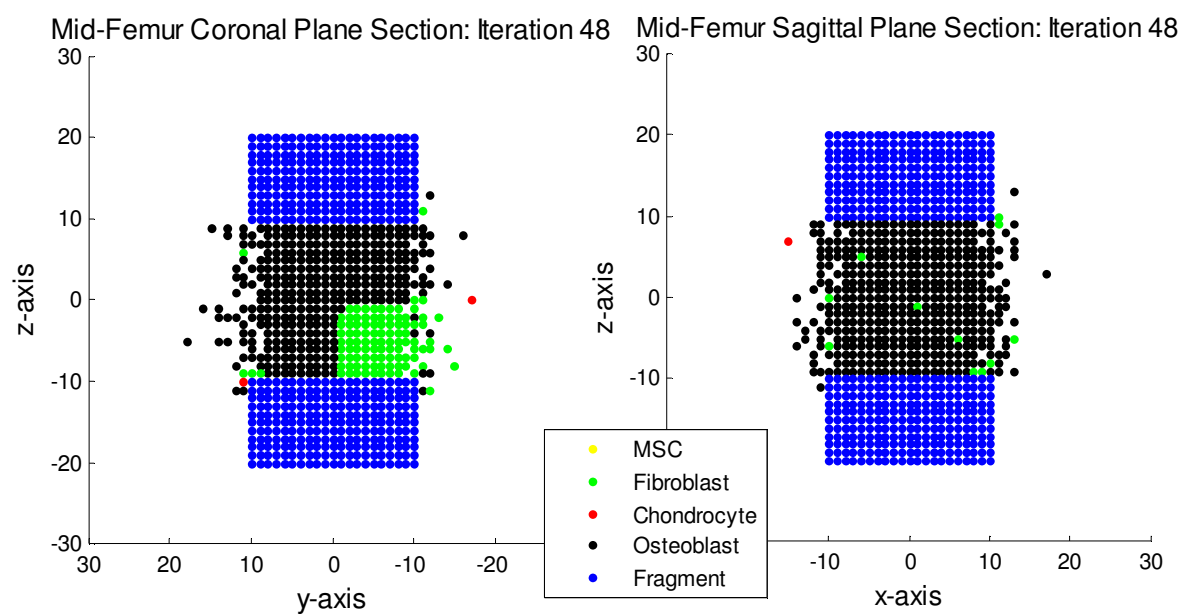
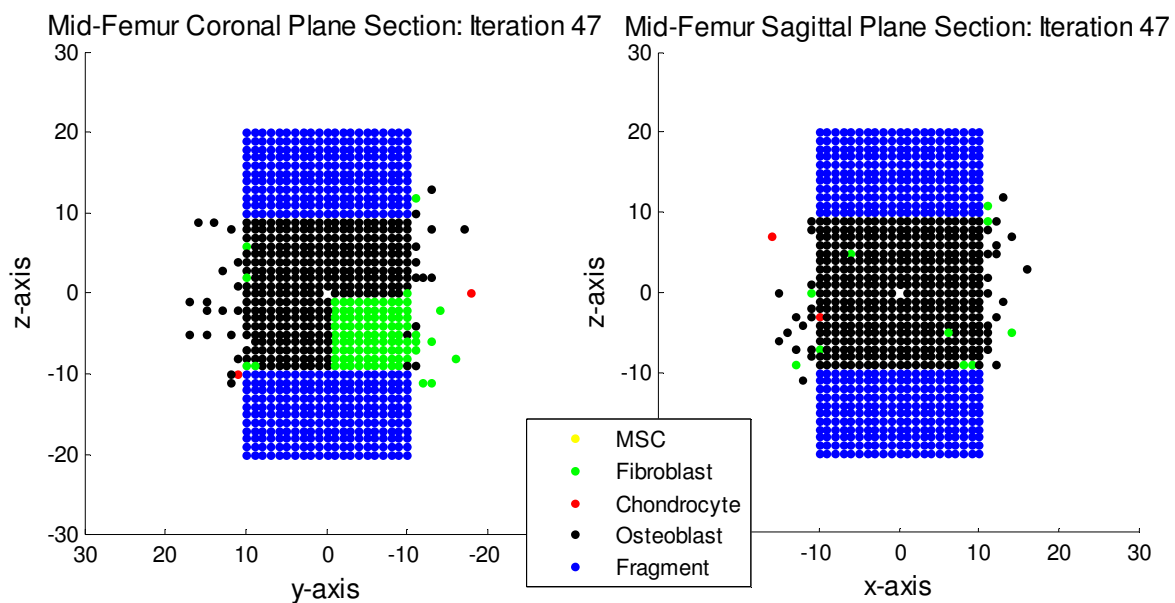


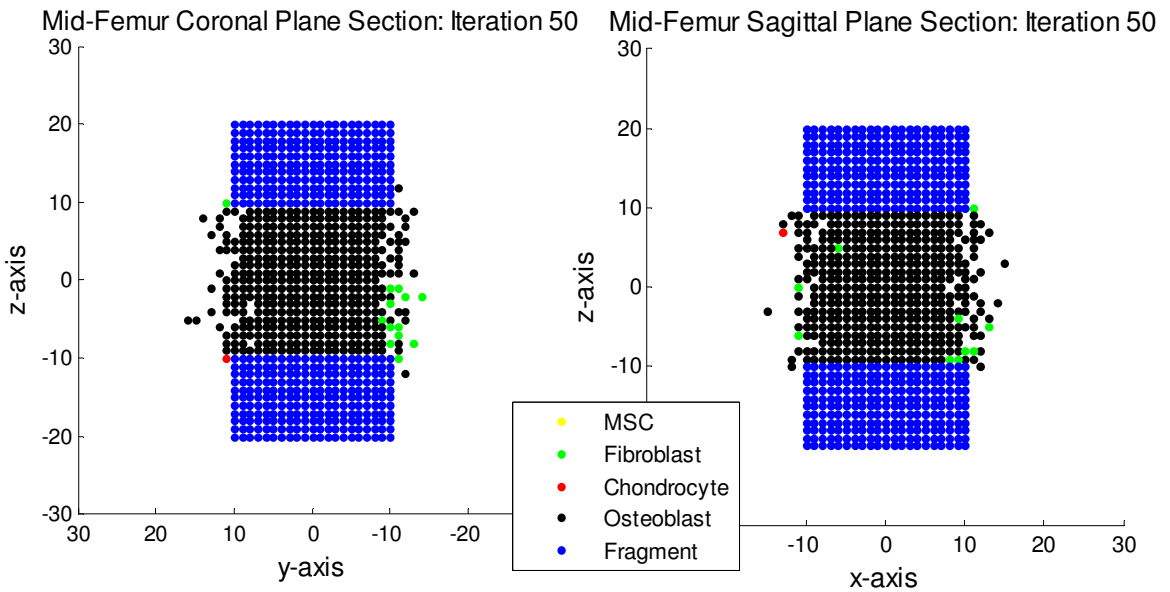
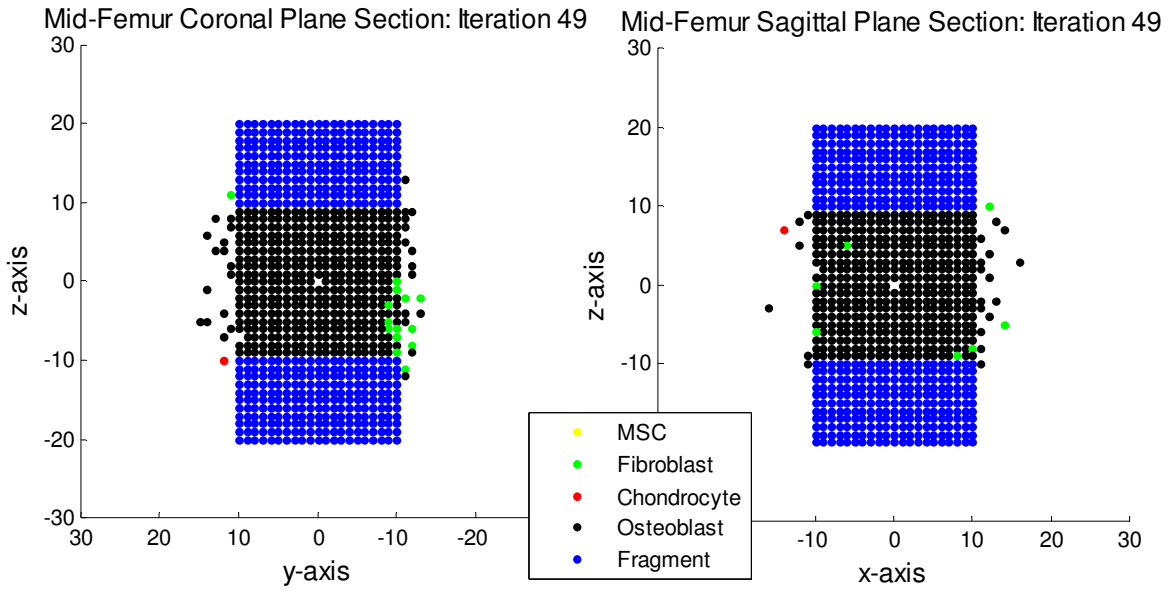
Mid-Femur Coronal Plane Section: Iteration 46

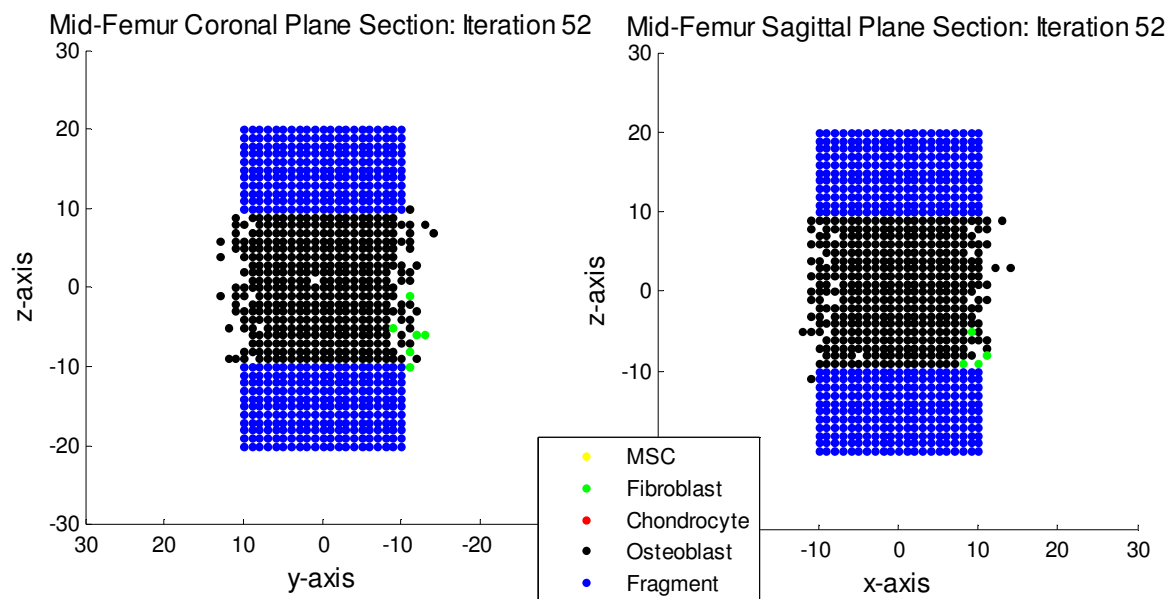
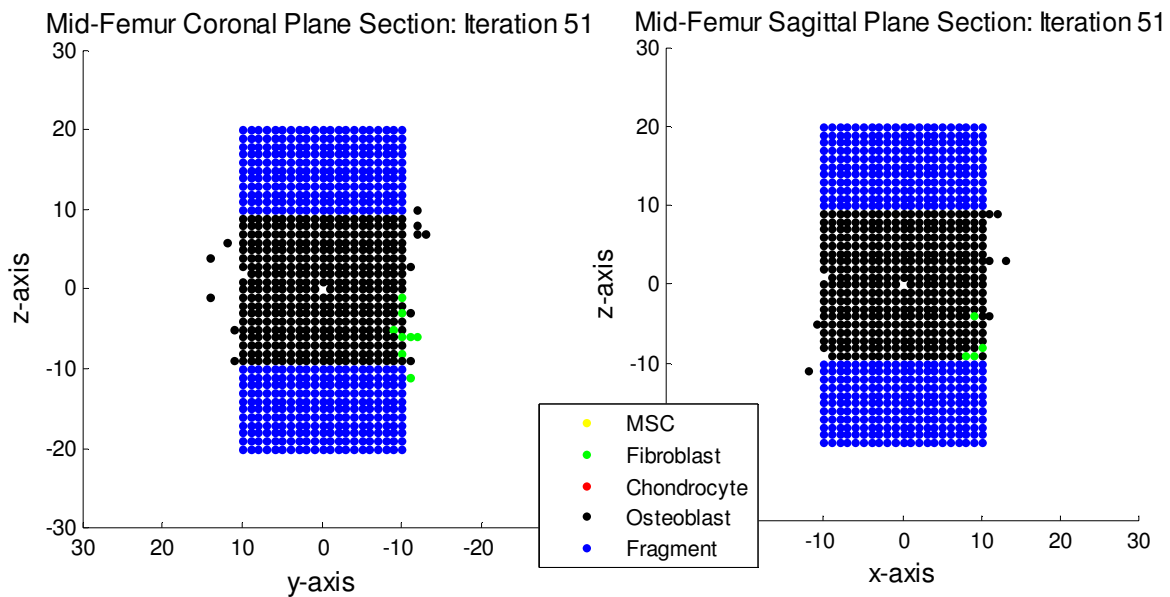


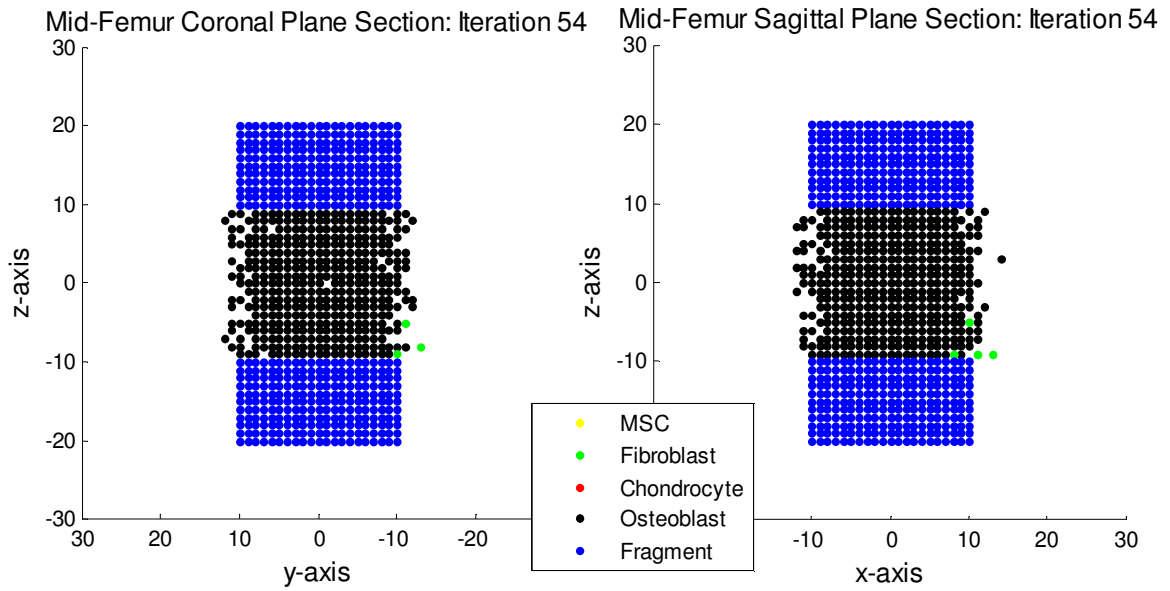
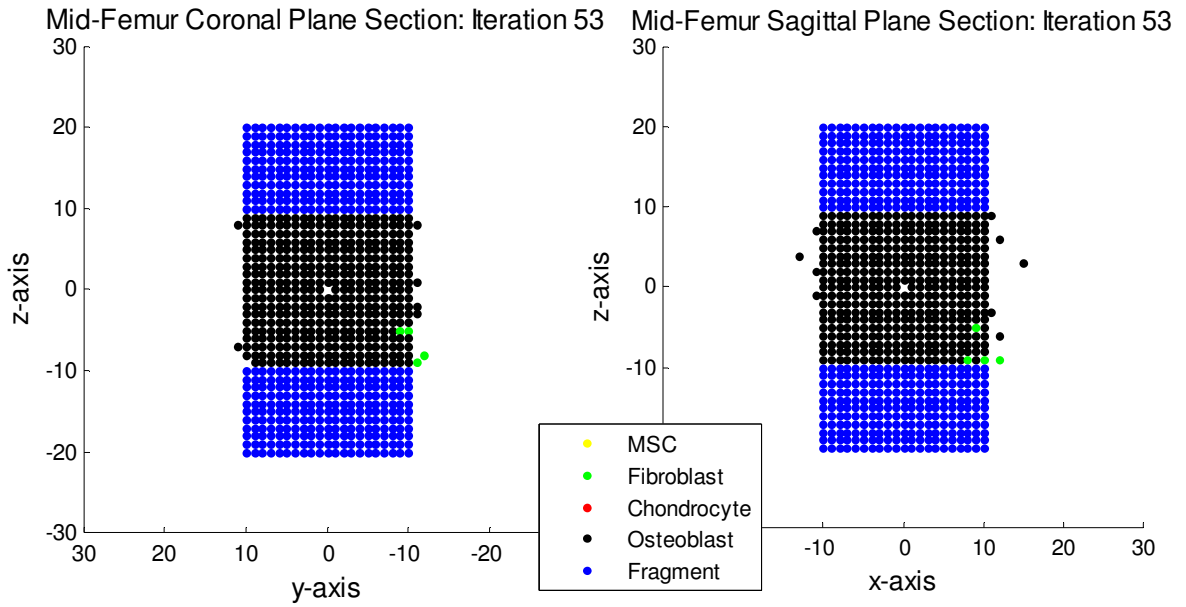
Mid-Femur Sagittal Plane Section: Iteration 46

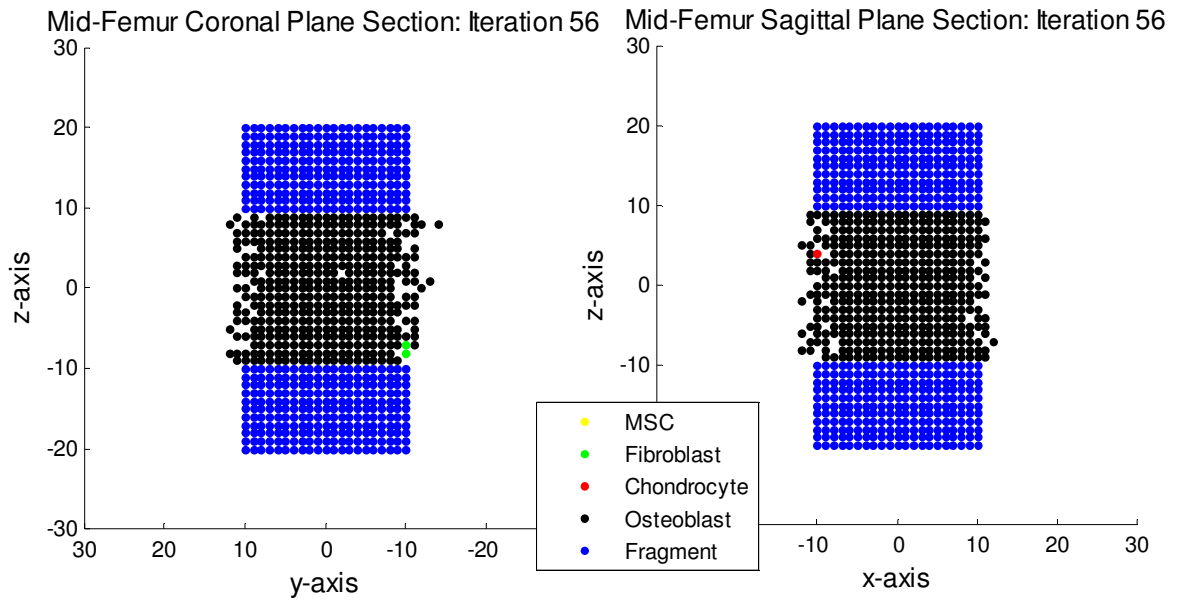
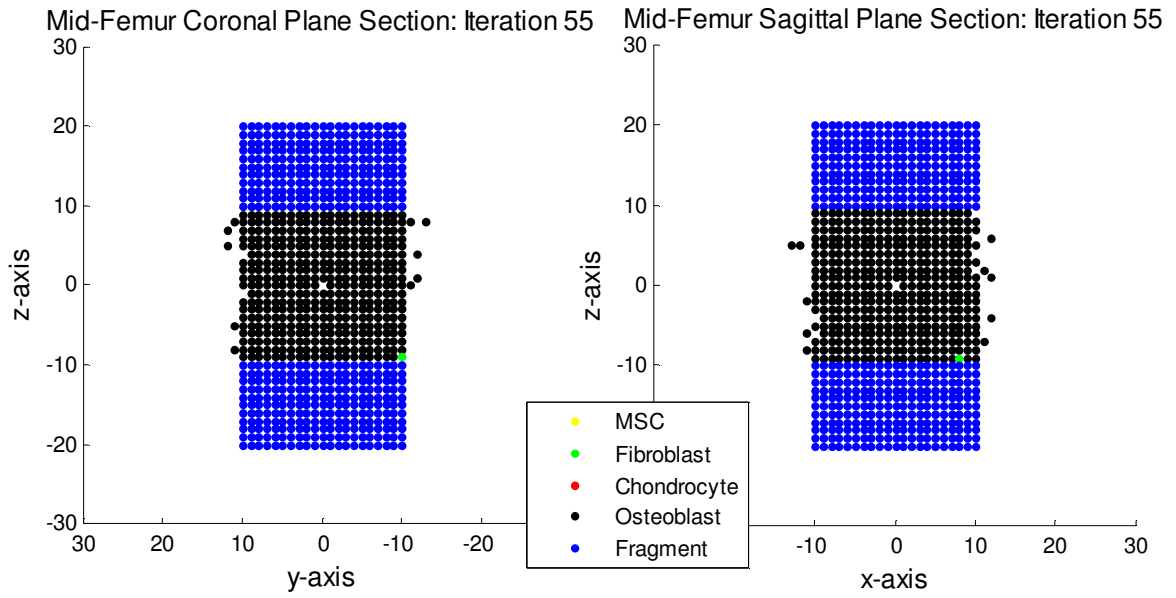




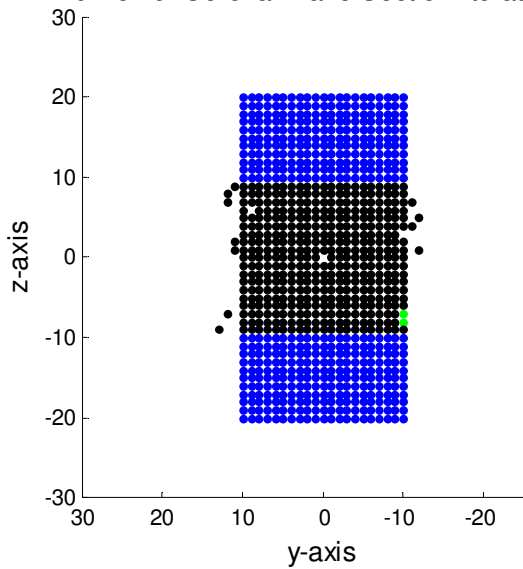




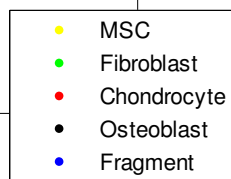
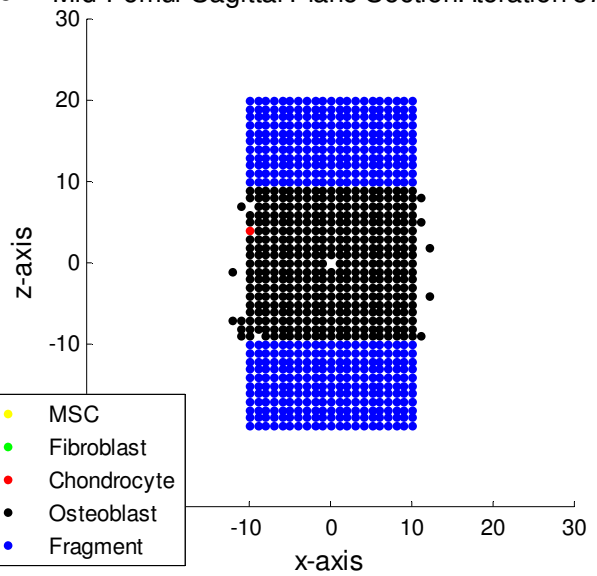




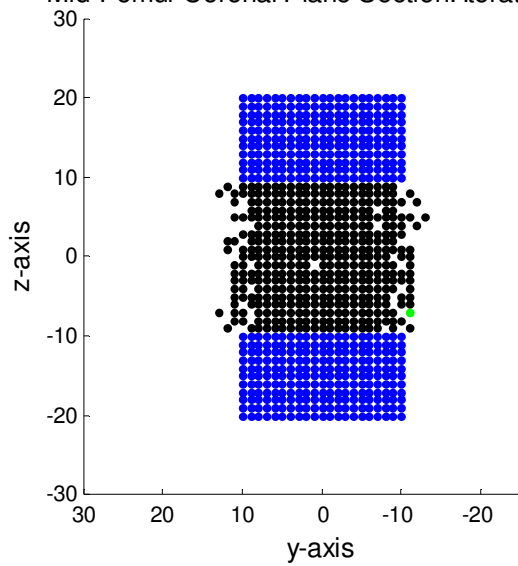
Mid-Femur Coronal Plane Section: Iteration 57



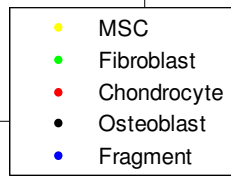
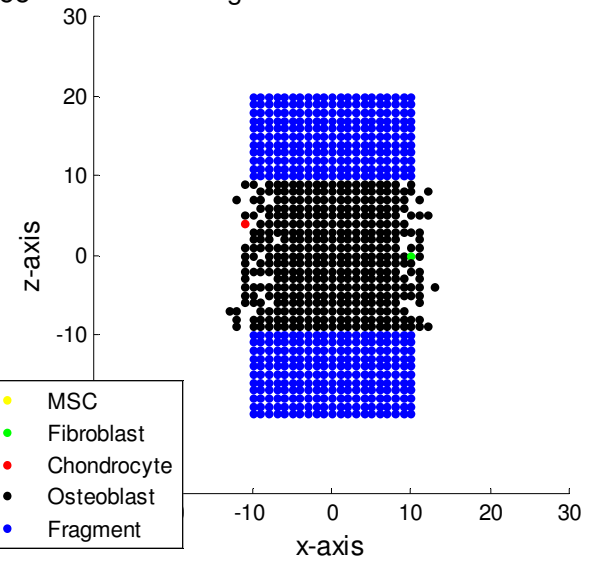
Mid-Femur Sagittal Plane Section: Iteration 57



Mid-Femur Coronal Plane Section: Iteration 58



Mid-Femur Sagittal Plane Section: Iteration 58



References

- [1] Berg HC. 1993. *Random Walks in Biology*. Princeton University Press: Princeton.
- [2] Carter DR, Beaupre GS, Giori NJ, Helms JA. 1998. Mechanobiology of Skeletal Regeneration. *Clinical Orthopaedics and Related Research*. 355S: S41-S55.
- [3] Carter DR, Blenman PR, Beaupre GS. 1988. Correlations between mechanical stress history and tissue differentiation in initial fracture healing. *Journal of Orthopaedic Research*. 6: 736-748.
- [4] Claes LE, Heigele CA. 1999. Magnitudes of local stress and strain along bony surfaces predict the course and type of fracture healing. *Journal of Biomechanics*. 32: 255-266.
- [5] Cowin SC. 2006. On the Modeling of Growth and Adaptation. *Mechanics of Biological Tissues*. Ed: Holzapfel GA, Ogden RW. *Mechanics of Biological Tissue*. Springer-Verlag. 29-46.
- [6] Doblare M, Garcia JM, Gomez MJ. 2004. Modelling bone tissue fracture and healing: a review. *Engineering Fracture Mechanics*. 71: 1809-1840.
- [7] Einhorn TA. 1998. The Cell and Molecular Biology of Fracture Healing. *Clinical Orthopaedics and Related Research*. 355S: S7-S21.
- [8] Frost HM. 1988. The Biology of Fracture Healing: An Overview for Clinicians. *Clinical Orthopaedics and Related Research*. 248: 283-293.
- [9] Fung YC. 1993. *Biomechanics: Mechanical Properties of Living Tissues*. Springer Verlag: New York.
- [10] Garcia-Aznar JM, Kupier JH, Gomez-Benito MJ, Doblare M, Richardson JB. 2007. Computational simulation of fracture healing: Influence of interfragmentary movement on the callus growth. *Journal of Biomechanics*. 40: 1467-1476.
- [11] Gardner TN, Mishra S. 2003. The biomechanical environment of a bone fracture and its influence upon the morphology of healing. *Medical Engineering & Physics*. 25: 455-464.
- [12] Gomez-Benito MJ, Garcia-Aznar JM, Kuiper JH, Doblare M. 2005. Influence of fracture gap size on the pattern of long bone healing: a computational study. *Journal of Theoretical Biology*. 235: 105-119.

- [13] Gomez-Benito MJ, Garcia-Aznar JM, Kuiper JH, Doblare M. 2006. A 3D Computational Simulation of Fracture Callus Formation: Influence of the Stiffness of the External Fixator. *Transactions of the ASME*. 128: 290-299.
- [14] Huiskes R, van Driel WD, Prendergast PJ, Soballe K. 1997. A biomechanical regulatory model for periprosthetic fibrous-tissue differentiation. *Journal of Materials Science: Materials in Medicine*. 8: 785-788.
- [15] Isaksson H, Wilson W, van Donkelaar CC, Huiskes R, Ito K. 2006. Comparison of biophysical stimuli for mechano-regulation of tissue differentiation during fracture healing. *Journal of Biomechanics*. 39: 1507-1516.
- [16] Lacroix D, Prendergast PJ, Li G, Marsh D. 2002. Biomechanical model to simulate tissue differentiation and bone regeneration: application to fracture healing. *Medical & Biological Engineering & Computing*. 40: 14-21.
- [17] Lacroix D, Prendergast PJ. 2002. A mechano-regulation model for tissue differentiation during fracture healing: analysis of gap size and loading. *Journal of Biomechanics*. 35: 1163-1171.
- [18] Natali AN, Meroi EA. 1989. A review of the biomechanical properties of bone as a material. *Journal of Biomedical Engineering*. 11: 266-276.
- [19] Nawar EW, Niska RW, Xu J. 2007. National Hospital Ambulatory Medical Care Survey: 2005 Emergency Department Summary. National Center for Health Statistics. no. 386.
- [20] Pauwels F. 1960. Eine neue theorie uber den einflub mechanische reize auf die differenzierung der stutzgewebe. *Z Anat Entwicklungsgeschichte*. 121: 478-515.
- [21] Perez MA, Prendergast PJ. 2007. Random-walk models of cell dispersal included in mechanobiological simulations of tissue differentiation. *Journal of Biomechanics*. 40: 2244-2253.
- [22] Perren SM. 1979. Physical and Biological Aspects of Fracture Healing with Special Reference to Internal Fixation. *Clinical Orthopaedics and Related Research*. 138: 175-196.
- [23] Prendergast PJ, Huiskes R, Soballe K. 1997. Biophysical stimuli on cells during tissue differentiation at implant interfaces. *Journal of Biomechanics*. 30: 539-548.
- [24] Scripture taken from the Holy Bible, New International Version. Copyright © 1973, 1978, 1984 International Bible Society. Used by permission of Zondervan Bible Publishers.

- [25] Tarantino U, Guiseppa C, Domenico L, Monica C, Irene C, Iundusi R. 2007. Incidence of fragility fractures. *Aging Clinical and Experimental Research*. 19: 7-11.
- [26] Turner CH, Burr DB. 1993. Basic Biomechanical Measurements of Bone: A Tutorial. *Bone*. 14: 595-608.
- [27] van der Meulen MCH, Huijskes R. 2002. Why mechanobiology? A survey article. *Journal of Biomechanics*. 35: 401-414.
- [28] Wolff J. 1892. *Das Gesetz der Transformation der Knochen*. Berlin, A. Hirshwald.
- [29] Woolf AD, Akesson K. 2001. Understanding the burden of musculoskeletal conditions. *British Medical Journal*. 322: 1079-1080.
- [30] Yamagishi M, Yoshimura Y. 1955. The biomechanics of fracture healing. *Journal of Bone and Joint Surgery*. 37A: 1035-1068.